

# **Radiation-induced pneumonitis and fibrosis**

-

## **Defining the role of immune cells and regulatory molecules**

Inaugural-Dissertation

zur

Erlangung des Doktorgrades

Dr. rer. nat.

der Fakultät für

Biologie

an der

Universität Duisburg-Essen

vorgelegt von

Federica Cappuccini

Aus Rom, Italien

Mai 2013



Die der vorliegenden Arbeit zugrunde liegenden Experimente wurden im Institut für Zellbiologie AG1, Universitätsklinikum Essen, Universität Duisburg-Essen durchgeführt.

1. Gutachter: Prof. Dr. Verena Jendrossek

2. Gutachter: Prof. Dr. Astrid Westendorf

Vorsitzender des Prüfungsausschusses: Prof. Dr. Perihan Nalbant

Tag der mündlichen Prüfung: July, 31st 2013

**Index**

<b>1</b>	<b><u>INTRODUCTION</u></b>	<b>7</b>
1.1	RADIATION-INDUCED PNEUMOPATHY AND ITS PATHOLOGY	7
1.2	PREVENTION AND THERAPEUTIC APPROACHES	9
1.3	MODELS OF RADIATION-INDUCED PNEUMOPATHY	10
1.4	ADENOSINERGIC/PURINERGIC SIGNALLING AND LUNG INJURY	12
1.4.1	ADENOSINE AND ADENOSINERGIC PATHWAY	12
1.4.2	ADENOSINERGIC PATHWAY AND FIBROSIS	14
1.5	MACROPHAGES AND LUNG INJURY	16
1.5.1	CHARACTERISTICS OF MACROPHAGES	16
1.5.2	LUNG MACROPHAGES - RADIATION RESPONSES AND ADENOSINERGIC PATHWAY	17
1.6	T LYMPHOCYTES AND LUNG INJURY	19
1.6.1	CHARACTERISTIC OF T LYMPHOCYTES	19
1.6.2	LYMPHOCYTES - RADIATION RESPONSES AND ADENOSINERGIC PATHWAY	21
1.7	AIM OF THE STUDY	24
<b>2</b>	<b><u>MATERIALS &amp; METHODS</u></b>	<b>25</b>
2.1	EQUIPMENT AND MATERIALS	25
2.2	CHEMICALS	27
2.3	BUFFERS AND SOLUTIONS	28
2.4	ANTIBODIES	29
2.5	SOFTWARES	31
2.6	MICE	31
2.7	METHODS	32
2.7.1	THORAX IRRADIATION	32
2.7.2	PIMONIDAZOLE HYDROCHLORIDE INJECTION FOR DETERMINATION OF TISSUE HYPOXIA	33
2.7.3	ISOLATION OF BLOOD CELLS	33
2.7.4	ISOLATION OF SPLENOCYTES	33
2.7.5	CD4 <sup>+</sup> T CELL ISOLATION, AUTOMACS® DEPLETION AND ADOPTIVE TRANSFER	34
2.7.6	ISOLATION OF LYMPH NODE CELLS	34
2.7.7	ISOLATION OF LUNG CELLS	35
2.7.8	FLOW CYTOMETRY	35

2.7.9	ISOLATION AND PREPARATION OF LUNG TISSUE FOR PARAFFIN SECTIONS AND CRYOSECTIONS	36
2.7.10	TISSUE MICROARRAY	37
2.7.11	HEMATOXYLIN AND EOSIN STAINING OF LUNG SECTIONS	37
2.7.12	MASSON'S TRICHROME STAINING OF LUNG SECTIONS	38
2.7.13	IMMUNOHISTOCHEMISTRY ON LUNG SECTIONS	38
2.7.14	IMMUNOFLUORESCENCE ON LUNG SECTIONS	39
2.7.15	SEMITHIN SECTIONS AND ELECTRON MICROSCOPY SAMPLES	40
2.7.16	STATISTICAL ANALYSIS	40
<b>3</b>	<b><u>RESULTS</u></b>	<b><u>42</u></b>
<b>3.1</b>	<b>IMPORTANCE OF ADENOSINERGIC SIGNALLING PATHWAY FOR RADIATION-INDUCED FIBROSIS</b>	<b>42</b>
3.1.1	RADIATION-INDUCED CHANGES IN BODY WEIGHT AND SURVIVAL	42
3.1.2	HISTOLOGICAL CHANGES OF LUNG TISSUE IN IRRADIATED C57BL/6 WILD TYPE AND CD73 <sup>-/-</sup> MICE	44
3.1.3	CELLULAR CHANGES OF LUNG TISSUES IN IRRADIATED C57BL/6 WILD TYPE AND CD73 <sup>-/-</sup> MICE	51
3.1.4	LOCAL AND SYSTEMIC ADENOSINERGIC PATHWAY REGULATION IN T LYMPHOCYTES	56
3.1.5	LOCAL AND SYSTEMIC ANALYSIS OF REGULATORY T CELLS IN THE PNEUMONITIC PHASE	62
3.1.6	MACROPHAGE CHARACTERIZATION	64
<b>3.2</b>	<b>THE CONTRIBUTION OF LYMPHOCYTES IN RADIATION-INDUCED PNEUMOPATHY</b>	<b>74</b>
3.2.1	RADIATION INDUCED CHANGES IN BODY WEIGHT AND SURVIVAL	74
3.2.2	HISTOLOGICAL CHANGES OF LUNG TISSUES IN IRRADIATED RAG-2 <sup>-/-</sup> MICE	76
3.2.3	CELLULAR CHANGES OF LUNG TISSUES IN IRRADIATED RAG-2 <sup>-/-</sup> MICE	79
3.2.4	MACROPHAGE CHARACTERIZATION	81
<b>4</b>	<b><u>DISCUSSION</u></b>	<b><u>85</u></b>
<b>5</b>	<b><u>SUMMARY</u></b>	<b><u>100</u></b>
<b>6</b>	<b><u>BIBLIOGRAPHY</u></b>	<b><u>102</u></b>

<b>7 APPENDIX</b>	<b>115</b>
<b>7.1 SUPPLEMENTARY DATA</b>	<b>115</b>
7.1.1 RADIATION RESPONSE OF REGULATORY T CELLS IN C57BL/6 WILD TYPE MICE	115
7.1.2 EFFECT OF CD4 <sup>+</sup> T CELLS ON FIBROSIS DEVELOPMENT	116
<b>7.2 ABBREVIATIONS</b>	<b>118</b>
<b>7.3 FIGURE INDEX</b>	<b>121</b>
<b>7.4 TABLE INDEX</b>	<b>123</b>
<b>7.5 ACKNOWLEDGMENTS</b>	<b>124</b>
<b>7.6 CURRICULUM VITAE</b>	<b>125</b>
<b>7.7 DECLARATIONS</b>	<b>128</b>

# 1 Introduction

## 1.1 Radiation-induced pneumopathy and its pathology

Radiation-induced pneumopathy constitutes a dose-limiting adverse effect of thorax irradiation for the treatment of malignancies in the thoracic area, such as lung, breast or hematologic malignancies, as well as for whole body irradiation as part of the preconditioning before bone marrow transplantation. In general, the risk of radiation-induced side effects and the severity of lung injury are directly related to the irradiated tissue volume, the total radiation dose delivered, the dose rate, and concurrent chemotherapy applied (Gross, 1977; Jennings and Arden, 1961). Albeit many progresses have been made in the field of radiotherapy, this therapeutic intervention has still to cope with a critical dilemma: the contrast between the intrinsic radioresistance of malignant tumors and the high radiosensitivity of lung tissue, which is characterized by low regenerative capacity.

Radiation-induced pneumopathy has been intensively studied and, with respect to time-related reactions, cytotoxic effects of ionizing radiation (IR) have been differentiated in radiation pneumonitis and radiation fibrosis, considered as two types of lung injury that are not necessarily connected (Gross, 1977; Morgan and Breit, 1995). Radiation pneumonitis occurs 1 to 3 months following irradiation, with an incidence that ranges from 10 to 20 % of treated patients. Common clinical manifestations include dry cough, dyspnea and fever. Occasionally and depending on the severity and duration of the early effects, resolution and a full restoration of the normal tissue functions can occur (Davis et al., 1992; Ghafoori et al., 2008). Described morphologic changes in the early pneumonitic phase include degeneration of type I pneumocytes, ultrastructural changes to the lamellar bodies in type II pneumocytes, blebbing and vacuolation in endothelial cells and swelling of the basement membrane. Secondary changes, which characterize the so-called exudative phase of pneumonitis, consist of increased capillary permeability with subsequent leakage of serum proteins, edema of the interstitium, and in some cases increased number of alveolar macrophages and debris in the alveolar space (Morgan and Breit, 1995; Nakayama et al., 1996).

Manifested radiation pneumonitis does not always represent a premise for the development of radiation fibrosis, the delayed reaction that occurs 6 to 12 months after the completion of radiotherapy with similar clinical symptoms described for radiation pneumonitis.

Main histopathological abnormalities during development of radiation fibrosis are the thickening of alveolar septa, further degeneration of type II pneumocytes, loss of capillaries, and collagen deposition (Morgan and Breit, 1995; Nakayama et al., 1996).

The direct toxic effect of IR to the lung tissue is due to DNA damage and subsequent mitotic cell death, in addition to a local production of reactive oxygen species (ROS) in diverse resident cells. Most likely, radiation-induced direct toxicity involves alveolar epithelial cells (AEC) type I and II and microvascular structures. The series of pathologic events occurring after irradiation continues with the so-called latent period, during which release of cytokines and chemokines from the affected cells and a direct or indirect activation of parenchymal and immune cells is taking place (Fleckenstein et al., 2007a; Rubin et al., 1995). Lung injury is only appreciable after this phase with exudative and inflammatory reactions, and it reflects the specific turnover time of the affected cell populations. A subsequent cascade of molecular events presumably induces migration of inflammatory cells, alteration of the tissue microenvironment, chronic lung inflammation, cell proliferation, tissue destruction, and repair to re-establish normal lung architecture and functions.

In summary, lung damage following irradiation exerts an inflammatory response and activates the wound-healing machinery to re-establish tissue homeostasis. Such repair processes, as well as inflammatory reactions, if not properly regulated, can result in an inappropriate tissue regeneration leading to organ failure and death (**Fig. 1.1**) (Bentzen, 2006; Wynn, 2008).

Although several molecular factors that contribute to fibrosis development have been identified (e.g. platelet-derived growth factor (PDGF), transforming growth factor- $\beta$  (TGF- $\beta$ )) (Thornton et al., 1996; Yi et al., 1996), the molecular and cellular events that link direct tissue damage to chronic inflammation and that regulate and promote delayed tissue remodelling and lung fibrosis are not completely understood. Moreover, it is still matter of debate whether the pathological repair process initiated by radiation-induced pneumonitis is a prerequisite for fibrosis development.



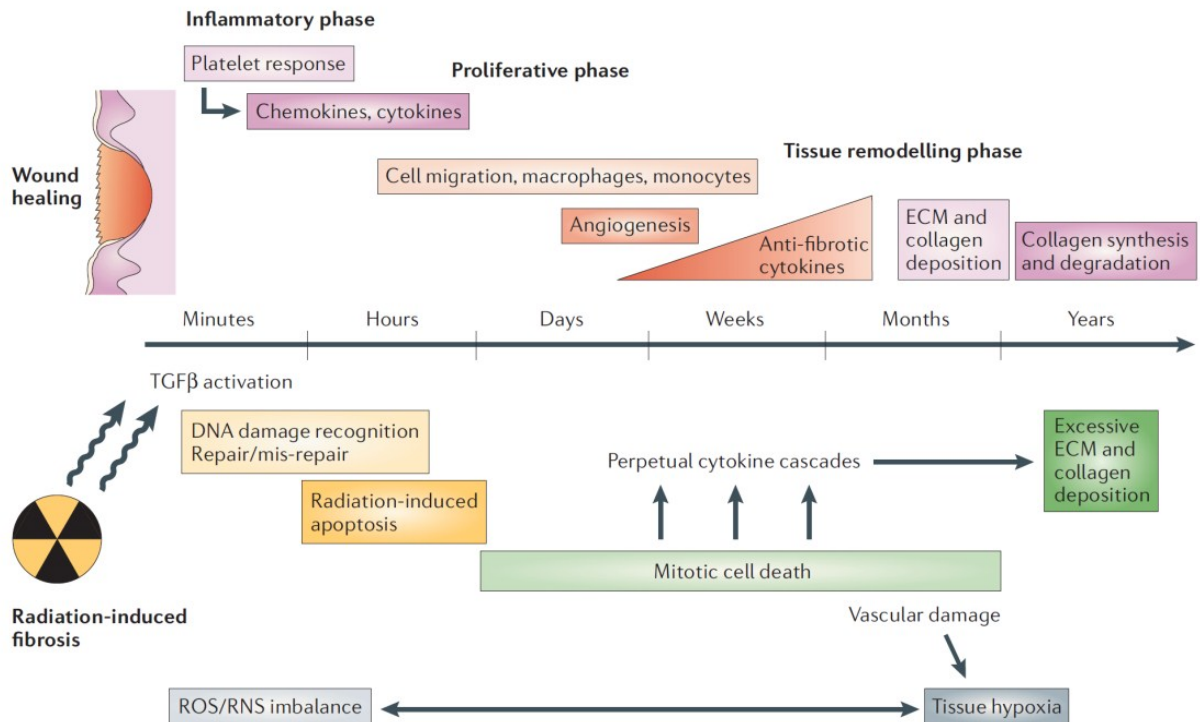


**Fig. 1.1 Normal wound healing vs radiation induced fibrosis.** Schematic overview of the well orchestrated wound healing machinery (above the timeline) activated in response to tissue injury, in comparison to the altered radiation-induced responses (below the timeline) which fail to re-establish tissue homeostasis (ECM = extracellular matrix; ROS = reactive oxygen species; RNS = reactive nitrogen species; TGF $\beta$  = transforming growth factor- $\beta$ ) (Bentzen, 2006).

## 1.2 Prevention and therapeutic approaches

The first approach to reduce radiation pneumonitis and fibrosis in cancer patients is a patient-specific radiation treatment schedule, aiming at limiting radiation doses and volumes. In addition, several pharmacological approaches have been used to reduce early and late side effects of radiation on lung tissue. Some of these will be listed.

Corticosteroids have been used to treat radiation pneumonitis. In mice, they have been shown to markedly improve survival and physiologic abnormalities. In some reports, though with no preventive effects, the administration of corticosteroids as clinical pneumonitis occurred in cancer patients have shown amelioration of the inflammation. However, steroid therapy had no effect on the late pulmonary fibrosis (Abid et al., 2001).

Amifostine is a cytoprotective compound in that it functions as a free-radical scavenger, and is under continued investigation in a number of clinical trials. Despite some reports described

amelioration of pneumonitis, others have shown no influence on the incidence of radiation pneumonitis (Bentzen, 2006; Tsoutsou and Koukourakis, 2006).

The efficacy of antioxidant drugs has also been investigated. Use on animal models could show that angiotensin-converting enzyme (ACE) inhibitors or superoxide dismutase (SOD) analogues ameliorate both radiation pneumonitis and fibrosis, but clinical studies on the effects of these drugs in patients have not been reported so far (Graves et al., 2010).

Recent studies showed significant protective effect for both early and late lung toxicity after prophylactic administration of the xanthine derivative pentoxifylline and vitamin E. Most of the patients obtained regression, and few the complete remission of fibrosis (Bentzen, 2006; Nakayama et al., 1996).

A promising strategy to reduce radiation-associated fibrosis would be the inhibition of fibrogenic mediators, such as TGF- $\beta$ . Pre-clinical studies already showed prevention or amelioration of radiation fibrogenesis and the targeting of TGF- $\beta$  in rodent models reduced the severity or the risk of radiation-induced lung injury (Bentzen, 2006; Graves et al., 2010).

Nevertheless, none of the mentioned approaches has been approved for treatment of radiation-induced pneumonitis and fibrosis. Therefore, a better understanding of the pathogenetic mechanisms of these lung disorders will help to identify critical regulators and to develop effective strategies for the prevention or treatment of radiation-induced pneumopathy.

### **1.3 Models of radiation-induced pneumopathy**

The pathological processes of radiation-induced lung injury have been extensively investigated using several animal models including rats (Burger et al., 1998; Pauluhn et al., 2001), pigs (Rezvani et al., 1989), rabbits (Rubin et al., 1992) and mice (Down and Steel, 1983; Sharplin and Franko, 1989). However, here the murine model will be discussed in more details.

Radiation induced-pneumonitis and fibrosis in mice are usually observed after a single exposure to hemithorax or whole thorax irradiation with 12-15 Gray (Gy) of dose. However, radiation effects are strain-dependent. Some strains show more severe or sub-acute pneumonitis and are fibrosis resistant, whereas others, such as C57BL/6 mice, have milder pneumonitis and are fibrosis prone (Franko et al., 1991; Moore and Hogaboam, 2008). Thus, C57BL/6 mice are the most widely used to investigate the pathogenesis of radiation-induced pneumopathy, with the additional advantage of the numerous genetic variants available.

Following thorax irradiation it has been shown that C57BL/6 mice display altered levels of cytokines, both within the lung tissue and in the bronchoalveolar lavage fluid (BALF) in comparison to sham irradiated mice (controls). An early increase of interleukin (IL)-1 in the first 2 weeks post irradiation (p.i.) was described and high levels of this cytokine, involved in macrophage and T cell recruitment, were noted at later time points up to 26 weeks p.i. In the same study, the two pro-fibrotic mediators TGF- $\beta$  and PDGF showed an early reduction (week 1), followed by a gradual increase and a peak at week 8. Control levels were reached again and a further increase was noted during the fibrotic phase, at 26 weeks p.i. (Rubin et al., 1995). Another study showed in addition increased levels of tumor necrosis factor alpha (TNF- $\alpha$ ), but only in the first 2 weeks p.i. (Chiang et al., 2005). Appreciable signs of radiation induced pneumonitis are usually observed starting at week 3-4 p.i., when lymphocytes, after an initial depletion, are gradually returning to control levels and further increase at later time points (Chiang et al., 2005). Fibrosis development is irreversible and usually occurs 24-30 weeks p.i., when excess of collagen and cellular infiltrates are also detected and fibrotic foci are observed mainly in the subpleural region (Haston and Travis, 1997). Details about macrophage and T cell response to radiation-induced lung damage will be discussed separately in paragraphs 1.5.2 and 1.6.2, respectively.

Many other animal models, with more or less clinical relevance, are currently used to investigate the mechanisms involved in fibrogenesis. They include bleomycin (BLM), silica fibers, or fluorescein isothiocyanate (FITC) treatments, as well as the use of transgenic mice (Moore and Hogaboam, 2008). The BLM model of lung fibrosis is extensively used in research, thus it will be shortly introduced. Bleomycin is an antibiotic isolated from *Streptomyces verticillatus* that has been firstly used in the clinic for its antineoplastic activity. However, its use was downsized because of pulmonary toxicity, a reflection of the low levels of inactivating enzyme in this tissue. Lung damage following BLM exposure is due to induction of DNA strand breaks and subsequent excess of ROS formation. These events result in signs of acute lung injury, inflammation, and subsequent fibrosis (Moore and Hogaboam, 2008). Despite the many advantages that this model provides including the variety of routes of administration and the fast development of fibrosis, as seen for the irradiation model the effect of BLM in mice is strain-dependent, but fibrosis is a self-limited response (Moore and Hogaboam, 2008).

The BLM model, although reproducing many features of human pulmonary fibrosis, is a model of acute lung injury, therefore the irradiation model is preferred to elucidate the development of chronic fibrosis.

Nevertheless, in the effort to understand the mechanisms linking chronic inflammation and fibrosis, the BLM model and the use of transgenic mice have helped in the identification of some important molecular and cellular mediators involved in the fibrogenic process. In particular, one such mediator is adenosine (Ado), a signalling nucleoside that plays an important role in lung physiology, inflammation and fibrosis.

## 1.4 Adenosinergic/purinergic signalling and lung injury

### 1.4.1 Adenosine and adenosinergic pathway

The purine nucleoside adenosine is involved in many physiological and pathological events and is a critical regulator of inflammatory responses. In normal physiologic conditions, adenosine levels in the extracellular space are relatively low, but during inflammation, hypoxia, infection and other pathological situations, they can rapidly increase. This evolutionary well-preserved mechanism activated during immune reactions aims at protecting cells and tissues from excessive damage (Bours et al., 2006). Adenosine can be produced intracellularly from adenosine monophosphate (AMP) by cytosolic 5'-nucleotidase, and passively diffused or actively secreted in the pericellular space via equilibrative nucleoside transporters. Alternatively and particularly after injury, the main source of adenosine is the catabolic extracellular hydrolysis of precursor nucleotides, such as adenosine triphosphate (ATP), a potent danger signal commonly released during tissue damage and cellular stress. The sequential phosphohydrolysis of ATP or adenosine diphosphate (ADP) in AMP is catalyzed through the enzymatic activity of the membrane-bound ectoapyrase cluster of differentiation (CD) 39 (NTDPase1 - ectonucleoside triphosphate diphosphohydrolase-1). AMP can be further hydrolysed to adenosine by the rate-limiting ecto-5'-nucleotidase CD73 (NT5E) (**Fig. 1.2**). Extracellularly and intracellularly, adenosine can be metabolised and converted to inosine by the enzyme adenosine deaminase (ADA), or phosphorylated to generate AMP by adenosine kinase (AK) (Fredholm, 2007; Zimmermann, 2000).

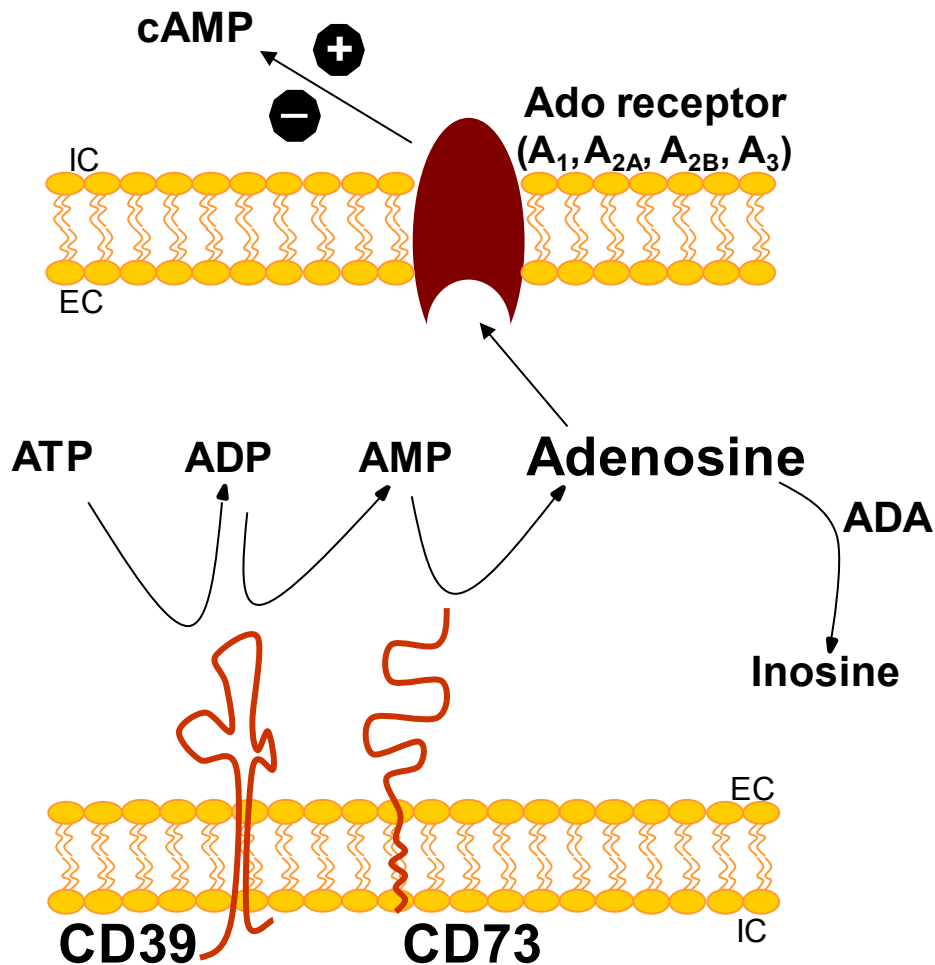


**Fig. 1.2 Schematic overview of the extracellular purine metabolism.** The extracellular generation of adenosine relies on the enzymatic activity of the ectonucleotidases CD39 and CD73. These ecto-enzymes stepwise convert ATP in adenosine, which can bind to specific adenosine receptors (A<sub>1</sub>, A<sub>2A</sub>, A<sub>2B</sub>, A<sub>3</sub>) leading to differential regulation of intracellular cyclic AMP (cAMP) in the target cell. Alternatively, extracellular adenosine can be converted into inosine by the action of the enzyme adenosine deaminase (ADA) (EC= extracellular; IC= intracellular).

Adenosine exerts anti- or pro-inflammatory actions mainly through its binding to four G-protein-coupled receptors, namely adenosine receptors A<sub>1</sub>, A<sub>2A</sub>, A<sub>2B</sub> and A<sub>3</sub>. These receptors are widely expressed on immune cells, but also on endothelial and epithelial cells. They differ in their binding affinity and in their downstream effects, with the G<sub>i/o</sub>-coupled A<sub>1</sub> and A<sub>3</sub> receptors inhibiting adenylyl cyclase, thereby decreasing intracellular cyclic AMP (cAMP) levels, and the G<sub>s</sub>-coupled A<sub>2A</sub> and A<sub>2B</sub> receptors, activating adenylyl cyclase and protein kinase A, therefore increasing cAMP levels in the cell (Hasko et al., 2008).

The ectonucleotidase CD73 belongs to the 5'-nucleotidases, a family of soluble and membrane-bound enzymes that catalyse the hydrolysis of 5'-nucleotides. CD73 is a 70-kDa

glycosyl phosphatidylinositol (GPI)-linked protein expressed on the cell surface of many cell types including endothelial cells, immune cells, epithelial cells and dendritic cells (DC). In humans, CD73 is expressed in approximately 30 % of peripheral blood T cells and 70 % of B cells, whereas monocytes and natural killer (NK) cells are negative for CD73 (Resta and Thompson, 1997). Differences in the tissue distribution and activity of this enzyme suggest a wide diversity of physiological activities that extend beyond its enzymatic properties. A role in tissue barrier function and cell adhesion has indeed been described (Airas et al., 1995; Koszalka et al., 2004; Lennon et al., 1998).

Among all the physiological properties of this molecule, adenosine has mainly anti-inflammatory effects exerted on a plethora of immune cells, therefore representing a beneficial response during acute injury states. On the contrary, elevated levels of adenosine are promoting and exacerbating tissue injury, contributing to progression of chronic disease state, including fibrosis. For example, in asthmatic patients or in patients suffering from chronic obstructive pulmonary disease (COPD) increased levels of adenosine have been found, suggesting a cause-and-effect role of adenosine in these disorders. Altered levels of adenosine were associated with increase of CD73, reduction of ADA activity, as well as with upregulation of some Ado receptors (Driver et al., 1993; Fozard and Hannon, 1999; Huszar et al., 2002). These evidences lead to the hypothesis that CD73 could represent an essential mechanism in the regulation of adenosine extracellular levels. The role of CD73/Ado pathway in fibrosis development has been investigated and will be discussed in the next paragraph.

#### **1.4.2 Adenosinergic pathway and fibrosis**

As mentioned above (par. 1.3), several studies on chronic pulmonary diseases using mouse models of lung fibrosis described a detrimental or beneficial role of adenosine. The main findings will be discussed.

The first evidence of an implication of adenosine in lung inflammation, airway remodeling and chronic pulmonary injury was provided by the use of mice deficient for ADA, the purine catabolic enzyme responsible for the breakdown of adenosine. These mice present markedly elevated levels of adenosine in many organs including the lung, and die by 3 weeks of age from lung inflammation and pulmonary insufficiency. No signs of lung damage and respiratory failure were observed when exogenous ADA enzyme therapy was administered to these mice from birth. Even more interestingly, mice treated after the establishment of the pulmonary

damage could restore lung adenosine to control levels, recover and survive (Blackburn et al., 1998; Blackburn et al., 2000; Chunn et al., 2001). In following investigations, experiments on ADA deficient mice treated with high dose or low dose of exogenous ADA enzyme could confirm that chronic elevations in lung adenosine correlate with fibrosis development (Chunn et al., 2006; Chunn et al., 2005). Pro-fibrotic mediators, such as TGF- $\beta$ , were found to be elevated exclusively in the lung tissue of mice at low dose regimen, and the same mediators could be significantly reduced when lowering levels of endogenous adenosine through the replacement of ADA treatment with the high dose regimen. Similarly, a decrease of tissue adenosine through ADA therapy was shown to be beneficial in a mouse model with specific lung overexpression of interleukin (IL)-13, a pluripotent T helper cell type 2 (T<sub>H</sub>2) cytokine implicated in the pathogenesis of asthma. These mice develop features of chronic lung disease and fibrosis resembling the ADA deficient phenotype, with adenosine accumulation and a decreased ADA activity in the lung (Blackburn et al., 2003). Other studies have been useful to identify in the ADA deficiency model the A<sub>1</sub> and the A<sub>2B</sub> receptors as mediators of anti-inflammatory/tissue protective and pro-fibrotic/tissue destructive effects of adenosine respectively (Sun et al., 2005; Sun et al., 2006).

In contrast with the above mentioned studies, the use of the BLM model of lung fibrosis could demonstrate that elevations of adenosine through CD73 are not necessary for the development of pulmonary fibrosis. In details, lung tissue of BLM challenged mice displayed adenosine accumulation and this increased level correlated with elevations in CD73 enzymatic activity. On the contrary, the administration of BLM to CD73 deficient mice was not leading to adenosine accumulation in the lung. In addition, these mice showed no compensatory increase in activity of other nucleotidases. BLM challenge was also differentially altering inflammation in the lung of CD73 deficient mice, which showed marked increase of inflammatory foci within the tissue and a greater level of total cells recovered from the BALF in comparison to CD73 proficient mice. Interestingly, loss of CD73 resulted in enhanced collagen production and deposition, in addition to enhanced expression of pro-inflammatory and pro-fibrotic mediators and a lower survival following BLM exposure. Moreover, the intranasal administration of exogenous nucleotidase could elevate lung adenosine levels and reduce inflammation and collagen deposition in mice challenged with BLM, in the absence or presence of endogenous CD73. In this report, the production of adenosine by CD73 emphasizes an anti-inflammatory/tissue-protective role of this nucleoside (Volmer et al., 2006).

In summary, these models pointed out a crucial role of key components of Ado metabolism and signalling in respect to chronic lung pathologies, showing how therapeutic strategies addressed to regulate Ado levels (e.g. ADA enzyme replacement therapy, A<sub>2B</sub> receptor inhibitors) could improve the outcome of pulmonary pathology. Albeit the strong association between increased levels of adenosine and progressive inflammation and fibrosis, mechanisms regulating adenosine formation after lung injury are still considerably unexplored. In this context the indication of a key role for CD73 in the control of adenosine production is highly comprehensible, as suggested also by Volmer *et al.*. However, up to date the role of CD73/adenosine in radiation-induced pneumonitis and fibrosis remains unknown.

## 1.5 Macrophages and lung injury

### 1.5.1 Characteristics of macrophages

Macrophages are major players in the innate immune response and are considered as professional antigen-presenting cells (APCs) with the ability to initiate specific lymphocyte effector mechanisms. Macrophages derive from monocytic precursor cells originated in the bone marrow from a common myeloid progenitor. Circulating peripheral blood mononuclear cells (PBMCs) differentiate and acquire specialized functions when migrating in different anatomical locations. Tissue macrophage functions involve homeostatic clearance processes and remodeling and repair of tissues after inflammation (Gordon and Taylor, 2005). Different stimuli can rapidly trigger macrophage activation and secretion of a multitude of inflammatory mediators leading to their participation in a variety of immune responses. Due to their remarkable plasticity and depending on the stimuli and the microenvironment, activated macrophages show a broad spectrum of phenotypes that influence their role in the initiation and the resolution of inflammation. The simplest scenario conceives two major macrophage phenotypes. Classically activated (M1) macrophages are induced by exposure to T helper cell type 1 (T<sub>H</sub>1) cytokines and interferon-gamma (IFN- $\gamma$ ) and are considered as pro-inflammatory and cytotoxic. This phenotype is associated with massive production of nitric oxide (NO), ROS and pro-inflammatory cytokines involved in cytotoxicity and microbicidal activity, such as IL-1 $\beta$ , IL-6, IL-12 and TNF- $\alpha$ . In contrast, alternatively activated (M2) macrophages are induced by T<sub>H</sub>2 cytokines (IL-4 and/or IL-13) and are involved in phagocytosis of apoptotic



cells, tissue repair, wound healing and resolution of inflammation. M2 macrophages produce anti-inflammatory cytokines such as IL-10, TGF- $\beta$  and IL-1R antagonist, express high levels of arginase-1 (Arg1) and inhibit the production of pro-inflammatory cytokines. Moreover, alternatively activated macrophages are characterized by an increase in extracellular matrix remodeling, being therefore involved in tissue repair and homeostasis more than in immune defense (Gordon and Taylor, 2005; Mosser, 2003; Mosser and Edwards, 2008). However, the classification into two polarized states oversimplifies the complex and dynamic functional activity of these cells, which are able to differentially modulate their responses inducing peculiar gene expression patterns, in addition to rapidly adapt to progressive changes in the microenvironment (Martinez et al., 2008; Stout et al., 2005; Stout and Suttles, 2004). A tight regulation of macrophage functions and their cytokine production, as well as a balanced activity of the diverse macrophage populations are needed to avoid dangerous consequences. It is widely accepted that an aberrant regulation of M1 macrophages can lead to host tissue destruction, whereas uncontrolled repair processes driven by M2 macrophages can have a role in fibrosis development (Lupher and Gallatin, 2006; Martin and Leibovich, 2005; Mosser and Edwards, 2008).

### **1.5.2 Lung macrophages - radiation responses and adenosinergic pathway**

Lung macrophages primarily originate from circulating monocytes, although local proliferation of a self-renewing population has been also described (Bitterman et al., 1984; Tarling and Coggle, 1982). Macrophages represent the most abundant immune effector population in the lung and comprehend cells residing in the interstitium and cells on the alveolar wall, namely alveolar macrophages (AM). The natural AM turnover is very slow but it can be accelerated after acute lung inflammation via recruitment of monocytes, which replace the resident alveolar macrophage population (Maus et al., 2006).

Compared with other tissue macrophages, AM constitute a peculiar population exhibiting unique properties including unusual phenotypic features, such as the expression of high levels of CD11c and low expression of CD11b (Lambrecht, 2006; Lohmann-Matthes et al., 1994). The highly exclusive lung microenvironment provides specific signals, among those the macrophage colony-stimulating factor (M-CSF), granulocyte-macrophage CSF (GM-CSF), as well as surfactant proteins, which influence the development, growth and survival of these cells (Akagawa et al., 1988; Chen et al., 1988; Laskin et al., 2001).

Alveolar macrophages constantly survey the pulmonary surface to maintain the sterility of alveolar surfaces and proper gas exchange. In homeostatic conditions, AM retain a quiescent state, in that they show production of small amounts of inflammatory cytokines and little phagocytic activity. Moreover, they have been shown to actively suppress DC and T cells in the lung through the release of IL-10 and TGF- $\beta$  (Lambrecht, 2006). At the same time, AM are the main initiators of inflammatory responses as a consequence of lung injury, being rapidly able to respond to insults, infectious agents or dangerous particles.

Modulation of macrophage responses, as previously mentioned, has a major role in determining the progress and the resolution of inflammatory reactions, in that excessive repair processes driven by M2 macrophages have been associated to fibrosis development. One regulator of macrophage polarization and effector functions is adenosine. Due to the anti-inflammatory effect and the ability to decrease expression of several pro-inflammatory mediators in macrophages such as ROS and NO production, Ado can prevent excessive classical macrophage activation (Hasko et al., 2007). Moreover, with its positive regulation on anti-inflammatory cytokines, such as IL-10, Ado has been suggested to contribute to the phenotype switching of macrophages during inflammatory responses, a mechanism involved in the resolution of inflammation (Bours et al., 2006).

As described in par. 1.1 and par. 1.3, lung inflammatory cells, both resident and recruited, take part in the tissue response to irradiation possibly determining the progression of radiation pneumonitis to fibrosis development. Among those, macrophages are of particular interest. In response to thorax irradiation, an initial decrease in the numbers of macrophages within the BALF has been described (1 week p.i.). Despite their dose- and fractionation-dependent sensitivity, AM show an immediate production of inflammatory mediators such as TGF- $\beta$ , IL-1, TNF- $\alpha$  or PDGF- $\beta$ . Subsequent to the initial decrease, AM rapidly repopulate the lung tissue. Macrophage numbers return to control levels by week 2 p.i., and a significant but not dramatic increase is noted between 3 and 6 months p.i. (Chiang et al., 2005). Lung interstitial macrophages respond to irradiation differently, in that they are involved in delayed inflammatory responses.

Radiation-induced changes in macrophages include an increase in size and the presence of multinuclei, mainly at 3 week p.i and then again at later time points (6 months p.i.) (Chiang et al., 2005; Hong et al., 2003). The increase in size is also dependent on lipid accumulation in these cells, in that both in the BALF and in the tissue, an early appearance of foamy lung

macrophages has been documented. These enlarged foamy macrophages reappear during the late phase, at 6 months p.i. (Cappuccini et al., 2011; Chiang et al., 2005; Gross and Balis, 1978; Hong et al., 2003). Despite its common occurrence after thoracic irradiation during the pneumonitic phase, in none of these studies a specific marker for these cells could be identified. As mentioned above, activated AM, through the immediate release of different cytokines and chemokines can regulate and/or recruit many other cell types at the site of injury (Coggle et al., 1986; Hong et al., 2003; Morgan and Breit, 1995; Rubin et al., 1992). A radiation-dependent release of pro-fibrotic cytokines has been documented also using *in vitro* assays. Cultured alveolar macrophages isolated from BALF of patients just prior to thoracic irradiation, secreted PDGF- $\beta$  in a dose- and time-dependant manner after *in vitro* irradiation. In addition, BALF macrophages isolated from the same patients 4-6 weeks after radiation treatment, showed the spontaneous production of TNF- $\alpha$  and PDGF- $\beta$  (Thornton et al., 1996). In a rat model of thorax irradiation, AM actively produced TGF- $\beta$  when irradiated *in vitro* and BALF AM isolated 1 month after *in vivo* irradiation were able to stimulate fibroblast proliferation via TGF- $\beta$  (Rubin et al., 1992).

These studies highlighted the role of the alveolar macrophage population in early responses to irradiation. However, the role of macrophages in the pathogenic process linking initial tissue damage in response to whole thorax irradiation to chronic inflammation and fibrosis remains still largely unknown.

## 1.6 T lymphocytes and lung injury

### 1.6.1 Characteristic of T lymphocytes

The T cell population plays a central role in humoral and cellular immune responses, and with B lymphocytes constitutes the adaptive immunity. T lymphocytes originate in the thymus, where T cell clones with a receptor (TCR) recognizing self major histocompatibility complex (MHC) antigens on stromal cells are positively selected and will later develop into effector cells. Mature T cells will then be able to recognize peptide antigen in peripheral lymphoid organs in a MHCI context (CD8<sup>+</sup>) or MHCII context (CD4<sup>+</sup>). On the contrary, T cell clones with higher affinity to self antigens will be negatively selected to avoid autoimmune reactions.

Naïve T cells, upon TCR recognition of the specific antigen and with appropriate co-stimulatory signals, proliferate and differentiate into effector cells. Different subsets of T cells with distinct functions have been characterized. A short description of the main T cell subpopulations follows (2008).

CD4<sup>+</sup> naive T cells are mainly differentiating into T<sub>H</sub>1 and T<sub>H</sub>2 subsets, involved in the stimulation of innate cellular immunity, and contributing in the humoral response influencing B lymphocyte properties. The classification depends on the specific cytokines produced by these cells. T<sub>H</sub>1 cells are induced by IFN- $\gamma$  and IL-12 and secrete IFN- $\gamma$  and IL-2, whereas T<sub>H</sub>2 differentiation is favored by IL-4 and these cells produce IL-4 and IL-5. As a consequence, each activated T<sub>H</sub> subtype produces signals to amplify the differentiation towards its specific subtype, to generate T<sub>H</sub>1 or T<sub>H</sub>2 driven immune responses. A third CD4<sup>+</sup> T cell subset is the T<sub>H</sub>17 population, mostly involved in the recruitment of neutrophils to sites of infection. T<sub>H</sub>17 cells are differentiated in the presence of IL-6 and TGF- $\beta$  and characteristically secrete IL-17, but not IFN- $\gamma$  or IL-4. The expansion and development of this subset rely on the presence of IL-23 (2008).

CD4<sup>+</sup> regulatory T cells (T<sub>reg</sub>) have also been described, with the main function of suppressing T cell activation in the periphery therefore preventing excessive immune responses and autoimmunity during acute immune reactions. This subset produces TGF- $\beta$  and IL-10, inhibitory cytokines involved in the suppression of T cell proliferation and activation. There exist natural T<sub>reg</sub> cells (nT<sub>reg</sub>), committed to a regulatory differentiation in the thymus, and induced T<sub>reg</sub> cells (iT<sub>reg</sub>), that differentiate directly in the periphery depending on specific environmental conditions. Both subsets of nT<sub>reg</sub> and iT<sub>reg</sub> cells specifically express the transcription factor forkhead box P3 (Foxp3), which activates genes that mediate the suppressive phenotype and silences many effector T cell genes (Sakaguchi et al., 2008).

CD8<sup>+</sup> T cells, also named cytotoxic T cells (CTLs), actively recognize and kill infected cells inducing apoptosis via direct membrane-binding or through release of cytotoxic granules containing granzymes and perforin. Costimulatory signals for CD8<sup>+</sup> T cell activation are provided by APCs, such as DC, or by CD4<sup>+</sup> T<sub>H</sub> cells (2008).

The extinction of T cell immune responses after removal of the inflammatory threat consists in the apoptotic death of most of the activated cells, whereas only few will become long-lived memory cells (Bours et al., 2006).

### 1.6.2 Lymphocytes - radiation responses and adenosinergic pathway

Generally, it is suggested that a shift from a  $T_H1$  to a  $T_H2$  response is likely to play an important role in the progression of inflammation to fibrosis. A dysregulation in the equilibrium of anti-fibrotic  $T_H1$ -associated cytokines and pro-fibrotic  $T_H2$ -associated cytokines could contribute to fibrogenesis (Thannickal et al., 2004; Wynn, 2008). Pro-fibrotic effects of  $T_{reg}$  cells have also been postulated. In the attempt to dampen inflammation, these cells produce TGF- $\beta$  and therefore may contribute to fibrosis (Luzina et al., 2008). Moreover,  $T_{reg}$  cells have been shown to promote the activation of macrophages towards an M2 polarization state (Tiemessen et al., 2007).

In general, CD73 is recognized as a maturation marker in lymphocytes due to its developmentally regulated expression, and has also been identified as a signal transducing molecule. In T lymphocytes, the binding of specific antibodies to CD73 in combination with suboptimal T cell receptor engagement was shown to be potent co-stimulatory signal for T cell activation and proliferation. Unfortunately, neither a specific interaction partner, nor mechanisms mediating CD73 effects have been clarified, though the GPI anchor and the enzymatic activity of CD73 were not absolutely required for CD73-mediated signal transduction (Dianzani et al., 1993; Gutensohn et al., 1995; Massaia et al., 1990; Resta et al., 1994; Thompson et al., 1989). Noteworthy, it has been relatively recently discovered that  $T_{reg}$  cells co-express high levels of CD39 and CD73. It is now widely approved that extracellular Ado generation constitutes a potent additional suppressive mechanism of these cells. Interestingly, Ado engagement of the  $A_{2A}$  receptor has been shown to promote the generation of  $iT_{reg}$  cells (Zarek et al., 2008).

Radiation pneumonitis is characterized by increased infiltration of immune cells in the lung tissue and T lymphocytes represent a significant part of these infiltrating cells. In rodent models of thorax irradiation, after an initial depletion lymphocyte numbers recovered by 3 weeks and further increased in a dose-dependent manner, persisting also at later time point during the fibrotic phase (Chiang et al., 2005; Johnston et al., 2004). A selective increase in the  $CD4^+$  T cell subset was noted at 4 weeks p.i.. This cell population has been reported to express IL-4, indicative of a  $T_H2$  response, until later phases (Westermann et al., 1999).

In regard to T cell radiation responses in humans, a phenomenon named lymphocytic alveolitis (alveolar lymphocytosis) has been described in breast and lung cancer patients receiving therapeutic radiation treatment. Cell counts performed on the BALF of these patients after

completion of radiotherapy showed an increased number of lymphocytes with a predominance of the CD4<sup>+</sup> subset. This reaction has been described to correlate with the degree of clinical symptoms of radiation pneumonitis, therefore more pronounced in symptomatic patients in comparison to asymptomatic patients. Moreover, the increase of lymphocytes infiltration was not only confined to the field of irradiation (Cordier et al., 1984; Gibson et al., 1988; Martin et al., 1999; Nakayama et al., 1996; Roberts et al., 1993). T cell sensitivity to IR could also be used as a predictive parameter for late tissue injury. A low rate of apoptosis in CD4<sup>+</sup> and CD8<sup>+</sup> T cells isolated from blood of cancer patients before and after receiving radiotherapy directly correlated with late side effects. No association between apoptosis and early toxicity was found in this prospective study (Ozsahin et al., 2005).

Conflicting data have been published in the attempt to clarify the role of T cells in the fibrogenesis of the lung. Moreover, these studies were carried out using animal models of acute fibrosis. A short overview of the main findings follows.

Frequency and severity of alveolitis and fibrosis after intraperitoneal (i.p.) injection of the radiomimetic drug BLM in nude mice were shown to be comparable to BLM treated control mice (Szapiel et al., 1979). Some years later, Schrier *et al.* showed that athymic mice after a single intratracheal (i.t.) administration of BLM were partially protected against pneumonitis and fibrosis (Schrier et al., 1983). In line with this group, Piguet *et al.* showed that mice depleted of CD4<sup>+</sup> and CD8<sup>+</sup> T cells were prevented from fibrosis development after i.t. instillation of BLM (Piguet et al., 1989). In another report it was shown that, after i.t. inoculation of BLM, fibrosis development was abrogated in immunosuppressed mice, whereas severe combined immunodeficiency (SCID) mice showed no differences in their fibrotic response in comparison to control mice (Zhu et al., 1996). Helene *et al.*, using different mouse strains and the respective SCID counterparts, could confirm that the initial induction of this disease can be lymphocyte independent, though a different kinetic of collagen deposition was noted in BLM sensitive mouse strains (Helene et al., 1999). The T cell independent induction of lung fibrosis was also confirmed using FITC i.t. instillation. CD4<sup>+</sup> depleted recombination activating gene (RAG) knock out and SCID mice in this study were showing identical increase of lung collagen deposition when compared to immunocompetent control mice (Christensen et al., 1999).

The most data available in the literature describe the role of T cells in fibrotic processes in general. The impact of whole thorax irradiation on the time-dependent polarisation and

function of T cells recruited to the lung tissue is still largely unknown. Moreover, it is still unclear whether T cells play a functional role in the pathogenesis initiated by whole thorax irradiation and in the progression to lung fibrosis.

## 1.7 Aim of the study

Radiation-induced pneumopathy (pneumonitis and fibrosis) constitutes a severe and dose-limiting side effect of thorax and whole body irradiation. Acute tissue injury leads to an inflammatory response followed by chronic inflammation with or without fibrosis development. The current hypothesis proposes that acute tissue damage triggers a delayed inflammation (pneumonitis) as well as lung fibrosis, involving complex interactions of resident lung cells, fibroblasts, the extracellular matrix and the immune system. As observed for other fibrotic diseases, an impaired balance between inflammation and repair may be causative for extensive remodelling processes and finally fibrosis. However, despite many reports and studies, the underlying mechanisms leading to radiation-induced lung injury are still poorly understood. In particular, the primary target cells, the key soluble regulators and the network of signals involved in and regulating the sequence of pathophysiological events after irradiation have to be identified in the need of developing effective strategies for prevention or treatment of radiation-induced pneumopathy.

From other disease models it is known that tissue damage triggers the release of adenosine from resident cells and that chronically elevated extracellular levels of this immunomodulatory purine nucleoside are associated to fibrosis development. Therefore, the first focus of the experimental study was to analyze the role of the ecto-enzyme CD73, responsible for the last step of extracellular adenosine generation, in radiation-induced pneumopathy.

Moreover, it is still controversial whether inflammation is a prerequisite for progression to lung fibrosis. Thus, the second focus of the present work was to characterize the radiation-responses of the innate and adaptive immune systems, and to gain a better understanding of their putative role in driving radiation-induced lung reactions towards fibrosis development.

Overall, aim of the project was to investigate the processes linking radiation-induced tissue damage to tissue inflammation and fibrosis, and to characterize local and systemic radiation-induced immune changes in a murine model *in vivo*, using a single dose (15 Gray) of whole thorax irradiation on C57BL/6 wild type mice, as well as on CD73<sup>-/-</sup> and RAG-2<sup>-/-</sup> mice on a C57BL/6 background.



## 2 Materials & Methods

### 2.1 Equipment and materials

The equipment and materials used in this study are listed in **Tables 2.1** and **2.2** below.

**Table 2.1 Equipment**

<i>Item</i>	<i>Manufacturer</i>
autoMACS®	MiltenyiBiot, Bergisch Gladbach, Germany
Cell counter and analyzer CASY®	Innovatis AG, Reutlingen, Germany
Centrifuge Jouan CR422	Thermo Scientific, Dreieich, Germany
Cobalt-60 source Philips	Netherlands
Cryostat CM1850 UV	Leica Microsystems, Wetzlar, Germany
Embedding station Shandon Histocentre™ 2	Thermo Scientific, Dreieich, Germany
Flow cytometers FACS Calibur™, BD LSR II™, BD LSRFortessa™	Becton Dickinson, Heidelberg, Germany
Fluorescence microscope Axio Observer Z1, ApoTome, fluorescence filters (#49 DAPI, #38HE eGFP, #43 HE CY3)	Carl Zeiss, Jena, Germany
Incubator Heraeus Cytoperm 2	Thermo Scientific, Dreieich, Germany
Incubator	Memmert, Kirchheim u. Teck, Germany
Inverted light microscope DMIRB, AxioCam HRc	Leica Microsystems, Wetzlar, Germany Carl Zeiss, Jena, Germany
Micro-plate shaker	Oehmen, Essen, Germany
Microtome RM2235, water bath, flattening table	Leica, Wetzlar, Germany
Tissue arrayer MTABooster® OI	Alphelys, Plaisir, France
Tissue processor Shandon Excelsior™ ES	Thermo Scientific, Dreieich, Germany
Water bath Julab5B	Oehmen, Essen, Germany
Water bath	Köttermann, Uetze/Hänigsen, Germany

**Table 2.2 Disposables and materials**

<i>Item</i>	<i>Supplier</i>
96-well plates U-bottom Cellstar	Greiner bio-one, Frickenhausen, Germany
Barrier pen hydrophobic	Dako, Glostrup, Denmark
Cell culture dishes (6, 10 cm)	Sarstedt, Nümbrecht, Germany
Cell strainers (70, 100 µm)	BD Falcon, Heidelberg, Germany
Coverslips	Engelbrecht, Edermuende, Germany
Disposable glass capillaries	Brand, Wertheim, Germany
Disposable filters CellTrics (30, 50 µm)	Partec, Görlitz, Germany
Disposable scalpels Mediatech	Servoprax, Wesel, Germany
Embedding cassettes RotiLab	Roth, Karlsruhe, Germany
Micropipettes	Gilson, Middleton, USA
Microscope slides	Engelbrecht, Edermuende, Germany
Microscope slides Superfrost Plus	R. Langenbrinck, Teningen, Germany
Needles BD Microlance 3 (21, 23, 27 G)	BD, Drogheda, Ireland
Objective slides	Engelbrecht, Edermuende, Germany
Pasteur pipettes (3 ml) Plastibrand	Sigma-Aldrich, Deisenhofen, Germany
Pipet boy	Starlab, Hamburg, Germany
Pipet tips (100, 200, 1000 µl)	Greiner bio-one, Frickenhausen, Germany
Pipet tips Multi Kristall (0.5, 10 µl)	Roth, Karlsruhe, Germany
Plastic pipettes (1, 2, 5, 10, 25 ml)	Sarstedt, Nümbrecht, Germany
PP-tubes (1.3 ml)	Greiner bio-one, Frickenhausen, Germany
Scale Kern 474	Kern&Sohn, Balingen-Frommern, Germany
Surgical tools	B Braun, Melsungen, Germany
Syringes (1, 2 ml)	Terumo, Leuven, Belgium
(5 ml)	Dispomed, Gelnhausen, Germany
(10 ml)	Ameba, Limburg, Germany
Tubes (0.5, 1.5, 2 ml)	Sarstedt, Nümbrecht, Germany
Tubes (15, 50 ml)	Sarstedt, Nümbrecht, Germany
Tubes round-bottom (5 ml)	BD Falcon, Heidelberg, Germany

## 2.2 Chemicals

Chemicals, reagents and media used in this study are listed in **Table 2.3** below.

**Table 2.3 Chemicals, reagents, media and kits**

<i>Chemical/Reagent/Kit/Media</i>	<i>Manufacturer</i>
Acetic acid	Merck, Darmstadt, Germany
Ammonium chloride (NH <sub>4</sub> Cl)	Merck, Darmstadt, Germany
Bovine serum albumin (BSA)	Roth, Karlsruhe, Germany
CD4 <sup>+</sup> T cell Isolation Kit	MiltenyiBiot, Bergisch Gladbach, Germany
Cell culture media	Gibco, Karlsruhe, Germany
DMEM	
RPMI	
Collagenase type V	Sigma-Aldrich, Deisenhofen, Germany
Detection systems	Dako, Glostrup, Denmark
APAAP REAL™, Mouse	
DAB+ chromogen	
DAB+ substrate buffer	
Eosin G	Roth, Karlsruhe, Germany
Ethanol (EtOH)	Merck, Darmstadt, Germany
Ethylenediaminetetraacetic acid (EDTA)	Roth, Karlsruhe, Germany
Fetal calf serum (FCS)	Biochrom AG, Berlin, Germany
Fluorescent mounting medium	Dako, Glostrup, Denmark
Foxp3 Staining Buffer Set	eBiosciences, San Diego, USA
Hank's balanced salt solution (HBSS)	PAA Laboratories, Cölbe, Germany
Heparin-Natrium 25000	Ratiopharm, Ulm, Germany
Hoechst 33258	Invitrogen, Karlsruhe, Germany
Immersol	Carl Zeiss, Jena, Germany
Isoflurane	Abbott, Wiesbaden, Germany
Isopropanol	Sigma-Aldrich, Deisenhofen, Germany
Masson-Goldner-Trichrome kit	Roth, Karlsruhe, Germany
Mayer's hematoxylin	Roth, Karlsruhe, Germany
Mounting medium Roti Histokitt II	Roth, Karlsruhe, Germany
Normal goat serum (NGS)	Sigma-Aldrich, Deisenhofen, Germany
Octenisept	Schülke, Norderstedt, Germany
Paraformaldehyde (PFA)	Merck, Darmstadt, Germany
Phosphate buffered saline (PBS)	PAA Laboratories, Cölbe, Germany
Pimonidazole HCl (solid)	Hypoxiprobe Inc, Barlington, USA
Potassium bicarbonate (KHCO <sub>3</sub> )	Roth, Karlsruhe, Germany
Sodium chloride (NaCl)	Merck, Darmstadt, Germany
Sodium chloride 0.9 % (saline solution)	Fresenius Kabi, Bad Homburg, Germany
Tissue-Tek® O.C.T.™ Compound	Sakura Finetek, Torrance, USA

***Chemical/Reagent/Kit/Media***

Tris-base  
 Triton X 100  
 Xylene

***Manufacturer***

Roth, Karlsruhe, Germany  
 Roth, Karlsruhe, Germany  
 Applichem, Darmstadt, Germany

**2.3 Buffers and solutions**

All solutions and buffers (unless otherwise noted) were prepared using double distilled water (ddH<sub>2</sub>O) (Table 2.4).

**Table 2.4 Buffers and solutions**

<b><i>Name</i></b>	<b><i>Composition</i></b>
Ammonium chloride potassium buffer (ACK)	150 mM NH <sub>4</sub> Cl 10 mM KHCO <sub>3</sub> 0.1 mM EDTA
Antibodies solution	- TBS, 1.5 % BSA - PBS, 2% NGS
Blocking solutions	- PBS, 2% BSA - TBS, 5% BSA - PBS, 2 % NGS
Citrate buffer, pH 6.0	10 mM sodium citrate
Collagenase solution	HBSS 2 mg/ml collagenase
Complete media	DMEM/RPMI 10 % FCS
FACS buffer	PBS 0.5 % FCS 2 mM EDTA
FcR block solution	FACS buffer anti-CD16/32 1:200
Formalin 1 % solution	PBS 1 % PFA

<i>Name</i>	<i>Composition</i>
Formalin 4 % buffered solution, pH 7.2	PBS 4 % PFA
Permeabilization solution	PBS 0.1 % Triton
Quenching solution	PBS 50 mM NH <sub>4</sub> Cl
TBS	150 mM NaCl 10 mM Tris-base

## 2.4 Antibodies

Antibodies used in flow cytometry, immunohistochemistry and immunofluorescence are listed in **Table 2.5**. The combination of antibodies used in flow cytometric stainings of lung, spleen, blood and lymph nodes cells are listed in **Table 2.6**.

**Table 2.5 Antibodies**

<i>Antibody</i>	<i>Conjugate</i>	<i>Clone</i>	<i>Provider</i>
Actin, smooth muscle		ASM-1	Millipore
Arginase 1		19	BD Biosciences
CD3ε	APC	145-2C11	eBiosciences/BioLegend
	FITC	145-2C11	BD Biosciences
CD4	APC	RM4-5	eBiosciences
	FITC	GK1.5 / RM4-5	eBiosciences
	PE	RM4-5	BioLegend
CD8	APC	53-6.7	eBiosciences
	FITC	53-6.7	BD Biosciences
CD11b	FITC	M1/70	eBiosciences
	PerCP-Cy5.5	M1/70	BioLegend
CD11c	APC	N418	BioLegend
	PE	N418	eBiosciences
	PerCP-Cy5.5	N418	BioLegend/eBiosciences
CD16/CD32		93	eBiosciences
CD25	APC	PC61	BD Biosciences
	PE	PC61.5	eBiosciences

<i>Antibody</i>	<i>Conjugate</i>	<i>Clone</i>	<i>Provider</i>
CD36	PE	HM36	BioLegend
CD39	PE-Cy7	24DMS1	eBiosciences
CD45	eFluor 450	30-F11	eBiosciences
CD45	Pacific Blue	30-F11	BioLegend
CD45R/B220	FITC	RA3-6B2	BioLegend
	PE	RA3-6B2	BioLegend
	PerCP-Cy5.5	RA3-6B2	eBiosciences
CD73	PE	TY/11.8	BioLegend/eBiosciences
	PE-Cy7	TY/11.8	eBiosciences
CD115 (CSF-1R)	PE	AFS98	eBiosciences
CD206 (MMR)	PE	CO68C2	BioLegend
F4/80		CI:A3-1	AbD Serotec
	APC	BM8	eBiosciences
F4/80	PE	BM8	eBiosciences
	PE-Cy7	BM8	BioLegend/eBiosciences
Foxp3	APC	FJK-16s	eBiosciences
	PE	FJK-16s	eBiosciences
IgG	Cy 2		Jackson Immuno Research Labs
	Cy 3		Jackson Immuno Research Labs
IgG	HRP		Cell signaling/NEB
IgG isotype control	PE	eBR2a	eBiosciences
IL-10 R $\alpha$		polyclonal	R&D Systems
Ly-6G and Ly-6C (Gr-1)	FITC	RB6-8C5	BD Biosciences/eBiosciences
MAb1 (hypoxia)			Hypoxyprobe
MHC Class II	APC	M5/114.15.2	eBiosciences
NOS2 (iNOS)		C-11	Santa Cruz Biotechnology
TGF- $\beta$ 1,2,3		1D11	R&D Systems

**Table 2.6 FACS stainings*****Antibodies combination***

CD45\*, CD8, CD4, CD39, CD3  
 CD45\*, CD8, CD4, CD73, CD3  
 CD45, Gr1, B220  
 CD45, CSF1R, F4/80, CD11c  
 CD45, CD36, F4/80, CD11c  
 CD45, MMR, F4/80, CD11c, MHCII  
 CD45, F4/80, CD39, CD11c  
 CD45, F4/80, CD73, CD11c  
 CD45\*, CD4, Foxp3, CD25  
 \*antibody used only for lung tissue

***Tissue***

Lung, spleen, lymph nodes  
 Lung, spleen, lymph nodes  
 Lung  
 Lung  
 Lung  
 Lung  
 Lung  
 Lung  
 Lung, spleen, blood, lymph nodes

## 2.5 Softwares

Alphelys-TMA Designer® (version 1.6.8)

AxioVision (version 4.8)

BD CellQuest™ Pro (version 4.0.2)

BD FACSDiva™ software (version 5.0.2)

FlowJo (version 7.6.5)

GraphPad PRISM® (version 5.01)

ImageJ (version 1.47c)

## 2.6 Mice

All mice were bred in the central animal facility of the University Hospital Essen. The origins of the parental breeding pairs are listed in **Table 2.7**. Mice were housed in individually ventilated cages (IVC) at a room temperature of 20-22 °C with a 12 hours light/dark cycle. Food and drinking water were provided *ad libitum*.

All protocols for the animal experiments were approved by the University of Duisburg-Essen animal protection board in conjunction with the Landesamt für Natur, Umwelt und Verbraucherschutz Nordrhein-Westfalen (G 1094/09). Eight-to-twelve weeks-old males and females were enrolled in the study.

### Table 2.7 Mouse strains

C57BL/6 wild type

CD73<sup>-/-</sup> (C57BL/6 background)

RAG-2<sup>-/-</sup> (C57BL/6 background)

Charles River, Sulzfeld, Germany

Thompson *et al.*, 2004

Shinkai *et al.*, 1992

## 2.7 Methods

### 2.7.1 Thorax irradiation

Mice were anesthetized with 3-5 % isoflurane in oxygen and placed in holders to assure a correct position during irradiation. The setup for the lung irradiation, including distance from the source, dose and irradiation leakage, was performed by local radiation physicists. A field of irradiation of 1.5 cm in width was adjusted to the thoracic area using a laser positioning system. Four mice simultaneously received a single 15 Gray (Gy) dose of whole thorax irradiation using a Cobalt-60 source (dose rate 0.5 Gy/min) while anesthetized with 0.8 % isoflurane. Non-irradiated parts of the body were shielded with lead blocks (**Fig 2.1**). Mice were closely monitored until fully recovered from anaesthesia and housed following standard procedures. Appropriate control groups (sham irradiated) of littermate mice, matched according to age and weight, were anesthetized under identical conditions. At selected end time points of 3, 6, 12, 24 and 30 weeks after irradiation, mice were euthanized by carbon dioxide (CO<sub>2</sub>) inhalation and blood, spleen, lymph nodes, and lung tissue were collected for further analysis (**Fig 2.1**).

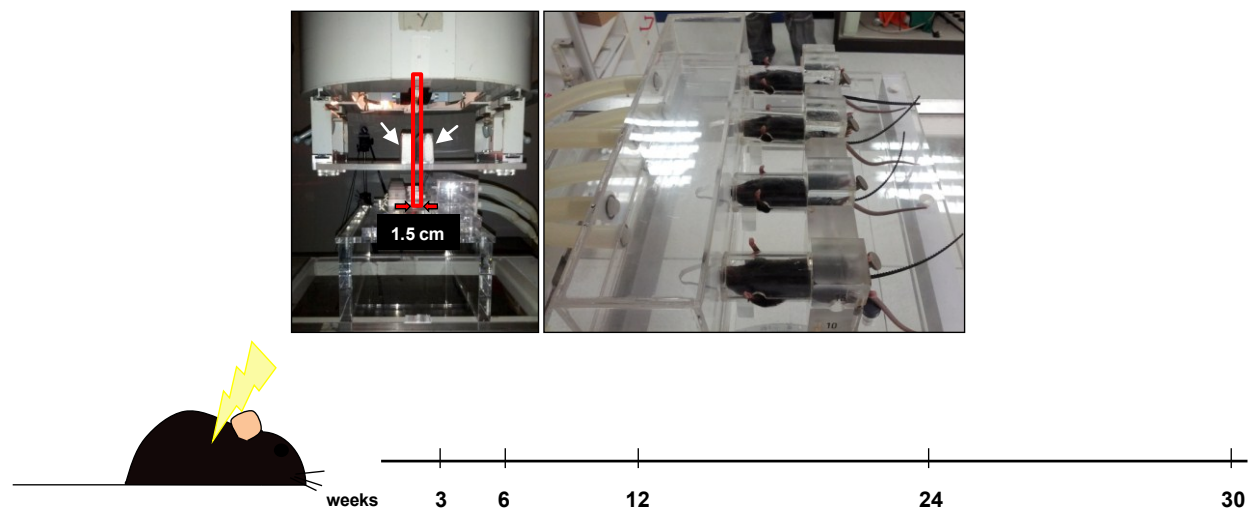


**Fig. 2.1 Mouse model of whole thorax irradiation - Experimental setup.** The cobalt-60 source is shown (upper left). The highlighted field of irradiation (in red) is defined by lead blocks (white arrows). Mice, placed in holders, receive 15 Gy whole thorax irradiation while anesthetized with isoflurane (upper right). At the indicated points (lower timeline), irradiated and sham irradiated mice are sacrificed and blood, spleen, lymph nodes and lung tissue isolated for further analyses.



### 2.7.2 Pimonidazole hydrochloride injection for determination of tissue hypoxia

For tissue hypoxia determination, pimonidazole hydrochloride solution in 0.9 % saline was administered intraperitoneally at 60 mg/kg 30 minutes (min) before euthanasia. This compound is reductively activated in hypoxic conditions and forms stable adducts with proteins, peptides and amino acids, which can be recognized by a specific antibody. At selected end time points, mice were euthanized by carbon dioxide (CO<sub>2</sub>) inhalation and lung tissue was collected for further histological analysis.

### 2.7.3 Isolation of blood cells

Mice were euthanized by CO<sub>2</sub> inhalation and, after fur disinfection, blood was immediately collected via cardiac puncture inserting a 27 Gauge needle below the xiphoid cartilage (cranial approach), or alternatively, at a perpendicular angle to sternum (perpendicular approach). Approximately 0.7-0.8 ml of blood per mouse were collected in 1.5 ml tubes. To avoid clotting, 200 µl of the collected blood were transferred in tubes containing 30 µl heparin and further processed for flow cytometric stainings.

In alternative, mice were anesthetized with isoflurane and approximately 0.1 ml of venous blood was regularly collected from the retroorbital plexus. To avoid clotting, the collected blood was transferred in tubes containing 10 µl heparin and further processed for flow cytometric stainings.

### 2.7.4 Isolation of splenocytes

Mice were euthanized with CO<sub>2</sub> inhalation and, after fur disinfection the skin was cut on the left side of the abdomen and peritoneum opened to collect the spleen. Isolated spleens were directly placed on 70 µm cell strainers in 60 mm Petri dishes and perfused with ice-cold ACK buffer (**Table 2.4**) to lyse red blood cells (RBCs). Cell suspensions were always kept on ice and then transferred in DMEM medium containing 10 % fetal calf serum (FCS) and centrifuged at 1500 rpm for 6 min at 4 °C. Complete DMEM medium was used to re-suspend cell pellets and spleen cells were counted using CASY® cell counter. From each animal, 1\*10<sup>6</sup> total spleen

cells (TSCs) was plated in a 96 U-well plate and processed for flow cytometric staining. In alternative, TSCs from untreated mice were used for CD4<sup>+</sup> T cell isolation.

### **2.7.5 CD4<sup>+</sup> T cell isolation, autoMACS® depletion and adoptive transfer**

Spleens isolated from healthy and untreated C57BL/6 wild type mice were used for isolation of CD4<sup>+</sup> T lymphocytes, taking advantage of the CD4<sup>+</sup> T Cell Isolation Kit, following manufacturer instructions. In brief, the splenocyte suspension was incubated with a cocktail of biotin-conjugated monoclonal antibodies, directed to all leukocytes, but CD4<sup>+</sup> T cells. Anti-biotin monoclonal antibodies conjugated to magnetic micro beads were then added to the cell suspension. In the next step, the autoMACS® separator was used to retain labelled cells in the MACS® columns magnetic field. The cell suspension was depleted of all non-CD4<sup>+</sup> T cells and unlabelled CD4<sup>+</sup> T cells were purified through this process of negative selection. Freshly purified cells were evaluated for purity and injected ( $5 \times 10^6$  cells/mouse) in the tail vein of RAG-2<sup>-/-</sup> mice 1 day after receiving irradiation.

### **2.7.6 Isolation of lymph node cells**

Euthanized mice were restrained on their back on the operating board. A sagittal cut was performed from the lower abdomen to the salivary gland and cervical lymph nodes were collected in complete medium in 60 mm Petri dishes and placed on ice; in some experiments all lymph nodes from the same treatment group were pooled. Lymph node cells were released in the medium disrupting the connective tissue capsule with the help of 23 Gauge needles and collected in 15 ml tubes, then centrifuged at 1500 rpm for 6 min at 4 °C and counted using CASY® cell counter. From each animal,  $1 \times 10^6$  lymph node cells (LNCs) per antibodies staining was plated in a 96 U-well plate.

### 2.7.7 Isolation of lung cells

Euthanized and restrained mice were dissected as mentioned before and peritoneum was cut to expose the thoracic cavity. After carefully cutting diaphragm and the excision of the rib cage, lungs were isolated and minced into small pieces on microscope glass slides using sterile surgical blades and then collected in a 2 mg/ml collagenase solution in Hank's balanced salt solution (HBSS) on ice. Enzymatic digestion of the tissue was performed in a water bath at 37 °C for 45 min and the reaction was stopped by adding ethylenediaminetetraacetic acid (EDTA) to a final concentration of 5 mM. The digested tissue was then mashed through a 70 µm cell strainer and, to reduce cell loss, the cell strainer was washed with phosphate buffered saline (PBS). After centrifugation of lung cells for 10 min at 1200 rpm, lysis of erythrocytes was obtained incubating the cell pellets with 2 ml of ice-cold ACK buffer for 1-2 min and stopped by adding PBS. Lung cell suspensions were centrifuged again for 10 min at 1200 rpm and cells re-suspended in fluorescence-activated cell sorting (FACS) buffer (**Table 2.4**), passed through a 30 or 50 µm cell strainer to remove residual debris aggregates and counted using CASY® cell counter.

From each animal,  $0.5 \times 10^6$  or  $1 \times 10^6$  total lung cells (TLCs) were plated in a 96 U-well plate and flow cytometric staining was performed.

### 2.7.8 Flow cytometry

Flow cytometry is a widely used method applied in medical and biological research. Generally, the use of flow cytometry allows to measure physical or chemical properties of single cells or particles. Briefly, cell suspensions are conveyed as single cell stream through beams of light. Scattered light or fluorescence emission, if cells have been labelled with fluorochromes, are collected through a system of optical filters and detectors, processed and returned as electrical signals that can be graphically plotted.

For flow cytometry staining,  $0.5 \times 10^6$  or  $1 \times 10^6$  isolated cells from the mentioned tissues were plated in a 96 U-well plate and centrifuged at 1200 rpm for 10 minutes at 4 °C. Supernatant was removed and cell pellets were loosened on a plate shaker; cells were then re-suspended in 100 µl FACS buffer containing the appropriate dilutions of the desired antibodies (**Table 2.6**) and incubated for 12 minutes at 4 °C in the dark. In case of TLCs, the staining step was performed adding 50 µl of the antibody solutions on cells that were pre-incubated for at least

15 min on ice with 50  $\mu$ l FACS buffer containing fragment crystallizable receptor (FcR) block (**Table 2.4**). Following a washing step with FACS buffer, cells were centrifuged and loosened as mentioned before, re-suspended in 100-150  $\mu$ l FACS buffer and transferred in 1.3 ml tubes. Alternatively, when cells could not be analyzed immediately, all probes were fixed in 1 % paraformaldehyde (PFA) solution in PBS and stored at 4 °C until measurement.

Intracellular staining for forkhead box p3 (Foxp3) was performed using Mouse Regulatory T Cell Staining Kit according to manufacturer's instructions. Briefly, after surface staining, cells were washed with FACS buffer, centrifuged, loosened after supernatant removal and incubated for at least 30 min with 100  $\mu$ l of the fixation/permeabilization working solution at 4 °C in the dark. Cells were then washed one time with 1X permeabilization buffer, centrifuged and loosened on a plate shaker. Incubation with anti-Foxp3 antibody or isotype control was performed in 1X permeabilization buffer for 30 min in the dark at 4 °C. Staining was then rinsed using FACS buffer and the plate centrifuged, supernatant discarded and cells loosened, resuspended in 100-150  $\mu$ l FACS buffer and transferred in tubes for flow cytometric measurement.

Staining data from TSCs and LNCs probes were acquired using a BD FACSCalibur™ flow cytometer and analysed using BD CellQuest™ Pro. Total lung cell probes were measured in a BD LSRFortessa™ or, alternatively, in a BD LSRII™ analyzer and staining data analysed with BD FACSDiva™ and FlowJo softwares.

### **2.7.9 Isolation and preparation of lung tissue for paraffin sections and cryosections**

Euthanized and restrained mice were dissected as mentioned before and peritoneum was opened to expose the thoracic cavity. The inferior vena cava was cut and the hearth perfused through the right ventricle with 2-4 ml of sterile PBS to remove any residual blood from the pulmonary vasculature. Next, using a 21 Gauge needle lungs were intratracheally inflated with 4 % (wt/vol) PFA in PBS, pH 7.2, placed in embedding cassettes and then fixed overnight in the same solution. Alternatively, for the inflation a 1:1 mixture of pre-warmed Tissue-Tek® O.C.T.™ Compound and PBS was used and lungs placed in O.C.T. embedding medium, pre-cooled on dry ice and stored at -80 °C.

For hematoxylin and eosin (H&E) staining, Masson's trichrome staining and immunohistochemistry, after dehydration in 70 % ethanol, PFA-fixed lungs were processed using automated standard procedures and subsequently embedded in paraffin. Five  $\mu$ m tissue

sections obtained with a Leica microtome were mounted on coated microscope slides. Seven  $\mu\text{m}$  cryosections mounted on superfrost Plus microscope slides were obtained using a Leica cryostat.

#### 2.7.10 Tissue microarray

The generation of tissue microarrays (TMAs) allows the analysis of numerous samples of tissue on a single slide. Tissue microarrays were built from 48 paraffin embedded lung tissues isolated from C57BL/6 wild type (22) and CD73<sup>-/-</sup> mice (26). In details, areas of interest were identified on H&E stained slides, and from each lung tissue paraffin block (donor block) two tissue cores were punched out using a needle 1 mm in diameter. The tissue cylinders were then placed into the recipient TMA paraffin block using MTA Booster<sup>TM</sup> OI manual tissue arrayer. The distribution and position of the cores were determined in advance with the TMA Designer<sup>TM</sup> software. Cores of C57BL/6 wild type and CD73<sup>-/-</sup> mice were incorporated in two different tissue array blocks. Five  $\mu\text{m}$  tissue sections obtained with a Leica microtome were mounted on coated microscope slides.

#### 2.7.11 Hematoxylin and eosin staining of lung sections

The most commonly used staining system in histology is the hematoxylin and eosin stain (H&E). The combination of these two dyes allows the easy identification of tissue structures and cells on histological sections. Hematein, the oxidative product of hematoxylin, is a natural dye and stains cell nuclei purplish blue; eosin is an acidic dye that stains cell cytoplasm proteins and connective tissue fibers in different shades of pink and red.

H&E staining on lung paraffin sections or cryosections was performed as follows. Lung slices (only paraffin sections) were deparaffinized by incubation at 65 °C over night and two additional incubation steps of 5 min in xylene. Rehydration of lung sections was obtained via 5 min incubations in graded ethanol solutions (100 %, 90 % and 70 % EtOH in bidest water) and bidest water (paraffin and cryosections). To assess morphological alterations, the slides were then stained in Mayer's hematoxylin for 5 minutes and rinsed in running tap water for 5-10 min. After 3 min incubation in 0.5 % eosin G in water, the slides were rinsed with bidest

water and subsequently dehydrated in graded ethanol solutions (70 %, 90 % and 100 % EtOH in bidest water) and xylene. Glass cover slips were mounted using ROTH mounting medium. Light microscopy pictures were obtained using a Leica DMIRB microscope equipped with a Zeiss AxioCam HRc color camera and Axiovision software.

Quantitative analysis of fibrotic areas in irradiated mice was performed on pictures of whole lung sections using ImageJ software. For each mouse, at least 3 different slides with a minimum distance of 250  $\mu\text{m}$  in depth were analysed.

### **2.7.12 Masson's trichrome staining of lung sections**

The trichrome stain is used to selectively identify connective tissue, muscle and collagen fibers in tissue sections, therefore is widely adopted to observe histological changes in all diseases characterized by alterations of the amount of collagen, such as fibrosis. Typically, the molecular size of the employed acid dyes differs and determines the selectivity of the tissue structures stained. For Masson's trichrome staining, all staining solutions were obtained from the Masson-Goldner-Trichrome staining kit from ROTH. After tissue deparaffination and rehydration, lung slides were stained for 5 min in a 1:1 solution of Weigert's hematoxylin components A and B, and subsequently rinsed under running tap water for 5-10 min. The slides were then stained with the solutions Goldner I (ponceau - acid fuchsin), Goldner II (phosphotungstic acid - orange G) and Goldner III (light green SF), alternating the staining steps with 30 seconds washes in 1 % acetic acid solution in ddH<sub>2</sub>O to remove the stain in excess. The incubation time in the mentioned staining solutions was always adjusted proportionately to the intensity of the staining. After the standard dehydration procedure, glass cover slips were mounted using ROTH mounting medium. Nuclei are visible in violet-black colour, cytoplasm and muscles in red, erythrocytes in orange, and connective tissue, including collagen, in green colour.

### **2.7.13 Immunohistochemistry on lung sections**

Generally, the binding of an antibody to its specific epitope is a widely used reaction in many laboratory techniques, and immunohistochemistry is one of those. The specificity of this

reaction helps to localize and discriminate cells or tissues of interest on histological sections; this is achieved by the use of antibodies directly labelled or, more commonly, by the use of a secondary labelling method.

Lung slides were prepared according to the instructions given in the H&E staining paragraph. After rehydration, antigen retrieval was performed incubating the tissue sections in 10 mM citrate buffer pH 6.0 in a water bath at 98 °C for 15 min. The slides were then left to cool down at room temperature for 20 min. Next, two washing steps of 5 min were carried out in bidest water and Tris-buffered saline (TBS), followed by a 45 min incubation in 5 % bovine serum albumin (BSA) blocking solution in TBS. The tissue sections were then circled with a hydrophobic barrier pen and incubated over night at 4 °C in a moisture chamber with the appropriate dilution in 1.5 % BSA/TBS of the antibody of interest (**Table 2.5**). To detect antibodies binding, the alkaline phosphatase-anti-alkaline phosphatase (APAAP) or 3,3'-diaminobenzidine (DAB) detection methods were chosen. For each staining, control slides were incubated with isotype control, with no primary antibodies or with only secondary antibodies. Counterstain was obtained with 5 min incubation in Mayer's hematoxylin. Glass cover slips were mounted using fluorescent mounting medium.

A minimum of 5 pictures per lung section was evaluated to obtain a quantitative analysis of positively stained areas using ImageJ software.

#### **2.7.14 Immunofluorescence on lung sections**

Immunofluorescent techniques are based on the same principle described in the previous paragraph. In immunofluorescence, the localization of an antibody bound to its specific antigen is recognized by the use of a fluorochrome. Five µm sections from lung tissue microarrays were deparaffinized according to the instructions given in par. **2.7.11** and antigen retrieval was performed as mentioned in par. **2.7.13**. Tissue sections were then circled with a hydrophobic barrier pen and permeabilized for 5 min with 0.1 % Triton in PBS. Next, the slides were rinsed 3 times with PBS for 1 min and quenched with 50 mM ammonium chloride in PBS for 15 min. A second round of washing steps in PBS was performed and unspecific binding sites were blocked for 1 hour in a 2 % normal goat serum (NGS) solution in PBS. Subsequently, the blocking solution was removed and the slides were incubated over night at 4 °C in a moisture chamber with the appropriate dilution in 2 % NGS/PBS of the antibodies of interest (**Table 2.5**). The antibody solution was then removed and 3 rinsing steps in PBS for 3 min were

performed. Incubation of lung sections in 2 % BSA/PBS containing the appropriate secondary antibodies, labelled with cyanine dyes Cy2 or Cy3, was carried out at room temperature for 1 h and 30 min. Slides were then washed 3 times for 3 min in PBS and cell nuclei stained for 15 min with Hoechst (1:1000 in PBS) in the dark. At last, slides were rinsed in PBS (3 times for 3 min) and mounted with fluorescent mounting medium.

Lung slides were imaged using an inverted Zeiss Cell Observer fluorescence microscope equipped with the respective filter sets, an apotome and an AxioCam MRm. Overlay was performed with AxioVision software.

Quantification of positively stained macrophages was performed on at least 4 pictures per mouse and a minimum number of 2 mice per condition.

#### **2.7.15 Semithin sections and electron microscopy samples**

Lung tissue samples used to obtain semi thin sections and analysed in electron microscopic studies were provided by Dr Eldh (University Hospital Tübingen). Mice in this case received a single dose irradiation of 15 Gy on the right hemithorax. The samples were kindly processed and prepared in the Institute of Anatomy at the University Hospital Essen (Dr Jastrow). In brief, 0.5 µm semithin sections were cut on a Reichert-Jung Ultracut-E. After drying at 90 °C, rinsed sections were stained with toluidine blue 1 %, methylene blue 1 %, and Azur-II 1 % solution in water (pH 8.0) plus 1 % sodium tetraborate. Preparation of electron microscopy samples was realized as follows. Glutaraldehyde fixed tissue contrasted with osmium tetroxide (OsO<sub>4</sub>), uranylacetate and lead citrate was investigated on a Zeiss EM902 transmission electron microscope. Images were acquired on a MegaViewII slow-scan-CCD camera using ITEM 5.0 software.

#### **2.7.16 Statistical analysis**

Results were analysed and graphically represented using Graph Pad Prism software. If not otherwise stated, data are presented as mean values ± standard deviation (SD). Statistical differences were assessed using unpaired t-test or two-way analysis of variances (ANOVA),



with p values  $\leq 0.05$  considered as significant. P values of survival curves were calculated by the log-rank (Mantel-Cox) test.

## 3 Results

### 3.1 Importance of adenosinergic signalling pathway for radiation-induced fibrosis

As mentioned in the introduction, pneumonitis and lung fibrosis still represent dose limiting side effects in cancer patients undergoing radiation therapy. The importance of CD73 and adenosine in many lung injuries has been broadly investigated and chronic elevation of adenosine levels within the lung tissue has been shown to be directly correlated to the inflammatory insult and fibrosis development (Blackburn et al., 2000); moreover, many studies describe the importance of the adenosinergic pathway in mouse models of lung fibrosis (Blackburn et al., 2000; Chunn et al., 2005; Volmer et al., 2006). However, the role of CD73 and adenosine in radiation-induced pneumonitis and fibrosis has not been investigated so far. C57BL/6 mice are sensitive to radiation and, after an initial pneumonitic phase at 6-16 weeks post irradiation (p.i.), they develop lung fibrosis (5-6 months p.i.). The experimental design to investigate radiation-induced pneumopathy was adapted from previous studies (Chiang et al., 2005; Heinzelmann et al., 2006). In order to determine the contribution of CD73 to the development of pulmonary inflammation and fibrosis, C57BL/6 wild type mice (WT) and CD73 deficient mice (CD73<sup>-/-</sup>) mice received 15 Gray (Gy) whole thorax irradiation, whereas sham irradiated animals were treated with isoflurane anaesthesia only (control mice).

#### 3.1.1 Radiation-induced changes in body weight and survival

Subsequent to whole thorax irradiation and throughout the 30 weeks of study, the body weight of control and treated C57BL/6 wild type (WT) and CD73<sup>-/-</sup> mice was monitored every week, as changes in weight are ordinarily associated to the general health condition of mice. In **Fig. 3.1 A** body weight changes are shown for each group as average of delta ( $\Delta$ ) values calculated for each mouse subtracting the respective weight measured at the beginning of the experiment. Up to week 8,  $\Delta$  values from all groups had approximately similar increase. While control mice and irradiated CD73<sup>-/-</sup> mice continuously gained in weight, irradiated WT mice had a slower increase in body weight reaching the maximum at week 22,

corresponding to a  $\Delta$  value of  $3.2 \pm 1.6$  grams (g). Thereafter this group of mice showed a slow reduction in body weight ending at a  $\Delta$  value of  $1.9 \pm 1.6$  g at 30 weeks. On the contrary, irradiated  $CD73^{-/-}$  mice showed a similar gain in weight as respective controls, with a final  $\Delta$  value of  $4.5 \pm 2.7$  g. Differences in  $\Delta$  weight were highly significant when comparing irradiated WT mice to respective controls, as well as to irradiated  $CD73^{-/-}$  mice.

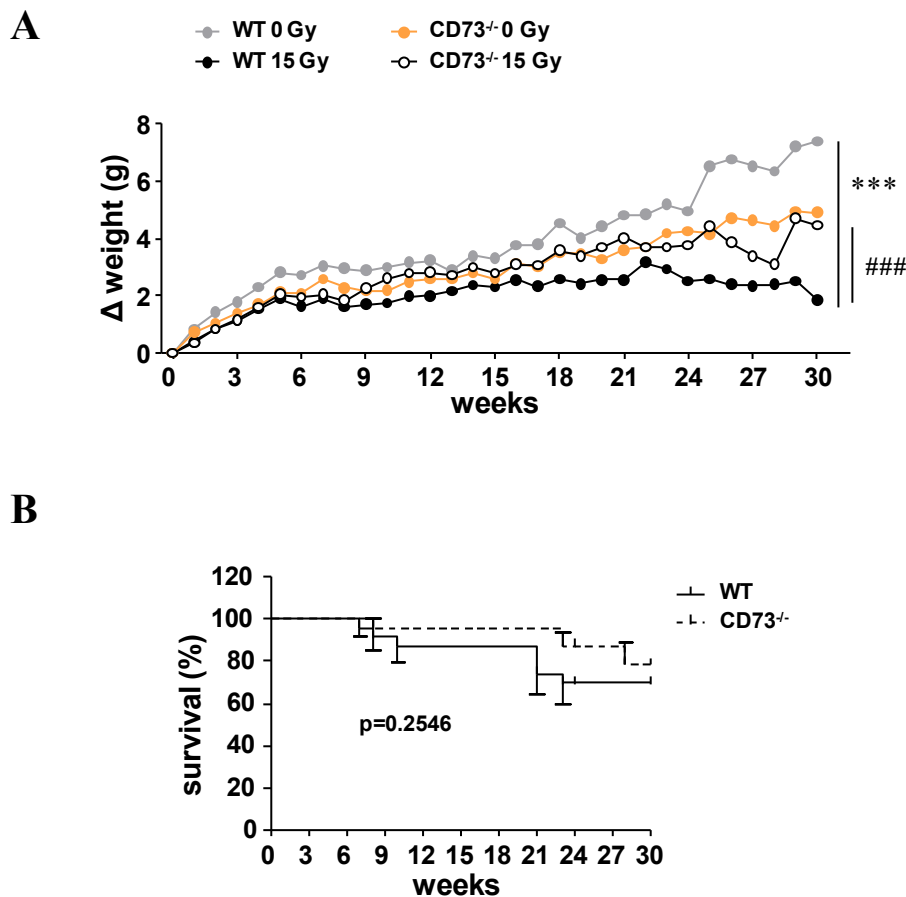


**Fig. 3.1 Changes in body weight and survival in C57BL/6 wild type and  $CD73^{-/-}$  mice.** Weights and survival of C57BL/6 wild type (WT) and  $CD73^{-/-}$  mice were monitored over time after 15 Gy whole thorax irradiation or sham irradiation (anaesthesia only). **A)** Changes in body weight are represented as mean delta values ( $\Delta$  weight = weight at day X – weight at day 0). Significant differences were calculated using two-way ANOVA test (\*\*\*,###  $p \leq 0.001$ ). **B)** Kaplan-Meier survival curves showing survival in percentage of irradiated WT ( $n=23$ ) and  $CD73^{-/-}$  mice ( $n=23$ ) at indicated time points. The shown  $p$  value was calculated by the log-rank (Mantel-Cox) test.

Some of the mice receiving irradiation did not survive until week 30, the chosen end time point of the study. Survival rates of irradiated WT and  $CD73^{-/-}$  mice are shown in the

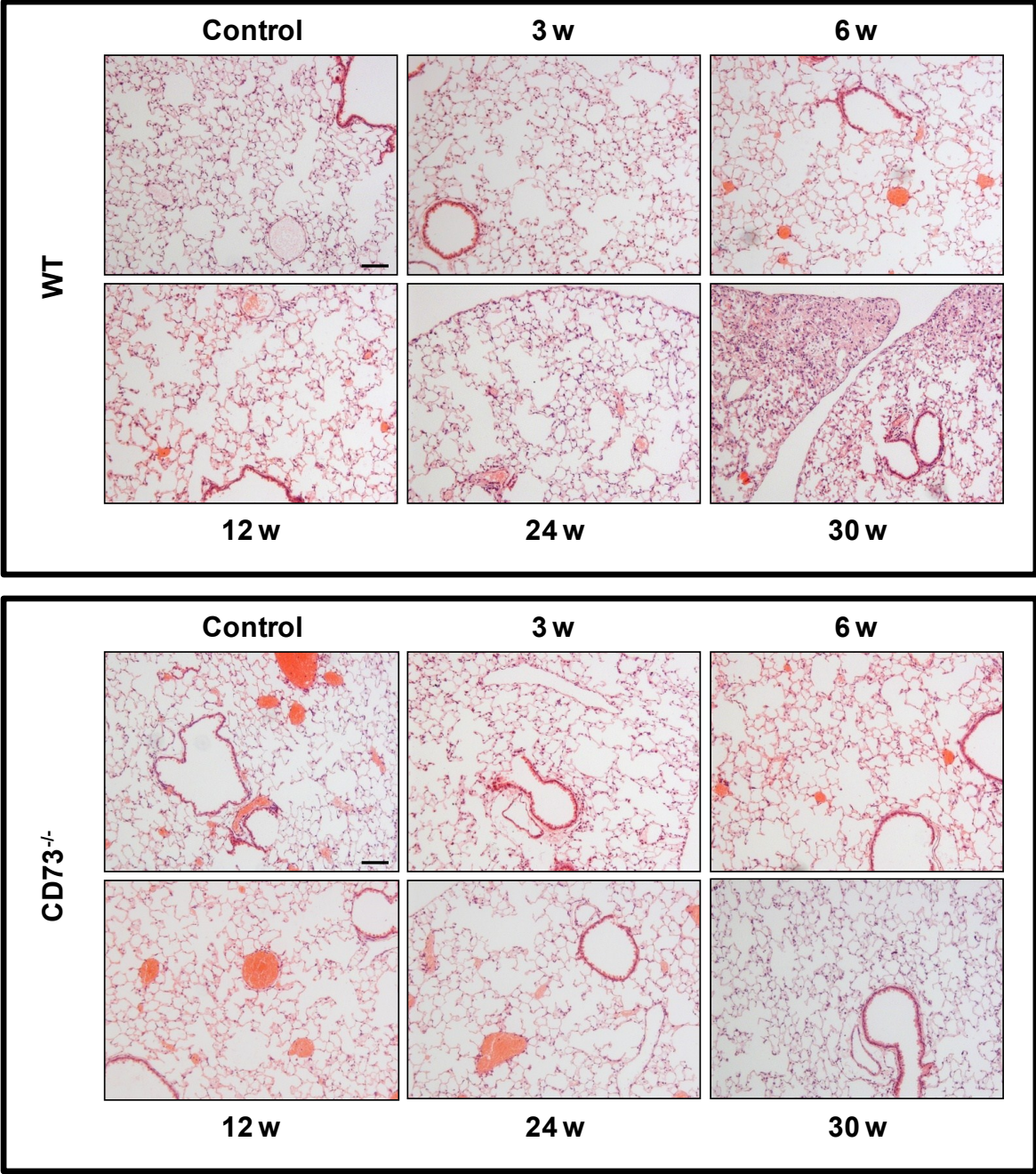
Kaplan–Meier survival curve of **Fig. 3.1 B**. Few irradiated mice died in the first 10 weeks p.i., with calculated survival rates at this time point of  $87.7 \pm 7 \%$  and  $95.6 \pm 4.2 \%$ , respectively in WT and CD73<sup>-/-</sup> mice. A second critical phase started at week 21 for WT mice and at week 23 for CD73<sup>-/-</sup> irradiated mice. By the end of the experiment survival percentages decreased to  $69.6 \pm 9.6 \%$  in irradiated WT mice and to  $78.3 \pm 10.4 \%$  in irradiated CD73<sup>-/-</sup> mice. Log-rank test analysis showed no significant difference in the survival curves between the two groups.

The significantly higher increase in  $\Delta$  weight and the slightly better survival of CD73<sup>-/-</sup> mice in comparison with irradiated WT mice suggest a distinct response of the two strains to irradiation. Therefore, in the next step lung tissue was isolated in order to assess local radiation-induced changes.

### **3.1.2 Histological changes of lung tissue in irradiated C57BL/6 wild type and CD73<sup>-/-</sup> mice**

To estimate radiation-induced tissue damage, lungs were isolated from the different groups at the time points of 3, 6, 12, 24 and 30 weeks p.i. and were processed for histological staining. In figure **Fig. 3.2 A**, representative pictures of hematoxylin and eosin (H&E) staining of lung sections from C57BL/6 wild type (WT; upper panel) and CD73<sup>-/-</sup> mice (lower panel) are shown. No marked sign of inflammation, neither a marked alteration of lung architecture were noticed in both strains during the early response to irradiation (up to week 12). At later time points, fibrotic foci formation was clearly detected at 30 weeks p.i. in WT mice, whereas mostly no fibrosis was appreciable in CD73<sup>-/-</sup> mice. Collagen deposition was also monitored over time using Masson's trichrome staining of lung sections, as shown in **Fig. 3.2 B** (upper panel: WT mice; lower panel: CD73<sup>-/-</sup> mice). Similar to the H&E staining, no obvious changes were detectable in WT and CD73<sup>-/-</sup> mice during the early phase p.i.. In contrast, enhanced collagen production associated with fibrotic areas was observed in the irradiated WT group.

A





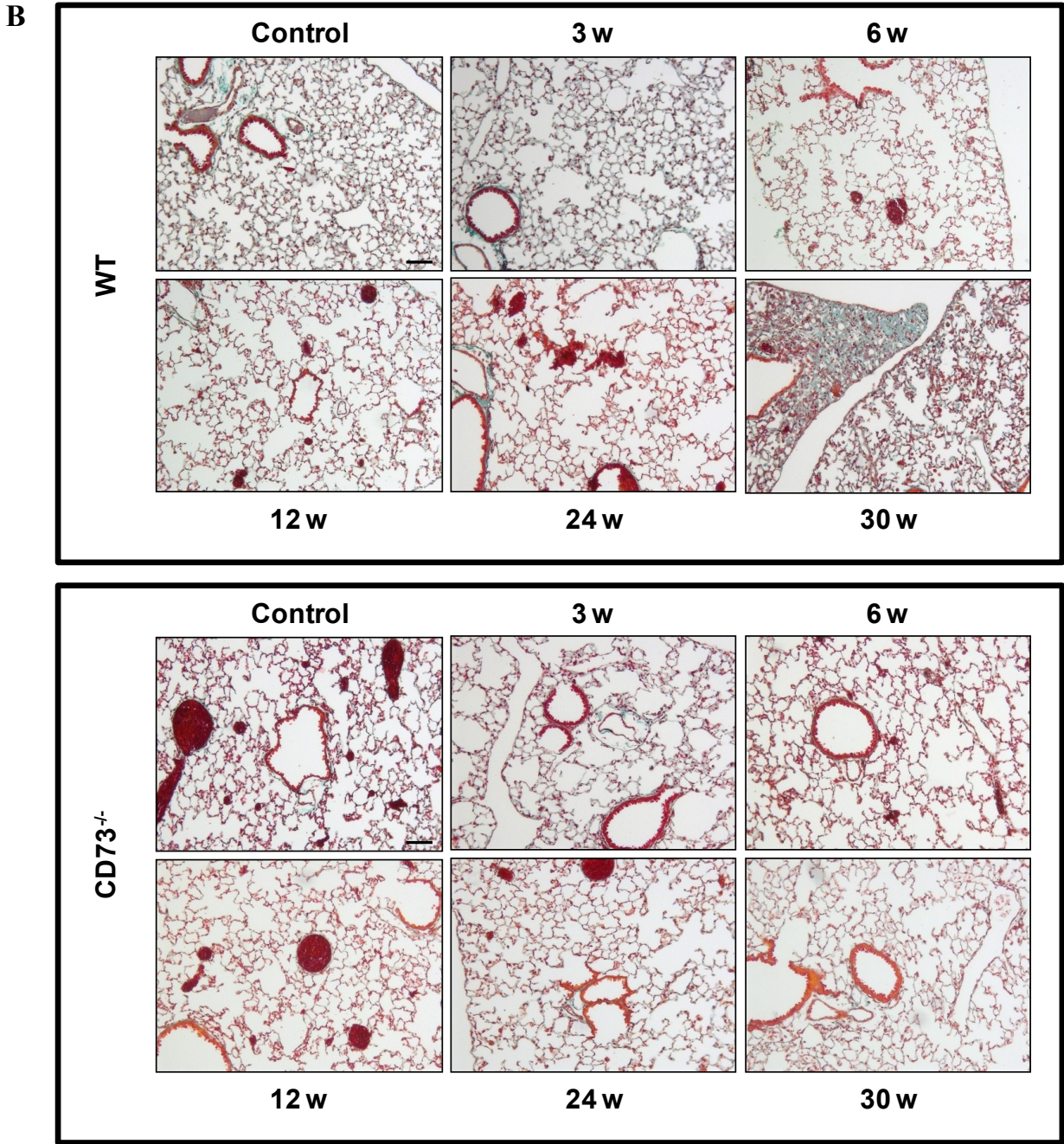


**Fig. 3.2 Lung histological changes in C57BL/6 wild type and CD73<sup>-/-</sup> mice.** Lung tissues were obtained 3, 6, 12, 24 and 30 weeks (w) after whole thorax irradiation with 15 Gy or 0 Gy and prepared for histological analysis. **A)** Representative light microscopy pictures of H&E stained lung sections (5 μm) from C57BL/6 wild type (WT - upper panel) and CD73<sup>-/-</sup> mice (lower panel) at all time points investigated (magnification x100; scale bars: 100 μm). **B)** Representative light microscopy pictures of Masson-Goldner trichrome stained lung sections from WT (upper panel) and CD73<sup>-/-</sup> mice (lower panel) investigated at indicated time points (magnification x100; scale bar: 100 μm).

In order to determine the degree of pulmonary fibrosis at 30 weeks p.i. in irradiated WT and CD73<sup>-/-</sup> mice, at least 2 additional tissue sections per animal were collected in a distal area of the lung (>250  $\mu$ m distance in depth), and the extent of fibrosis was quantified. At this purpose, the percentage of fibrotic areas and the number of fibrotic foci per mouse were calculated in both strains and compared. More than 60 % percent of WT animals deriving from 2 independent experiments showed fibrosis at 30 weeks (data not shown), with an average of  $5.1 \pm 5.7$  % of fibrotic areas (median value equivalent to 4 %), whereas only 50 % of CD73<sup>-/-</sup> mice showed minimal fibrosis development with less than 2 % of fibrotic tissue (median value equivalent to 0,7 %) (**Fig. 3.3 A**). The number of fibrotic foci in WT mice was more than 2-folds higher than in CD73<sup>-/-</sup> mice, with an average of  $7.2 \pm 7.0$  and  $2.3 \pm 3.8$  respectively. The scatter dot plot in **Fig. 3.3 B** shows the median values of fibrotic foci per lung, corresponding to 7 in WT mice and 0.8 in CD73<sup>-/-</sup> mice. Although a clear trend to increased fibrosis in irradiated C57BL/6 wild type as compared to CD73<sup>-/-</sup> mice was observed, the obtained values were not statistically different.

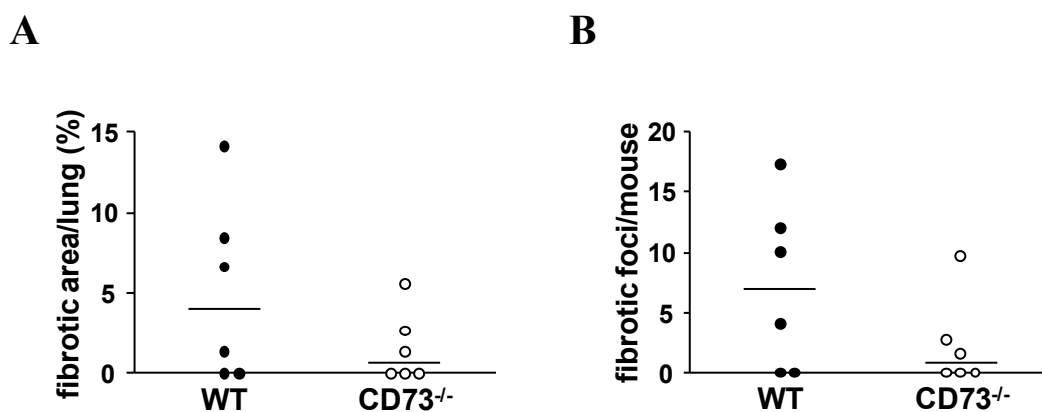


**Fig. 3.3 Quantitative analysis of fibrosis in C57BL/6 wild type and CD73<sup>-/-</sup> mice.** Lung sections were obtained from C57BL/6 wild type (WT) and CD73<sup>-/-</sup> mice 30 weeks after 15 Gy whole thorax irradiation, stained with H&E and analysed for the amount of fibrosis and the number of fibrotic foci. **A)** Quantification of fibrosis extent in mice 30 weeks p.i. expressed as percentage of lung area showing fibrosis. **B)** Quantification of fibrotic foci in mice 30 weeks p.i. Data represent median values obtained in  $\geq 3$  sections per mouse.

Several acute and chronic pulmonary disorders are characterized by a decreased lung tissue oxygenation. The progressive thickening of the alveolar septa leads to breathing difficulties,

disturbance of local blood supply, and eventually to the development of severe alveolar hypoxia (Tuder et al., 2007). To examine whether radiation-induced lung damage is also associated with tissue hypoxia, control and irradiated mice were intraperitoneally injected with a hypoxia-sensitive prodrug, pimonidazole hydrochloride, 30 min before euthanasia. Paraffin embedded lung sections of WT and CD73<sup>-/-</sup> mice from the different time points were subjected to immunohistochemical staining using a monoclonal antibody (MAb1) recognizing the hypoxia-related adducts mentioned above. **Fig. 3.4 A** shows the quantification of tissue hypoxia over time in irradiated and control WT and CD73<sup>-/-</sup> mice. Irradiated WT mice showed increasing hypoxia already 6 weeks p.i., reaching a first maximum at 12 weeks p.i.. Of note, a second increase in tissue hypoxia was observed from week 24 to week 30 in these mice, which displayed diffuse hypoxia mainly in the fibrotic areas (**Fig. 3.4 B**). In contrast, irradiated CD73<sup>-/-</sup> mice failed to develop significant tissue hypoxia neither during the early pneumonitic phase, nor during the late fibrotic phase (**Fig. 3.4 A**). Only minor hypoxic areas were detected in CD73<sup>-/-</sup> mice at 24 weeks p.i., primarily in peribronchial regions and single cells (**Fig. 3.4 B**). Thus, after whole lung irradiation CD73<sup>-/-</sup> mice presented a delayed onset and a lower level of tissue hypoxia compared to WT mice. At all time points, C57BL/6 wild type and CD73<sup>-/-</sup> sham irradiated mice showed no or rare positivity of single cells or tissue.

During the process of fibrogenesis, the enhanced synthesis of extracellular matrix is mainly attributed to the presence of myofibroblasts, activated fibroblasts producing collagen and other extracellular matrix proteins. Myofibroblasts overexpress  $\alpha$ -smooth muscle actin ( $\alpha$ -SMA), the primary stress fiber component involved in their strong contractile force (Hinz et al., 2007). TGF- $\beta$ 1 is a key regulator of ECM and has been shown to play a key role in fibrotic diseases. In pulmonary fibrosis, this cytokine contributes to myofibroblast differentiation and proliferation and is thought to be mainly produced by alveolar macrophages (Wynn, 2008). To corroborate the development of fibrosis, the presence of  $\alpha$ -SMA and TGF- $\beta$  was histologically evaluated in tissue microarrays generated from paraffin-embedded tissue blocks of control and irradiated WT and CD73<sup>-/-</sup> mice.



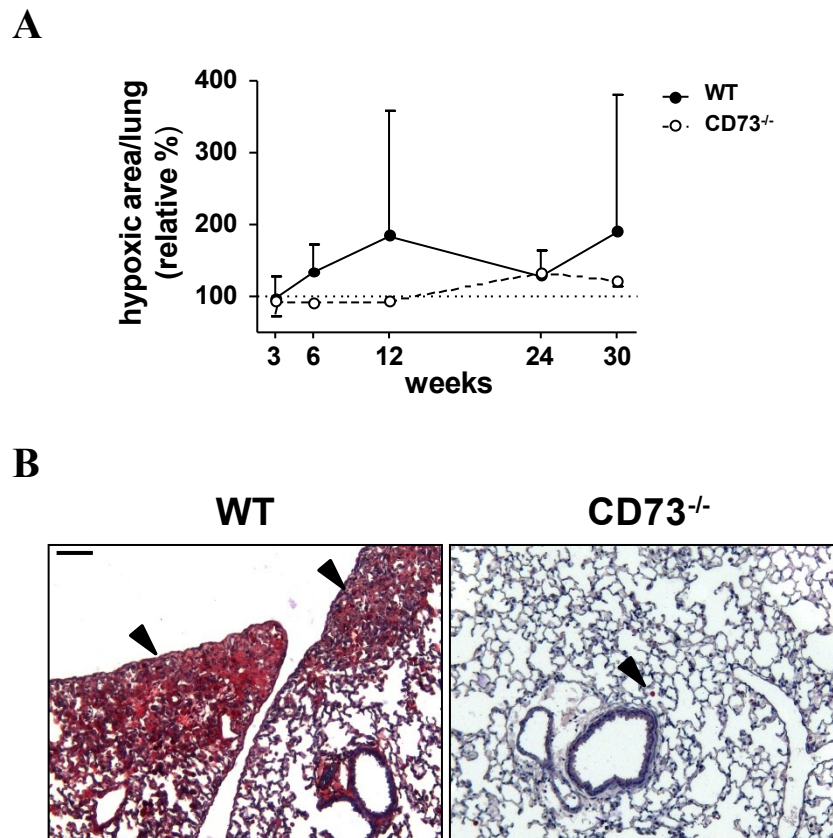


**Fig. 3.4 Quantitative analysis of hypoxic areas in C57BL/6 wild type and CD73<sup>-/-</sup> mice.** Irradiated and control C57BL/6 wild type (WT) and CD73<sup>-/-</sup> mice were injected with pimonidazole hydrochloride 30 min before sacrifice. Lung sections were obtained from tissue isolated after 3, 6, 12, 24 and 30 weeks and immunostained with the antibody reagent MAb1, which specifically recognizes hypoxic-related adducts. Quantification of positive staining was performed using ImageJ. **A)** Data represent relative mean values  $\pm$  SD compared to respective sham irradiated mice. At least 5 pictures per mouse were evaluated for positive staining ( $\geq 2$  mice per group). **B)** Representative light microscopy pictures of immunohistochemical staining for hypoxia of lung sections at 30 weeks p.i.. Positive staining is indicated (black arrows) (magnification x100; scale bar: 100  $\mu$ m).

As expected from previous results and in relation to fibrosis development, irradiated C57BL/6 wild type mice displayed a greater tissue positivity for both fibrotic markers at 30 weeks when compared to CD73 deficient mice (**Fig. 3.5 A**). Intriguingly, lung macrophages at this time point were highly positive for  $\alpha$ -SMA and TGF- $\beta$  in WT mice (**Fig. 3.5 B**). No significant alterations were observed in control and irradiated mice at earlier time points, when  $\alpha$ -SMA showed normal distribution surrounding blood vessels and bronchial airways, and no or weak staining for TGF- $\beta$  was noted (**Fig. 3.5 A** and data not shown).

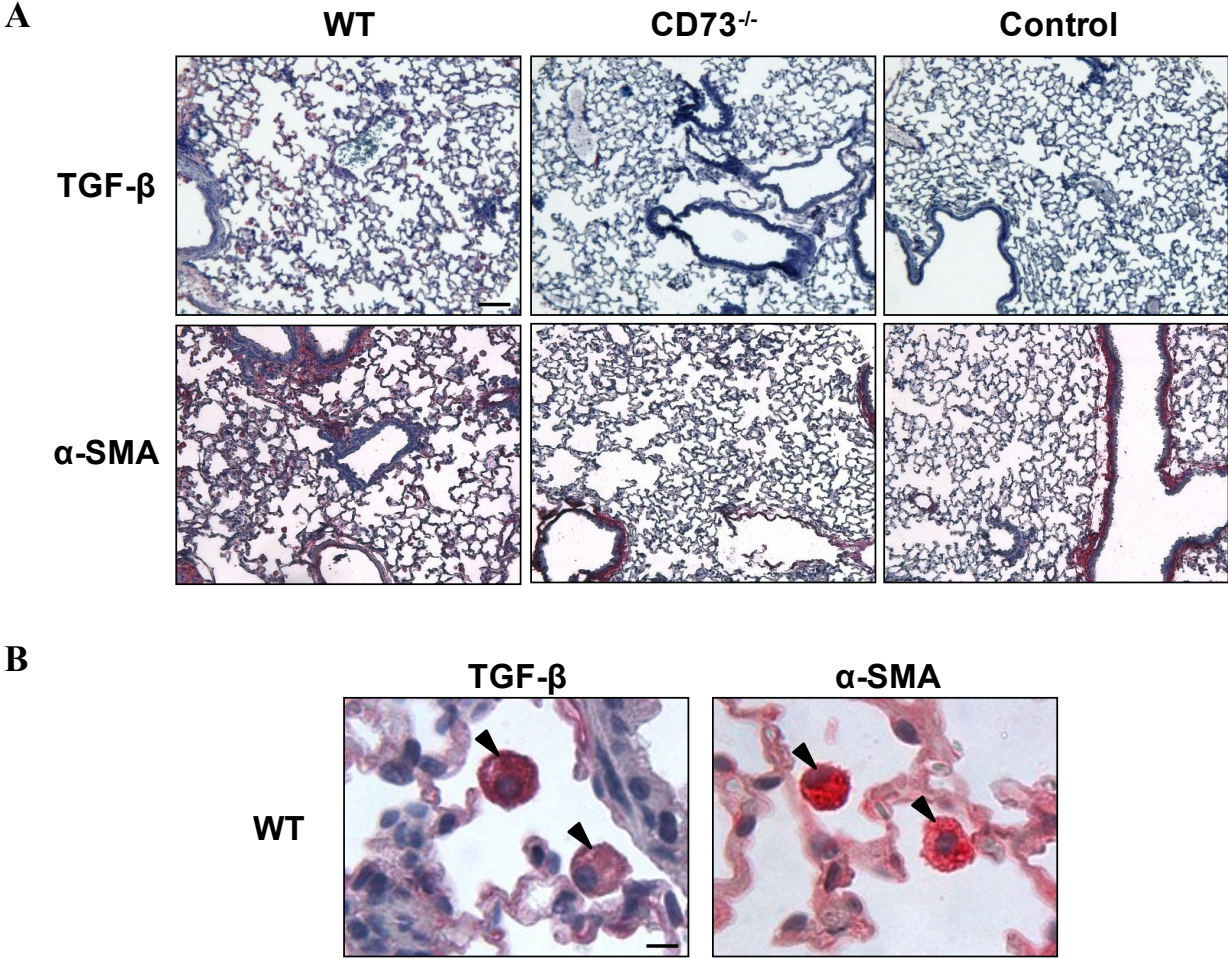


**Fig. 3.5 Immunohistochemical staining of TGF-β and α-SMA in lung sections.** Lungs isolated at 3, 6, 12, 24 and 30 weeks from irradiated and control C57BL/6 wild type (WT) and CD73<sup>-/-</sup> mice were embedded in paraffin and used for the generation of tissue microarrays. Sections of tissue microarrays were immunostained with monoclonal antibodies specific for TGF-β or α-SMA. **A)** Representative light microscopy pictures of immunohistochemical staining for TGF-β and α-SMA of lung tissues at week 30 p.i. (magnification x100; scale bar: 100 μm). **B)** Representative light microscopy pictures of positively stained macrophages (black arrows) in WT mice at 30 weeks p.i. (magnification x1000; scale bar: 10 μm).

### 3.1.3 Cellular changes of lung tissues in irradiated C57BL/6 wild type and CD73<sup>-/-</sup> mice

As mentioned in the introduction (par. 1.1), not all the fibrotic processes develop as a consequence of inflammation and it is still matter of debate whether radiation pneumonitis and fibrosis should be seen as a continuum.

Data from histological and immunohistochemical analyses suggested distinct tissue responses of irradiated C57BL/6 wild type and CD73<sup>-/-</sup> mice to IR and, above all, a noteworthy difference in fibrosis development related to endogenous expression of CD73. The CD73/adenosine system plays an important physiological role in the maintenance of lung homeostasis and therefore has been implicated in several airways disorders such as lung fibrosis, but is also a key regulator of many inflammatory processes (Cronstein, 1994; Spicuzza et al., 2006). In order to analyse whether loss of CD73 would alter radiation-induced lung inflammation and/or immune cell functions thereby decreasing radiation-induced late lung injury, the effects of whole thorax irradiation on immune cell infiltration were followed over time. Lung tissues from control and irradiated C57BL/6 wild type and CD73<sup>-/-</sup> mice were isolated at different time points, processed as described in par. 2.7.7, and evaluated by flow cytometry.

At first, the distribution of total leukocytes in the lung was compared. The glycoprotein CD45 is expressed at high levels on the cell surface of all nucleated hematopoietic cells and their precursors, and represents the leukocyte common antigen. Lung tissues isolated from control mice showed no variation in leukocytes content (CD45<sup>+</sup> cells) at all time points analysed, with average values ranging from 31.4 ± 9.1 % to 39.6 ± 4.1 % of total lung cells in WT mice and from 33.5 ± 6.1 % to 40.8 ± 3.7 % in CD73<sup>-/-</sup> mice (**Fig. 3.6 A**). In WT mice, whole thorax irradiation led to a significant increase of CD45<sup>+</sup> cells at 6, 12 and 24 weeks post irradiation. Similarly, in CD73<sup>-/-</sup> mice increased percentage of leukocytes was significant at 6, 12 and 24 weeks post irradiation, but was stably higher than control values even at week 30. The comparison of the relative increase of CD45<sup>+</sup> cells between WT and CD73<sup>-/-</sup> mice pointed out a similar response to irradiation, with a peak of infiltration at week 12 p.i. (**Fig. 3.6 A**).

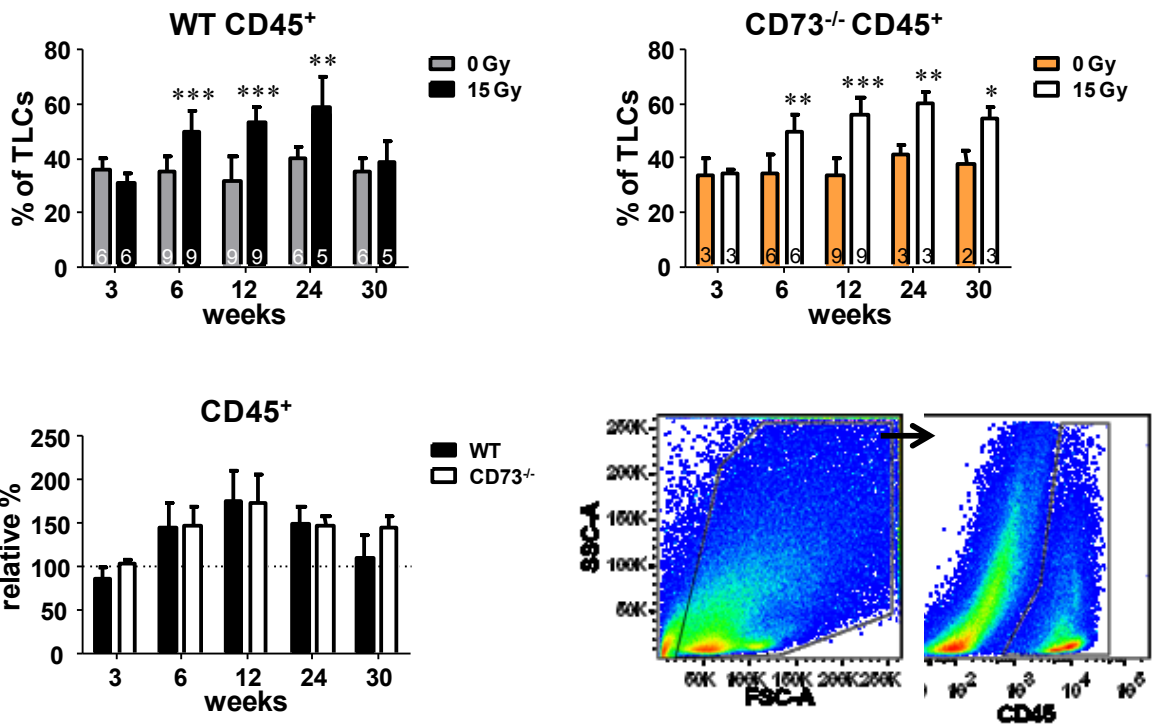
To gain insight into the contribution of specific immune cells to the inflammatory infiltrate, in a next step different sub-populations of infiltrating leukocytes were characterised. The gating strategy used for flow cytometric analysis of the different cell subsets is shown as dot plots in the corresponding figures.

Flow cytometric analysis of lung tissue did not show a significant alteration of granulocyte infiltration ( $\text{Gr1}^+$  cells) after irradiation in C57BL/6 wild type at all time points, while at 24 and 30 weeks a tendency to a higher local presence of  $\text{Gr1}^+$  cells was noted in  $\text{CD73}^{-/-}$  mice, with relative percentages corresponding approximately to a 2-fold increase compared to control mice (**Fig. 3.6 B**). B lymphocytes have also been compared in control and irradiated mice, and a significant 1.3-fold increase was displayed by WT mice at 12 weeks p.i., expansion not observed in  $\text{CD73}^{-/-}$  mice (**Fig. 3.6 C**). Overall only subtle differences in the composition of the immune cell infiltrate were observed between lungs of irradiated WT and  $\text{CD73}^{-/-}$  mice at specific time points p.i..

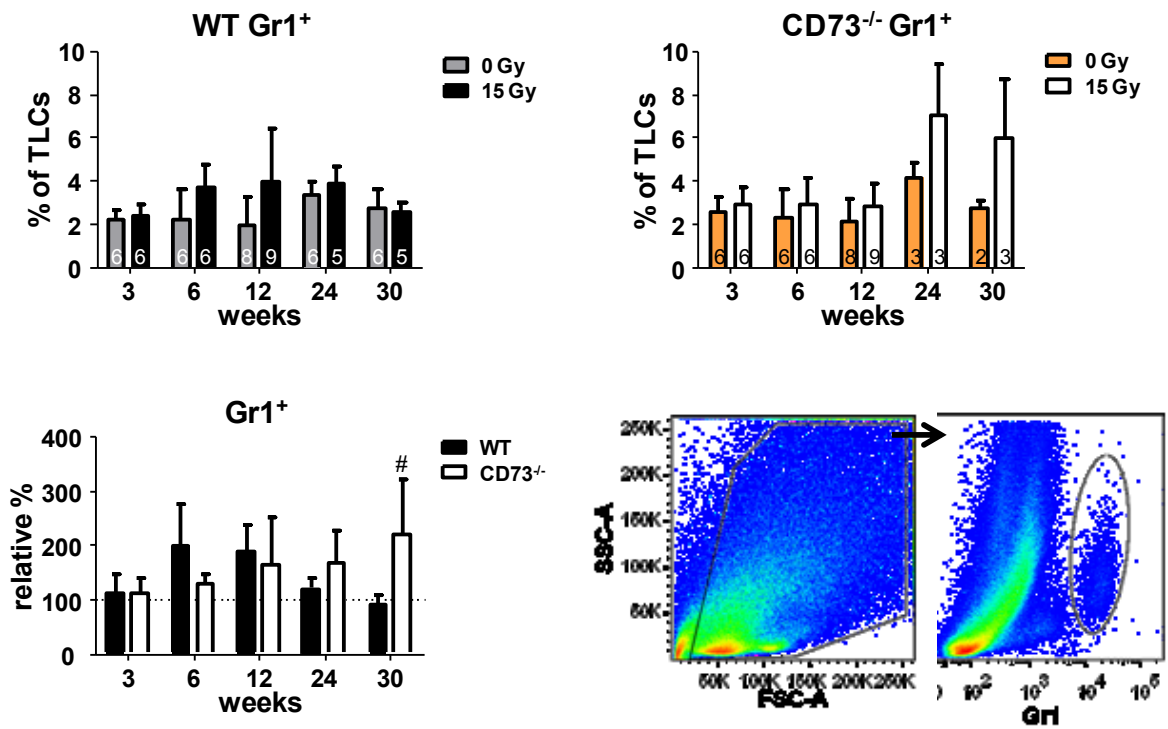
As mentioned in the introduction, IR is known to increase the number of leukocytes in the BALF of cancer patients, and in particular of T lymphocytes (par. 1.6.2), therefore it was particularly interesting to verify whether the mouse model could mirror such a common feature. In control mice, around 5 % of total lung cells were represented by  $\text{CD3}^+$  cells (**Fig. 3.6 D**) and whole thorax irradiation slightly reduced the percentage of T cells both in WT and  $\text{CD73}^{-/-}$  mice at week 3 p.i.. A significant T cell infiltration occurred in WT mice from week 6 until week 12, and the amount of infiltrating cells gradually decreased to control levels at later time points. Interestingly, in  $\text{CD73}^{-/-}$  mice the increase in T cells lasted longer, maintaining high levels until week 30. When comparing the two strains using percentages relative to respective control values, T lymphocytes of  $\text{CD73}^{-/-}$  mice showed higher resistance to radiation at the beginning of the inflammatory phase and a persistent lung infiltration (**Fig. 3.6 D**).

Lung resident macrophages can be distinguished from the newly recruited macrophages by the expression of the marker CD11c. Therefore the gating strategy based on the coupled expression of F4/80 and CD11c allows the identification of these two cell populations (**Fig. 3.6 E and F**).

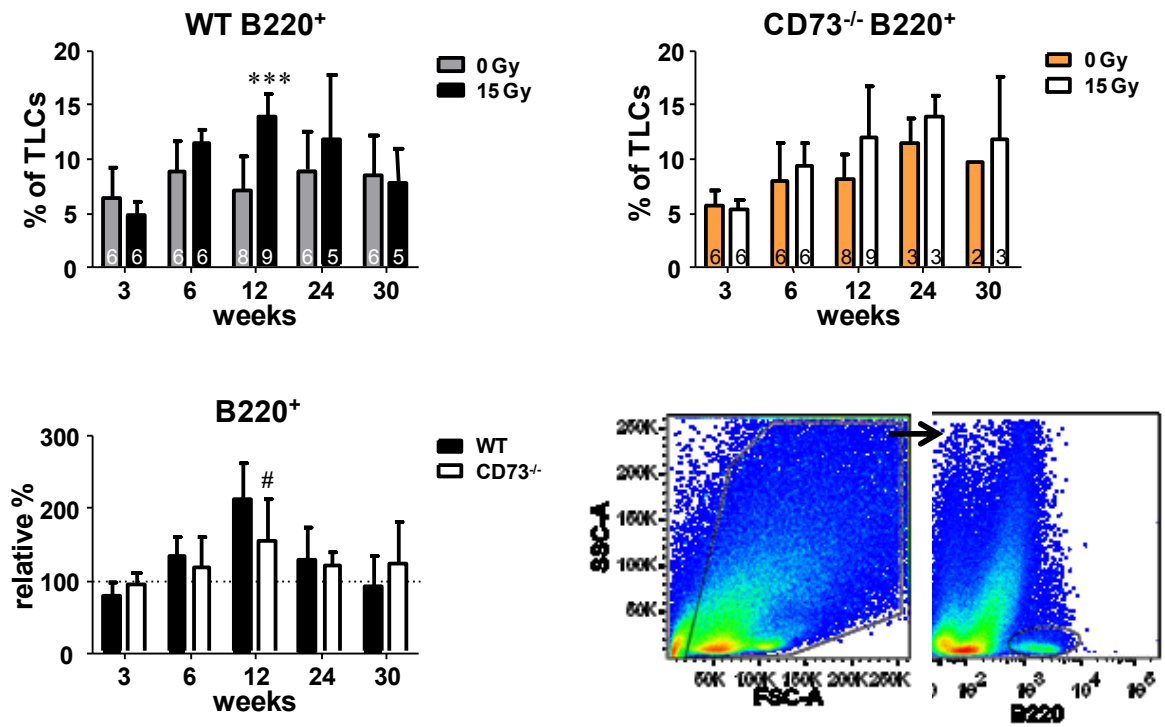
A



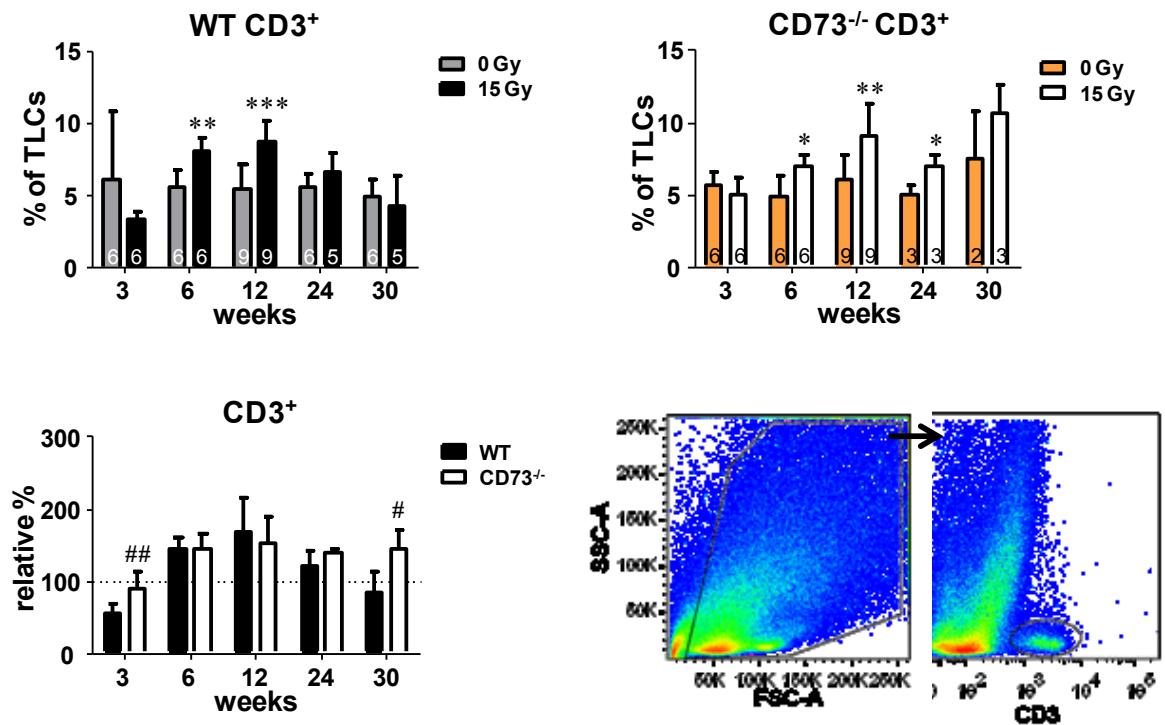
B



C

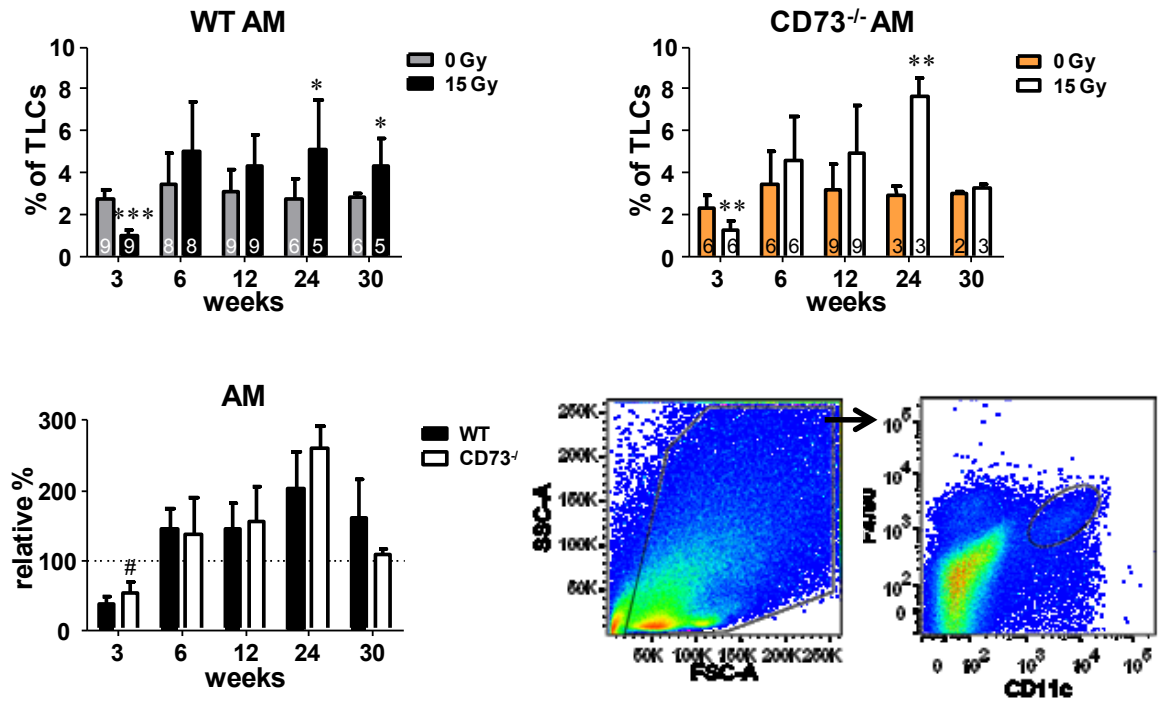


D





E



F

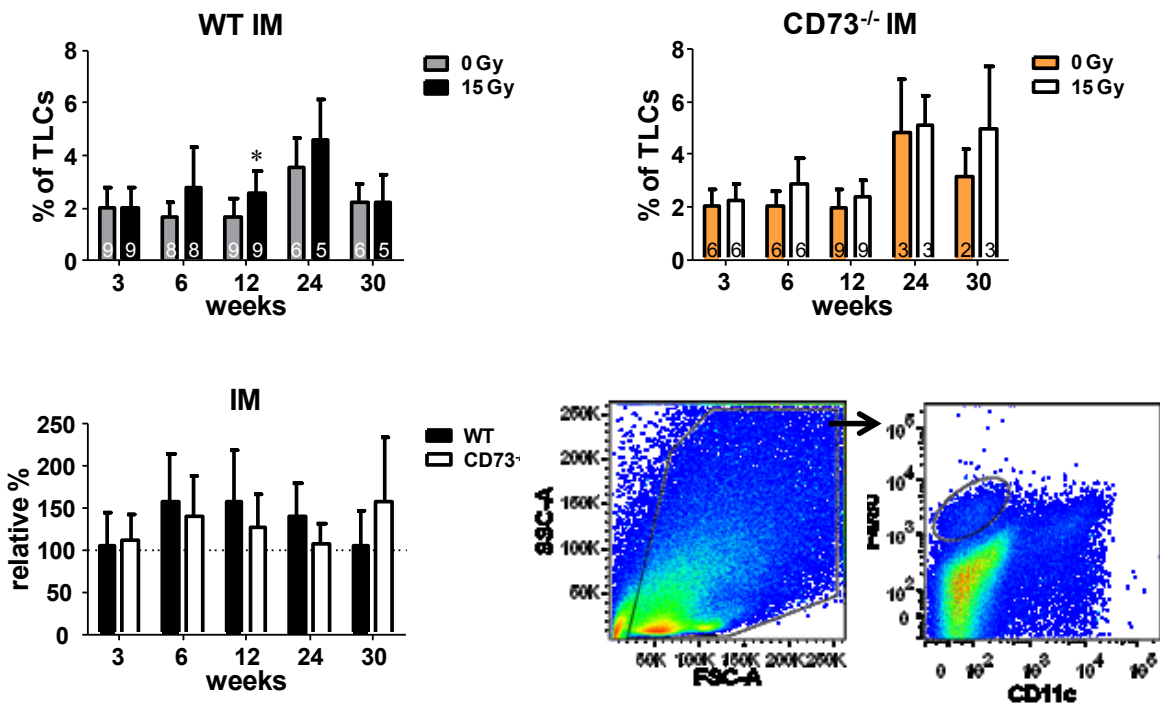


**Fig. 3.6 Determination of leukocyte content in lung tissue by flow cytometry.** C57BL/6 wild type (WT) and CD73<sup>-/-</sup> mice received 0 Gy or 15 Gy whole thorax irradiation. At 3, 6, 12, 24 and 30 weeks p.i. lung tissue was used for cell isolation and flow cytometric analysis using antibody stainings for (A) total leukocytes (CD45<sup>+</sup> cells), (B) granulocytes (Gr1<sup>+</sup> cells), (C) B lymphocytes (B220<sup>+</sup> cells), (D) T lymphocytes (CD3<sup>+</sup> cells), and alveolar (F4/80<sup>+</sup>CD11c<sup>+</sup>) or infiltrating (F4/80<sup>+</sup>) macrophages (E, F). Timelines of the indicated cell populations show mean percentages  $\pm$  SD calculated on total lung cells (TLCs). To compare radiation effects in WT and CD73<sup>-/-</sup> mice, mean values calculated in treated mice were normalized with respect to control values (lower left). For each cell population analysed, the respective gating strategy is shown as a dot plot (lower right). The number of mice used in the analyses is indicated within the bars (\*= 0 Gy vs 15 Gy; #= WT vs CD73<sup>-/-</sup>) (\*,# p $\leq$ 0.05; \*\*,## p $\leq$ 0.01; \*\*\*,### p $\leq$ 0.001; two-tailed unpaired t-test).

In the early phase of inflammation alveolar macrophages, unlike other immune cells in the lung, showed a significant reduction of their percentages compared to sham irradiated animals in both mouse strains. This macrophage population restored to control levels at week 6 p.i. and further increased peaking at week 24. Statistical analysis on relative percentages underlined a higher decrease of alveolar macrophages deriving from irradiated C57BL/6 wild type mice at week 3 p.i. in comparison to CD73<sup>-/-</sup> mice, with an approximately 3-fold and 2-fold decrease of this population in the lung, respectively. Both mouse strains displayed the same tendency to repopulate the tissue at later time points. With respect to infiltrating macrophages, whole thorax irradiation did not cause important changes at all time points investigated. Moreover, WT and CD73<sup>-/-</sup> mice showed a similar trend in maintaining lung homeostasis of the macrophage compartment.

### 3.1.4 Local and systemic adenosinergic pathway regulation in T lymphocytes

Histological analysis of lung tissue suggested that the absence of CD73 leads to a better outcome of whole lung irradiation with respect to fibrosis development. However, radiation induced only subtle changes in the immune cell composition. Therefore, in a next step the question was addressed whether radiation affects immune cell functions by altering the expression and/or activity of the adenosinergic pathway. To this end, T cells in the lung were analysed for the expression of CD73 and CD39, the ectonucleotidase acting upstream of CD73 (par. 1.4.1). For a more immediate interpretation of the data, only relative values of irradiated WT and CD73<sup>-/-</sup> mice compared to respective controls are shown (Fig. 3.7). In WT



mice a significant upregulation of CD39 on T cells was noted at late time points reaching maximum levels at week 30 p.i.. T cells in CD73<sup>-/-</sup> mice, though maintaining high levels of CD39 throughout the whole experiment, never showed significant differences in relative percentages at any time after irradiation.

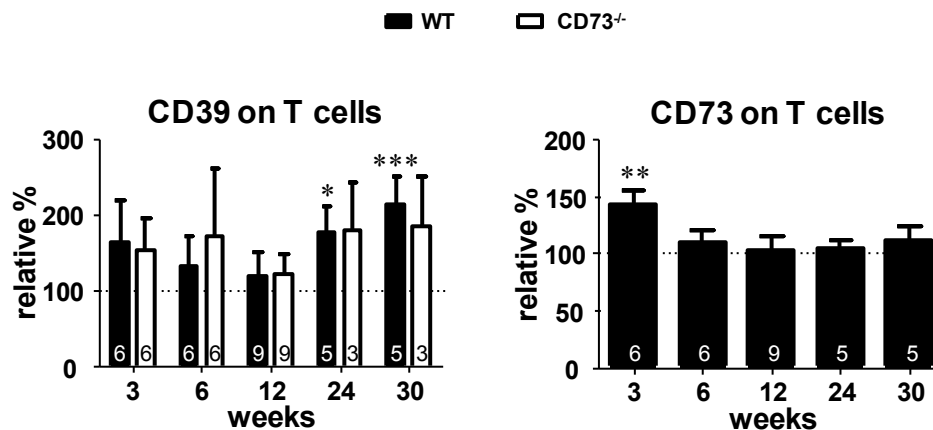


**Fig. 3.7 Determination of CD39 and CD73 expression on lung T cells by flow cytometry.** C57BL/6 wild type (WT) and CD73<sup>-/-</sup> mice received 0 Gy or 15 Gy whole thorax irradiation. At 3, 6, 12, 24 and 30 weeks time points, lung tissue was used for cell isolation and antibody staining for T lymphocytes (CD3<sup>+</sup> cells) in combination with anti-CD39 and anti-CD73 antibodies. To compare radiation effects in WT and CD73<sup>-/-</sup> mice, timelines show mean values  $\pm$  SD of CD39<sup>+</sup> or CD73<sup>+</sup> on CD3<sup>+</sup> cells in irradiated mice normalized with respect to control values. For each analysis, the number of mice used is indicated within the bars (\*= 0 Gy vs 15 Gy) (\*  $p \leq 0.05$ ; \*\*  $p \leq 0.01$ ; \*\*\*  $p \leq 0.001$ ; two-tailed unpaired t-test).

Whole lung irradiation also triggered upregulation of CD73 on T cells in WT mice. However, upregulation of CD73 was an early event, with a maximal upregulation of approximately 1.5-folds at 3 weeks p.i., while at later time points no significant alteration of CD73 expression on T cells could be observed.

Altogether, these results revealed radiation-induced changes in the percentage of T lymphocytes, as well as an altered regulation of the adenosinergic pathway in response to whole lung irradiation.

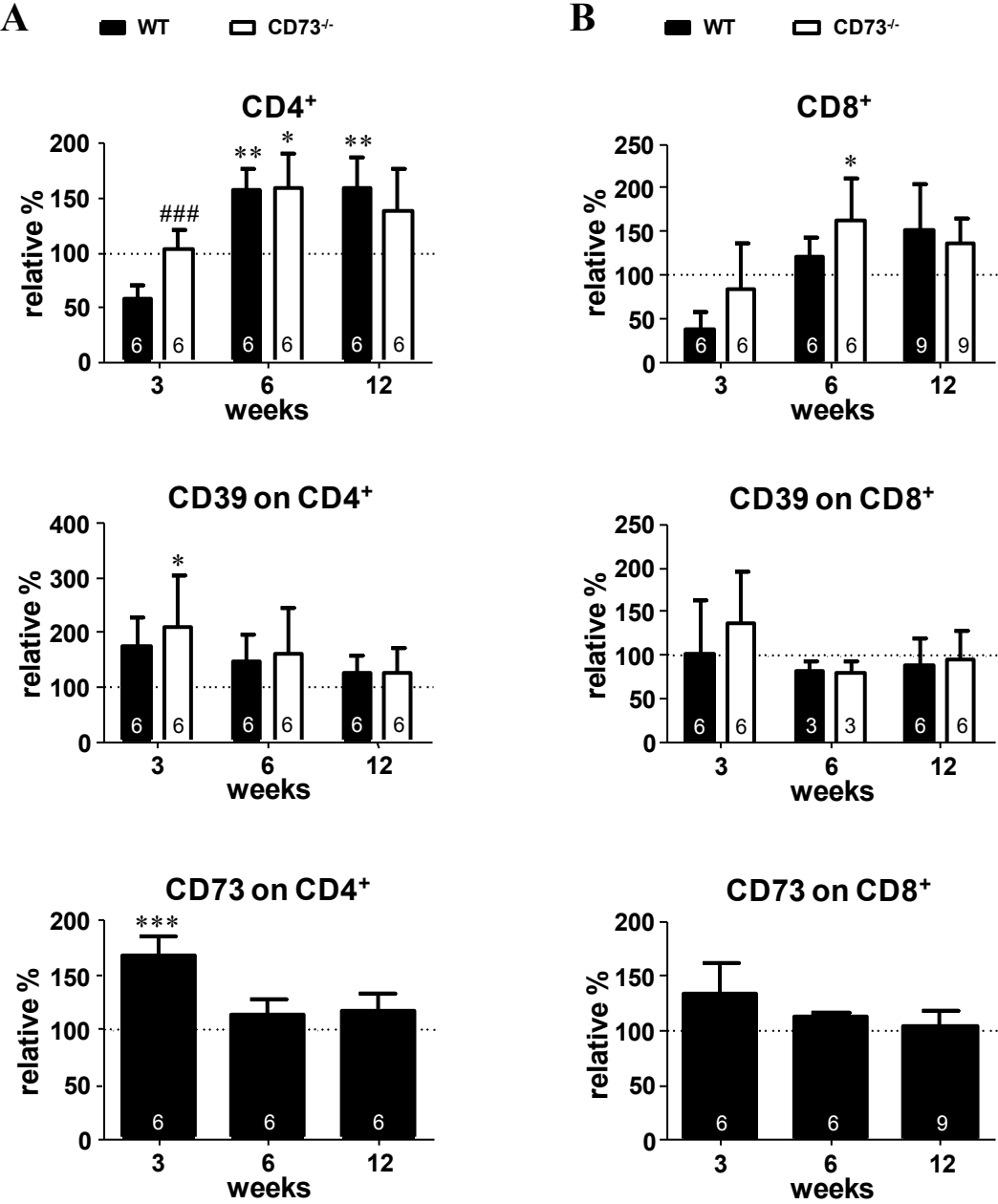


**Fig. 3.8** Determination of lung CD4<sup>+</sup> and CD8<sup>+</sup> T cells and their CD39 and CD73 expression by flow cytometry. C57BL/6 wild type (WT) and CD73<sup>-/-</sup> mice received 0 Gy or 15 Gy whole thorax irradiation. At 3, 6 and 12 weeks, lung tissue was used for cell isolation and flow cytometric measurement. (A) Relative percentages of CD4<sup>+</sup> T lymphocytes in irradiated lungs and surface expression of CD39 and CD73. (B) Relative percentages of lung CD8<sup>+</sup> population of irradiated mice in combination with anti-CD39 and anti-CD73 antibodies. Timelines show mean values ± SD calculated in treated mice normalized with respect to control groups. Absolute percentages of CD4<sup>+</sup> and CD8<sup>+</sup> cells were calculated on TLCs. For each analysis, the number of mice used is indicated within the bars (\*= 0 Gy vs 15 Gy; #= WT vs CD73<sup>-/-</sup>) (\* p≤0.05; \*\* p≤0.01; \*\*\*,### p≤0.001; two-tailed unpaired t-test).

Because of the role of adenosine in many function of T cells involved in inflammatory processes and the early changes observed in CD73 expression, it was next analysed to what extent whole lung irradiation would affect specific T cell subsets in their expression of CD39 and CD73, focusing on the pneumonitic phase.

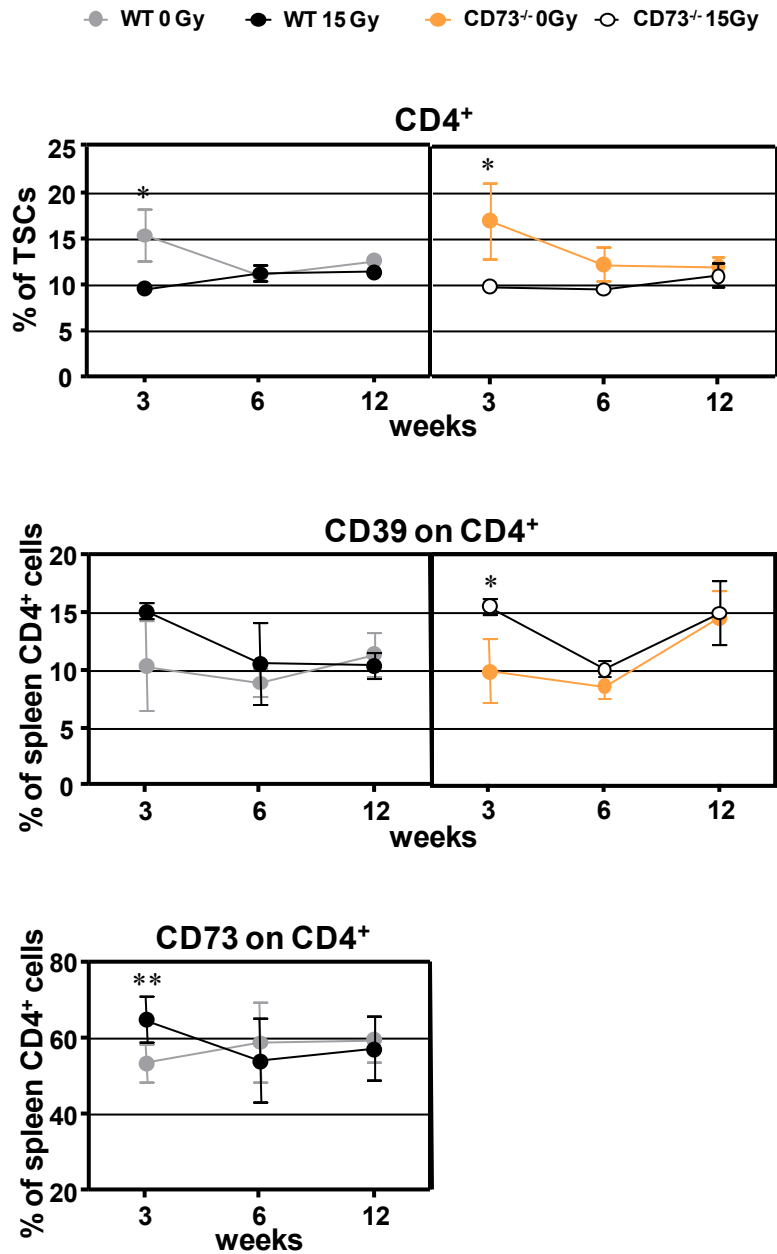
Similar to the results obtained in CD3<sup>+</sup> T cells, at week 3 after whole thorax irradiation relative percentages of CD4<sup>+</sup> T cells were significantly higher in CD73 deficient mice compared to C57BL/6 wild type mice. However, at later time points p.i. similar relative increases were found in WT and CD73<sup>-/-</sup> mice (**Fig. 3.8 A**). In both strains, a trend in the upregulation of CD39 on CD4<sup>+</sup> T cells was noted in the pneumonitic phase (weeks 3 to 12), especially in CD73<sup>-/-</sup> mice. Although percentages of lung CD4<sup>+</sup> T lymphocytes were largely decreased 3 weeks p.i. in WT mice, the remaining cells showed a significant upregulation of CD73 at this time point. CD73 expression reached the levels of controls at 6 and 12 weeks p.i., when the amount of CD4<sup>+</sup> cells on total lung cells was approximately 1.6-fold higher compared to sham irradiated mice (**Fig. 3.8 A**).

An analogous response to thorax irradiation was observed in the CD8<sup>+</sup> T cell population. In WT mice, a more prominent decrease in relative percentages was measured at 3 weeks p.i. as compared to CD73<sup>-/-</sup> mice, and at later time points both strains showed comparable increases of the CD8<sup>+</sup> T cell subset. Only minor or no radiation-induced effects were noted on the regulation of the CD39 and CD73 in this cell population (**Fig. 3.8 B**).

Radiation mainly affected percentages and CD39/CD73 surface expression of the CD4<sup>+</sup> T cell subset in the lung. In order to understand whether radiation could influence immune cells in the periphery, the systemic response was next investigated. At this purpose, lymphocytes isolated from spleen and cervical lymph nodes were also included in the study and results are shown in **Fig. 3.9**. Similarly to what was observed in the lung, radiation caused a significant reduction in the percentages of CD4<sup>+</sup> T cells in WT and CD73<sup>-/-</sup> mice at 3 weeks p.i., both in the spleen and lymph nodes, and control levels were restored at later time points. In the spleen, the decrease of CD4<sup>+</sup> T cells was accompanied by a 5 % increase in the expression of CD39 in both mouse strains (**Fig. 3.9 A**). In lymph node cells the upregulation of this enzyme was also observed, but to a lesser extent (**Fig. 3.9 B**). As already described for the lung tissue of WT mice, radiation significantly induced CD73 expression on CD4<sup>+</sup> T cells at week 3 p.i. in splenocytes and lymph nodes cells.

These data suggest that the systemic T cell response at least partially mimics the local T cell radiation-induced changes observed in the lung.

A



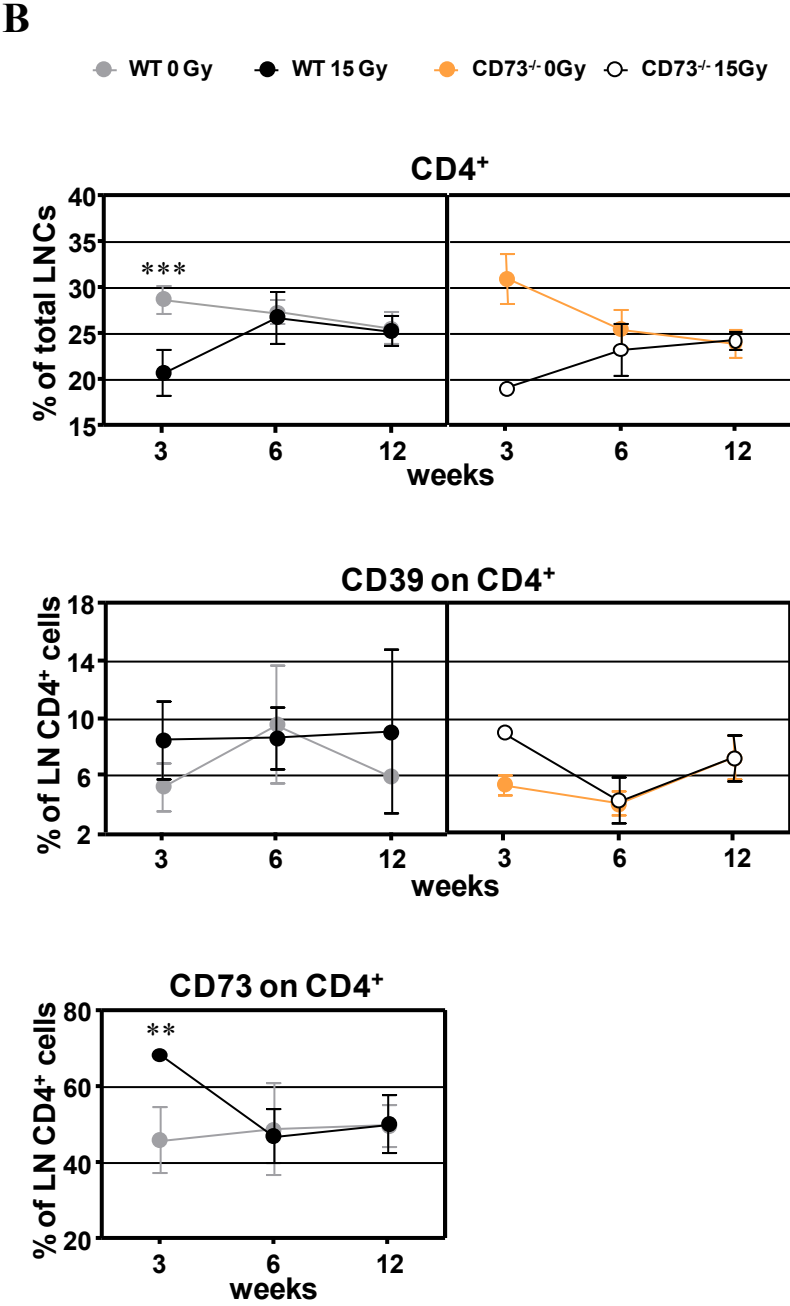


**Fig. 3.9 Determination of spleen and lymph nodes CD4<sup>+</sup> T cells and their CD39 and CD73 expression by flow cytometry.** C57BL/6 wild type (WT) and CD73<sup>-/-</sup> mice received 0 Gy or 15 Gy whole thorax irradiation. At 3, 6 and 12 weeks time points, spleen and lymph nodes were isolated and cells stained for flow cytometric analysis. (A) Percentages of spleen CD4<sup>+</sup> T lymphocytes on total spleen cells (TSCs) and surface expression of CD39 and CD73. (B) Percentages of CD4<sup>+</sup> T lymphocytes population in cervical lymph nodes (LN) in combination with anti-CD39 and anti-CD73 antibodies. Data represent mean percentages ± SD (n≥3 or pooled cells from n≥3; \* p≤0.05; \*\* p≤0.01; \*\*\* p≤0.001; two-tailed unpaired t-test).

### 3.1.5 Local and systemic analysis of regulatory T cells in the pneumonitic phase

Regulatory T cells ( $T_{reg}$ ) have been shown to co-express on their surface CD39 and CD73 and production of adenosine mediated by these two ecto-enzymes has been described as one of the mechanisms in the suppressive machinery of  $T_{reg}$  cells used to control immune responses (Deaglio et al., 2007; Kobie et al., 2006). Although earlier investigations in humans and rodents already showed infiltration of  $CD4^+$  (and  $CD8^+$ ) T cells into irradiated lungs, up to now the potential role of  $T_{reg}$  cells in the immune response of irradiated normal tissues, including the lung, is largely unexplored (par. 1.3 and 1.6.2). Therefore, it was of interest to investigate whether the early increase in CD39 and CD73 on  $CD4^+$  T cells observed in response to radiation was due to an expansion of regulatory T cells, both locally and systemically. As shown in Fig. 3.10, in the irradiated lung tissue,  $CD4^+CD25^+Foxp3^+$   $T_{reg}$  cells slightly increased in  $CD73^{-/-}$  mice compared to untreated control at 3 weeks, while a significant and higher than 4-fold expansion of these cells was detected in WT mice.

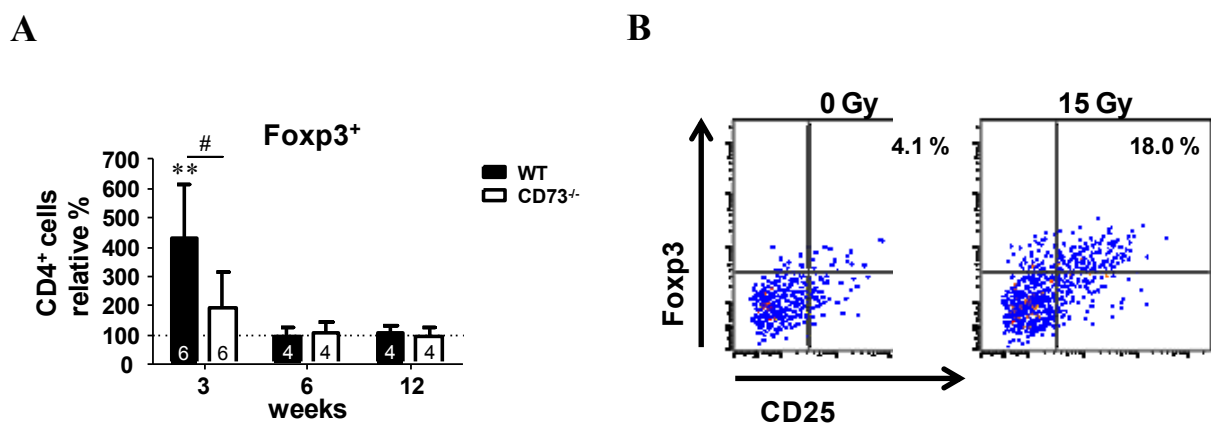


**Fig. 3.10 Determination of lung  $T_{reg}$  cells by flow cytometry.** C57BL/6 wild type (WT) and  $CD73^{-/-}$  mice received 0 Gy or 15 Gy whole thorax irradiation. At 3, 6 and 12 weeks p.i., lung tissue was used for cell isolation and flow cytometric measurement. (A) Timeline shows percentages  $\pm$  SD of  $CD4^+CD25^+Foxp3^+$  T lymphocytes population in irradiated lungs relatively to percentages of control mice. The number of mice used is indicated within the bars (\*= 0 Gy vs 15 Gy; #= WT vs  $CD73^{-/-}$ ) (#  $p \leq 0.05$ ; \*\*  $p \leq 0.01$ ; two-tailed unpaired t-test). (B) Representative dot plot showing the increase in  $Foxp3^+CD25^+$  cells from the  $CD4^+$  population detected in WT mice at week 3.

However, the increase in the  $T_{reg}$  cell population was only transient and was no longer observed at 6 and 12 weeks p.i.. Similar results were obtained in the spleen and cervical lymph nodes of WT mice (Fig. 3.11). Of note, WT mice showed a biphasic increase in  $T_{reg}$  cells in the irradiated lung tissue (Supplementary data, Fig. 7.1). Unfortunately, the data for  $CD4^+$  and  $T_{reg}$  cells are missing in the  $CD73^{-/-}$  mice because of experimental difficulties.

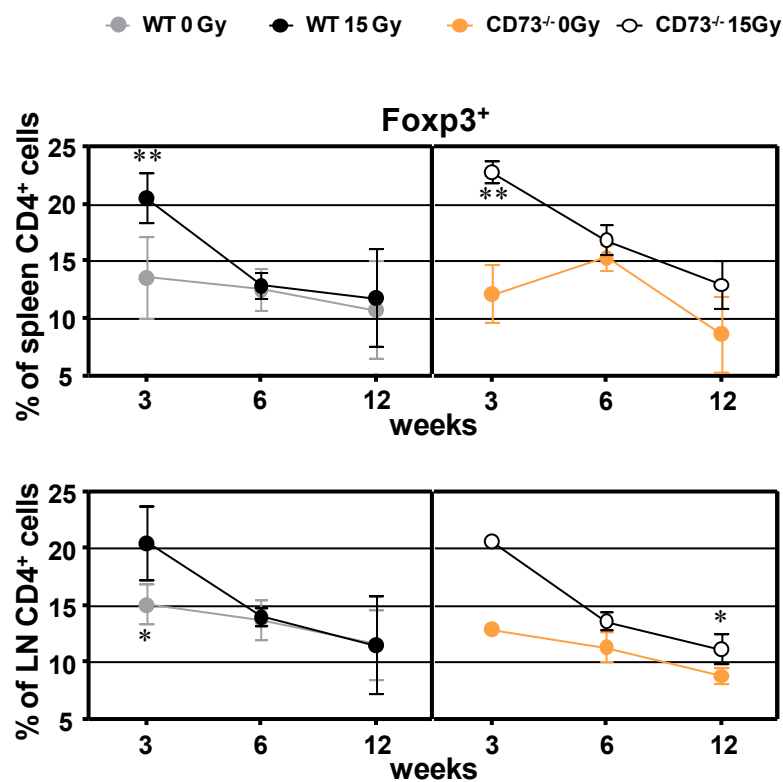


**Fig. 3.11 Determination of systemic  $T_{reg}$  cells by flow cytometry.** C57BL/6 wild type (WT) and  $CD73^{-/-}$  mice received 0 Gy or 15 Gy whole thorax irradiation. Lymphocytes were isolated from the spleen and cervical lymph nodes (LN) at 3, 6 and 12 weeks p.i., and used for flow cytometric measurement of  $T_{reg}$  cells. Timelines show absolute percentages  $\pm$  SD of  $CD4^+CD25^+Foxp3^+$  T lymphocytes population in the mentioned tissues of WT and  $CD73^{-/-}$  mice (\*  $p \leq 0.05$ ; \*\*  $p \leq 0.01$ ; two-tailed unpaired t-test).

A slightly different response to radiation was found in spleen and lymph nodes of  $CD73^{-/-}$  mice. Following an almost 2-fold increase measured at 3 weeks, irradiated mice seemed to maintain throughout the pneumonitic phase slightly higher levels of  $T_{reg}$  cells in these tissues

in respect to control mice. These data show that the systemic response at least partially mimics the local response of the immune system.

Altogether, results obtained indicated that whole thorax irradiation triggers time-dependent local and systemic activation of the adaptive immune system, and that the main differences between WT and CD73<sup>-/-</sup> mice can be found primarily in the activation of specific T cell subset and in the modulation of the surface expression of the adenosinergic pathway members, rather than in quantitative effects induced by radiation.

### **3.1.6 Macrophage characterization**

#### **3.1.6.1 Histological analysis of macrophages - morphology and phenotype**

The CD73/Ado system is not only of importance for the regulation of immunosuppressive functions of lymphocytes, but also contributes in the regulation of macrophage functions (Hasko et al., 2007; Linden, 2006).

Alveolar macrophages represent the first line of defence in the lung and they are rapidly involved in the initiation of immune responses whenever an inflammatory stimulus occurs locally. In addition, their extraordinary plasticity allows them to play also a central role in the modulation and resolution of inflammation (Stout et al., 2005). As a consequence, it was interesting to examine the quantitative reaction of macrophages to radiation-induced lung injury, as well as the potential of IR to affect their activation/polarization state. Moreover, because of the role of CD73 and adenosine in the regulation of macrophage activation and function, it was important to evaluate potential differences between the response of the macrophage compartment in WT and CD73<sup>-/-</sup> mice that may also be of relevance for the outcome of radiation-induced pneumopathy.

In a first step, semithin sections and electron microscopy samples of lung tissue from irradiated and control mice were analysed, and constituted a powerful magnifying glass to detect possible morphological changes in macrophages. All samples analysed had previously been collected at 3 and 6 weeks after right hemitorax irradiation (15 Gy) of C57BL/6 wild



type and  $CD73^{-/-}$  mice by Dr Therese Eldh (Tübingen). A striking finding in irradiated lungs was the presence of enlarged macrophages filled with non proteic content, which were barely found in control mice. Representative pictures are shown for both mouse strains in Fig. 3.12 A.

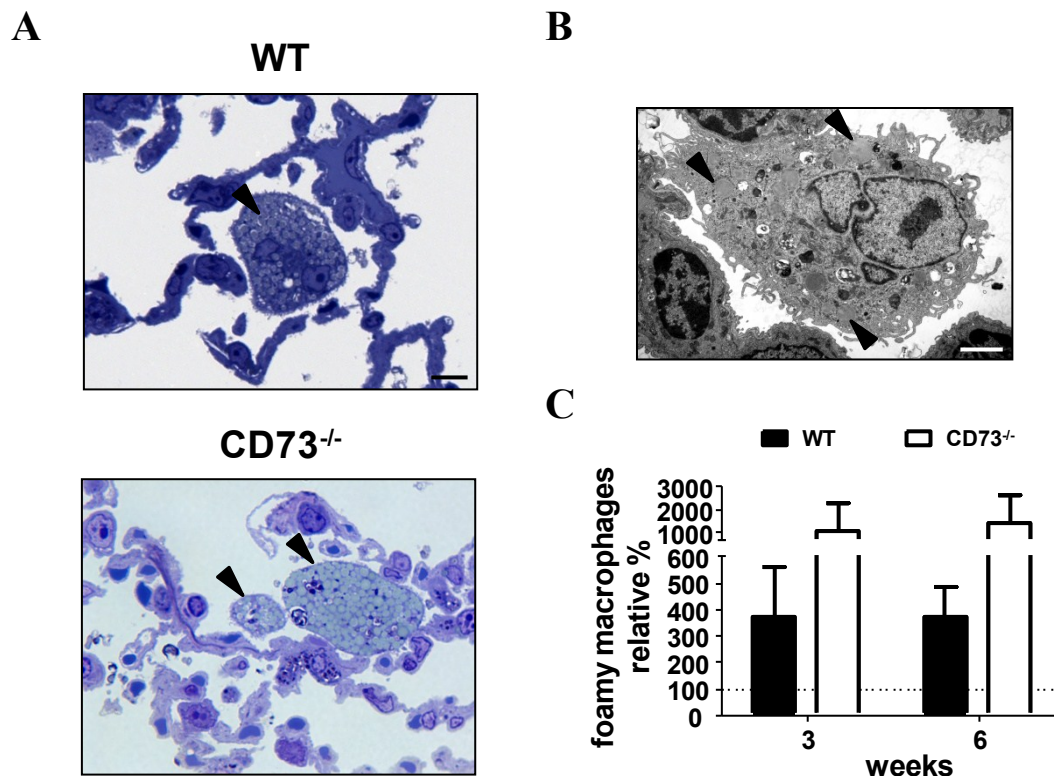


**Fig. 3.12 Foamy macrophages in C57BL/6 wild type and  $CD73^{-/-}$  mice lungs.** At 3 and 6 weeks after right hemithorax irradiation with 15 Gy or 0 Gy lung tissues were obtained and processed for electron microscopy. **A)** Representative light microscopy pictures of toluidine blue stained semithin sections (0.5  $\mu\text{m}$ ) from C57BL/6 wild type (WT) and  $CD73^{-/-}$  mice showing foamy macrophages (black arrows) (magnification  $\times 1000$ ; scale bar: 10  $\mu\text{m}$ ). **B)** Electron microscopy picture of a foamy macrophage; some lipid droplets are pointed (black arrows) (magnification  $\times 7000$ ; scale bar: 2  $\mu\text{m}$ ). **C)** Quantification of lipid loaded macrophages in semithin slices. Data represent relative mean percentage  $\pm$  SD of lipid loaded macrophages to respective control groups (=100%) ( $\geq 3$  different sections; 2 mice per group).

Electron microscopy on lung tissue deriving from the same samples confirmed the presence of lipid droplets in the cytoplasm of macrophages and, in addition, in other not well defined locations, most probably corresponding to the lung interstitium or to the cytoplasm of other

resident cells (**Fig. 3.12 B** and data not shown). A quantification of lipid-loaded macrophages was completed scanning whole tissue on semithin sections and counting normal and foamy macrophages. Results of the analysis in WT and CD73<sup>-/-</sup> mice are shown in **Fig. 3.12 C** as increases relative to respective controls (considered as 100 values). Both mouse strains showed a simultaneous and stable increase in the formation of foamy macrophages until week 6 p.i., but to a different extent. In details, IR led to an approximately 4-fold increase and a 10-fold increase of these cells in WT and CD73<sup>-/-</sup> mice, respectively. This analysis, even though not statistically validated, suggests that IR disturbs lipid metabolism of macrophages in the lung tissue, in particular in the absence of CD73.

It is largely accepted that, depending on the microenvironment and the inflammatory stimulus, macrophages have the ability to polarize toward a more inflammatory phenotype, named M1 or classically activated macrophages, or toward an alternative activation, namely the M2 phenotype, mainly involved in wound healing processes and inflammatory resolution. To characterize the role of macrophages in the regulation of the lung tissue response to IR, further analyses aimed at characterizing potential changes in the macrophage phenotype after whole thorax irradiation. At this purpose, tissue microarrays from C57BL/6 wild type and CD73<sup>-/-</sup> mice were subjected to immunofluorescence staining and macrophage phenotype was distinguished either by the use of the anti-iNOS antibody for the classical activation, or by the anti-Arg1 and anti-IL-10 $\alpha$  antibodies for the alternative activation (**Fig. 3.13**). Histograms in **Fig. 3.13 A** represent percentages, relative to sham irradiated mice, that were obtained by counting F4/80<sup>+</sup> cells positive for the phenotype marker of interest, in relation to F4/80-only positive macrophages. Exemplary immunofluorescence pictures are also shown (**Fig. 3.13 B**). In both strains, lung macrophages expressing iNOS, defined as M1 macrophages, showed only a slight increase in their percentage at late time points after irradiation, and at an earlier time point in CD73<sup>-/-</sup> mice when compared to WT mice. Arg1 is produced in alternative to iNOS and characterizes a M2 phenotype. Presence or absence of CD73 seemed not to alter the induction of Arg1, in consideration of a similar trend observed in the percentage of double positive macrophages after irradiation, with early reductions, peaks at 12 weeks and late low levels of F4/80<sup>+</sup>Arg1<sup>+</sup> cells. Interleukin-10 is an anti-inflammatory cytokine involved in the resolution of acute inflammation but has also been associated with fibrosis, as well as with alternative activation of macrophages.

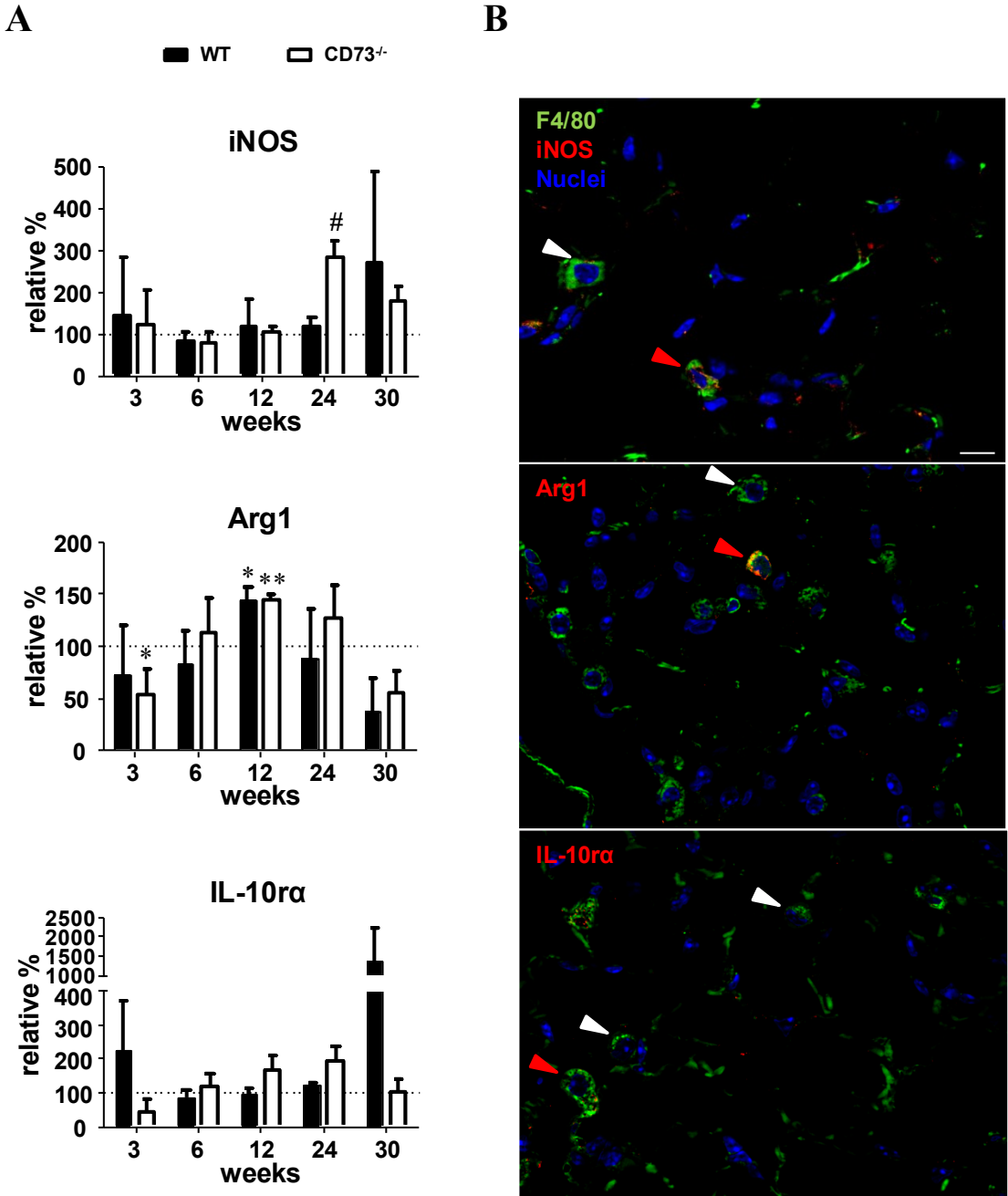


**Fig. 3.13 Macrophages and iNOS, or Arg1 or IL-10 $\alpha$  immunofluorescence staining.** Lungs isolated at 3, 6, 12, 24 and 30 weeks from irradiated and control C57BL/6 wild type (WT) and CD73<sup>-/-</sup> mice were embedded in paraffin and used in the production of tissue microarrays. Sections of microarrays were immunostained with monoclonal antibodies anti-F4/80 in combination with anti-iNOS, or with anti-Arg1, or with anti-IL-10 $\alpha$ . Hoechst was used for nuclei counterstaining. **A)** Quantification of double positive macrophages in irradiated mice. Data represent mean percentages  $\pm$  SD of double positive cells relative to respective control groups (=100%) ( $\geq 4$  pictures per mouse;  $\geq 2$  mice per group) (\*= 0 Gy vs 15 Gy; #= WT vs CD73<sup>-/-</sup>) (\*,#  $p \leq 0.05$ ; \*\*  $p \leq 0.01$ ; two-tailed unpaired t-test). **B)** Representative fluorescence microscopy pictures of the different stainings. F4/80<sup>+</sup> cells (white arrows) and double positive macrophages (red arrows) are indicated (magnification x630; scale bar: 10  $\mu$ m).

An increase in the expression of IL-10 receptor on macrophages can be considered as a marker for alternative activation, or at least for one subtype of M2 macrophages (Bogdan and Nathan, 1993; Gordon and Taylor, 2005; Moore et al., 2001; Sun et al., 2011). Whole thorax irradiation seemed to differentially affect the percentages of IL-10 $\alpha$  positive macrophages in the two mouse strains. F4/80<sup>+</sup>IL-10 $\alpha$ <sup>+</sup> cells slowly increased in WT mice and reached a 13-fold expansion at week 30 p.i., while in CD73 deficient mice only a slight increase in the amount of these cells was detected, with a peak at 24 weeks and subsequent decrease to percentages of control animals.

These data indicate that a very distinct regulation of the macrophage compartment is accompanying the response to radiation injury, and that loss of CD73 leads to partial alteration of the ordinary tissue reaction to whole thorax irradiation.

### 3.1.6.2 Flow cytometric analysis of macrophages - survival and lipid metabolism

The analysis of lung macrophage morphology and phenotype, respectively performed on semithin sections and by the use of immunofluorescence on tissue microarrays, gave clear indications about changes occurring on these cells after radiation treatment. However, only small portions of tissue can be analysed using these approaches. Therefore, flow cytometry on whole lung was performed to further support results already obtained.

Survival, proliferation and differentiation, as well as chemotaxis of mononuclear phagocytes are driven by the CSF-1 growth factor, and all members of the mononuclear phagocytic lineage express the CSF-1 receptor tyrosine kinase (Pixley and Stanley, 2004). The first investigation aimed at detecting a potential radiation-induced alteration of the expression of this key macrophage regulator. Results of the analysis are shown in **Fig. 3.14**. As observed in the absolute number of lung macrophages at 3 weeks p.i. (**Fig. 3.6 E and F**), the CSF-1R surface expression was equally and drastically downregulated at this time point in C57BL/6 wild type and CD73<sup>-/-</sup> mice, displaying normalized percentages corresponding to  $23.6 \pm 2.6$  and to  $25.4 \pm 1.7$ , respectively. At all the other time points included in the study only minor changes were detected, albeit WT mice seemed to progressively increase CSF-1R expression during the late fibrotic phase (24 and 30 weeks), especially in the infiltrating population.

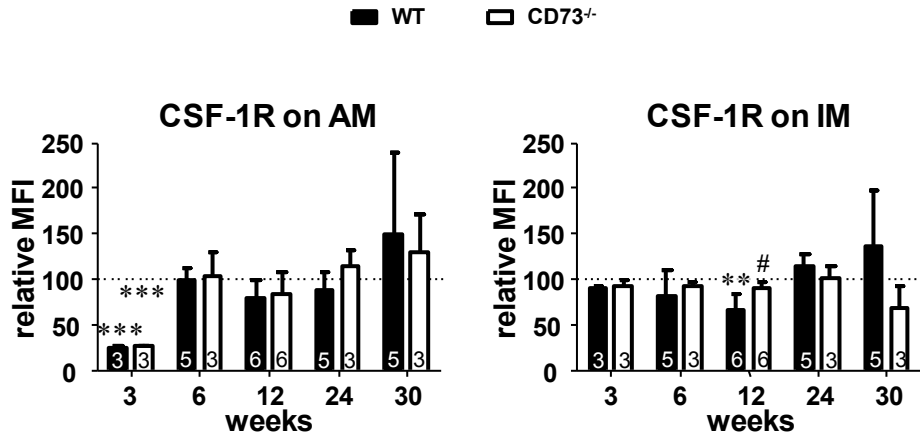


**Fig. 3.14 Analysis of CSF-1R expression on lung macrophages.** C57BL/6 wild type (WT) and CD73<sup>-/-</sup> mice received 0 Gy or 15 Gy whole thorax irradiation. Lung tissue isolated at 3, 6, 12, 24 and 30 weeks was used in flow cytometry staining. Alveolar (AM) and infiltrating macrophages (IM) were investigated for the expression of CSF-1R. Timelines show mean values ± SD of the geomean fluorescence intensity (MFI), normalized with respective MFIs of the same populations isolated from control animals. For each time point, the number of mice used is indicated within the bars (\*= 0 Gy vs 15 Gy; #= WT vs CD73<sup>-/-</sup>) (# p≤0.05; \*\* p≤0.01; \*\*\* p≤0.001; two-tailed unpaired t-test).

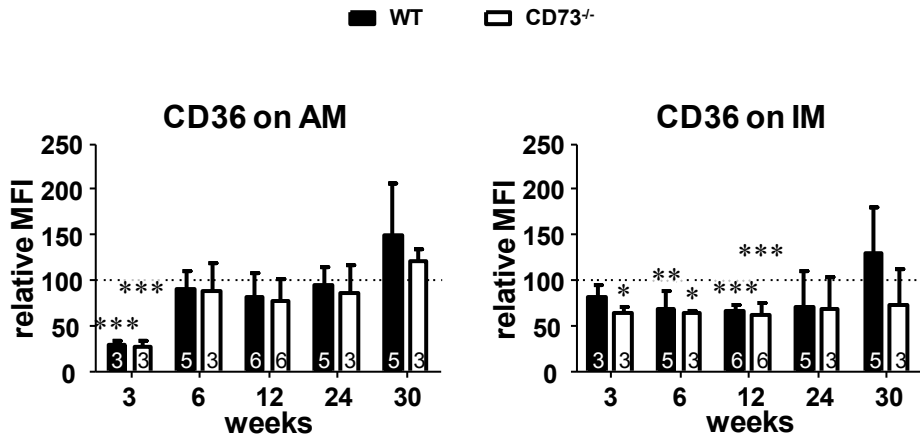


**Fig. 3.15 Analysis of CD36 expression on lung macrophages.** C57BL/6 wild type (WT) and CD73<sup>-/-</sup> mice received 0 Gy or 15 Gy whole thorax irradiation. Lung tissue isolated at 3, 6, 12, 24 and 30 weeks was used in flow cytometry staining. Alveolar (AM) and infiltrating macrophages (IM) were investigated for the expression of the scavenger receptor CD36. Timelines show mean values ± SD of the geomean fluorescence intensity (MFI) normalized with respective MFIs of the same populations isolated from control animals. For each time point the number of mice used is indicated within the bars (\*= 0 Gy vs 15 Gy) (\* p≤0.05; \*\* p≤0.01; \*\*\* p≤0.001; two-tailed unpaired t-test).

FACS analysis was also used to elucidate the dysregulation of lipid metabolism observed in lung macrophages after radiation treatment. In monocytes/macrophages one of the molecules responsible for oxLDL recognition, internalization and subsequent foam cell formation is the scavenger receptor CD36 (Rahaman et al., 2006). Therefore, expression of this protein was followed overtime on alveolar and infiltrating macrophages (**Fig. 3.15**). The 3 weeks time point was the most critical with regard to alveolar macrophages, when CD36 surface expression was reduced to less than 1/3<sup>rd</sup> as compared to control cells, with no significant changes at later time points. On the contrary, most of the effects were noticed in infiltrating macrophages, which, in both mouse strains, constantly downregulated CD36 during the inflammatory phase. CD36 expression slowly reached control levels during the late phase, with a slight increase in WT mice at 30 weeks.

### 3.1.6.3 Flow cytometric analysis of macrophages - Adenosinergic pathway

As already mentioned, the absence of CD73 seemed to protect mice from late side effects of thorax irradiation. Due to the diffuse presence of this enzyme on the surface of several immune cell types and the immunoregulatory properties of adenosine, the expression of CD39 and CD73 was additionally investigated on lung macrophages over time.

Once more, histograms of flow cytometric analyses show relative values of irradiated mice compared to respective sham irradiated animals. Whole thorax irradiation led to a distinct response in the regulation of the two ecto-enzymes on lung macrophages, in comparison to the one that has been already described for T lymphocytes. Indeed, significant overexpression of CD39 on alveolar macrophages (AM) and especially in C57BL/6 wild type mice was early occurring and persisted throughout the time points analysed, but little or no effects were observed on the infiltrating population (**Fig. 3.16**). In details, the two mouse strains showed a similar regulation of CD39 expression over time, with the only exception at 3 weeks, when a 2.9-fold and 2.1-fold increases were measured in WT and CD73 mice, respectively. It is important to underline that the highest expression of CD39 specifically arose when this cell population was profoundly affected by IR (**Fig. 3.6 E**).

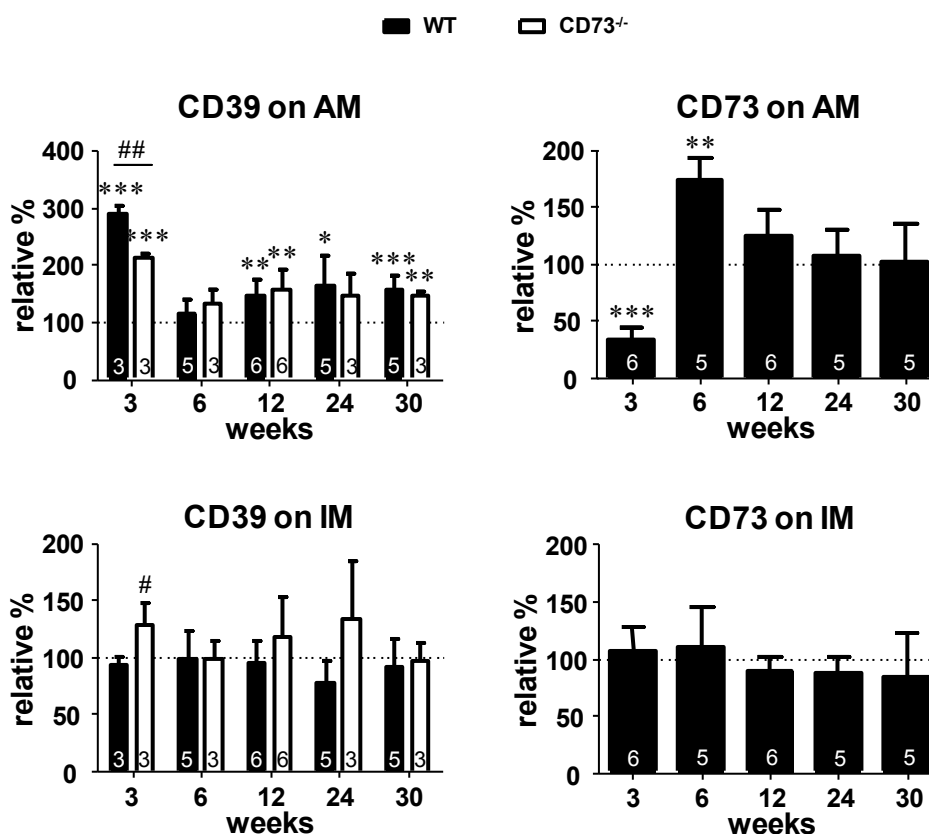


**Fig. 3.16** Determination of CD39 and CD73 expression on macrophages by flow cytometry. C57BL/6 wild type (WT) and CD73<sup>-/-</sup> mice received 0 Gy or 15 Gy whole thorax irradiation. At 3, 6, 12, 24 and 30 weeks time points lung tissue was used for cell isolation and antibody staining for alveolar or infiltrating macrophages in combination with anti-CD39 and anti-CD73 antibodies. To compare radiation effects in WT and CD73<sup>-/-</sup> mice, timelines show mean values  $\pm$  SD calculated in treated mice normalized with respect to control values. For each analysis the number of mice used is indicated within the bars (\*= 0 Gy vs 15 Gy; #= WT vs CD73<sup>-/-</sup>) (\*, #  $p \leq 0.05$ ; \*\*, ##  $p \leq 0.01$ ; \*\*\*, ###  $p \leq 0.001$ ; two-tailed unpaired t-test).

A distinct regulation of CD73 was found in WT mice. At week 3 alveolar macrophages significantly decreased their surface expression of CD73 in comparison to control mice. The observed reduction was rapidly followed by a significant upregulation at week 6, when irradiation led to a 1.7-fold increase of CD73 on AM. The alveolar population gradually restored normal surface expression at later time points, with no significant changes in the late fibrotic phase. Again, infiltrating macrophages (IM), similarly to what has been depicted for the ecto-enzyme CD39, were not affected by irradiation in their expression of CD73.

It is worth to remark a discrepancy in the regulation of the two ecto-enzymes involved in the adenosine formation, with radiation altering CD39 surface expression on alveolar

macrophages throughout the time points analysed, and CD73 surface expression only in the very early phase of pneumonitis.

#### 3.1.6.4 Flow cytometric analysis of macrophages – M1 and M2 phenotype

To corroborate data about macrophage activation obtained at a histological level, changes in the percentage of M1 and M2 macrophages in the lung tissue were determined by flow cytometry. Whole lung cells were stained for macrophages in combination with the markers MHCII and MMR to detect M1 or M2 phenotypes, respectively. Histograms in **Fig. 3.17 A** and **B** show timelines with values of fluorescence intensity measured in cells isolated from treated mice normalized with values of respective negative controls. The radiation treatment induced similar reactions in WT and CD73<sup>-/-</sup> mice in regard to the expression of MHCII on alveolar macrophages. At week 3 p.i., an acute increase of 12.5-folds in WT mice and 11.9-folds in CD73 mice was followed by the maintenance of increased, but lower levels of MHCII. While the inflammatory marker was still significantly upregulated at week 30 p.i. on CD73 deficient macrophages, WT mice showed only a trend in the increase of MHCII at this time point. No significant alterations in MHCII surface expression were detected in infiltrating macrophages in response to IR.

As expected, alveolar macrophages showed a complete opposite regulation of the M2 marker MMR when compared to the M1 marker MHCII. At almost all time points analysed, a constant trend to a downregulation of this marker was measured in irradiated mice as compared to controls. At week 3 MMR was critically and differently reduced on macrophage surface in both WT and CD73<sup>-/-</sup> mice. At later time points no or few changes were observed. Of note, MMR was largely upregulated in irradiated WT mice at week 30 p.i., pointing to the appearance of M2 macrophages in the fibrotic phase. Unfortunately, data concerning MMR staining for AM in CD73<sup>-/-</sup> mice at 24 and 30 weeks are not available, so that a comparison between the two mouse strains at these time points is not achievable. The regulation of MMR expression in infiltrating macrophages, even though a significant difference between WT and CD73<sup>-/-</sup> mice was observed during the pneumonitic phase, did not show drastic changes when comparing irradiated mice to the corresponding controls.



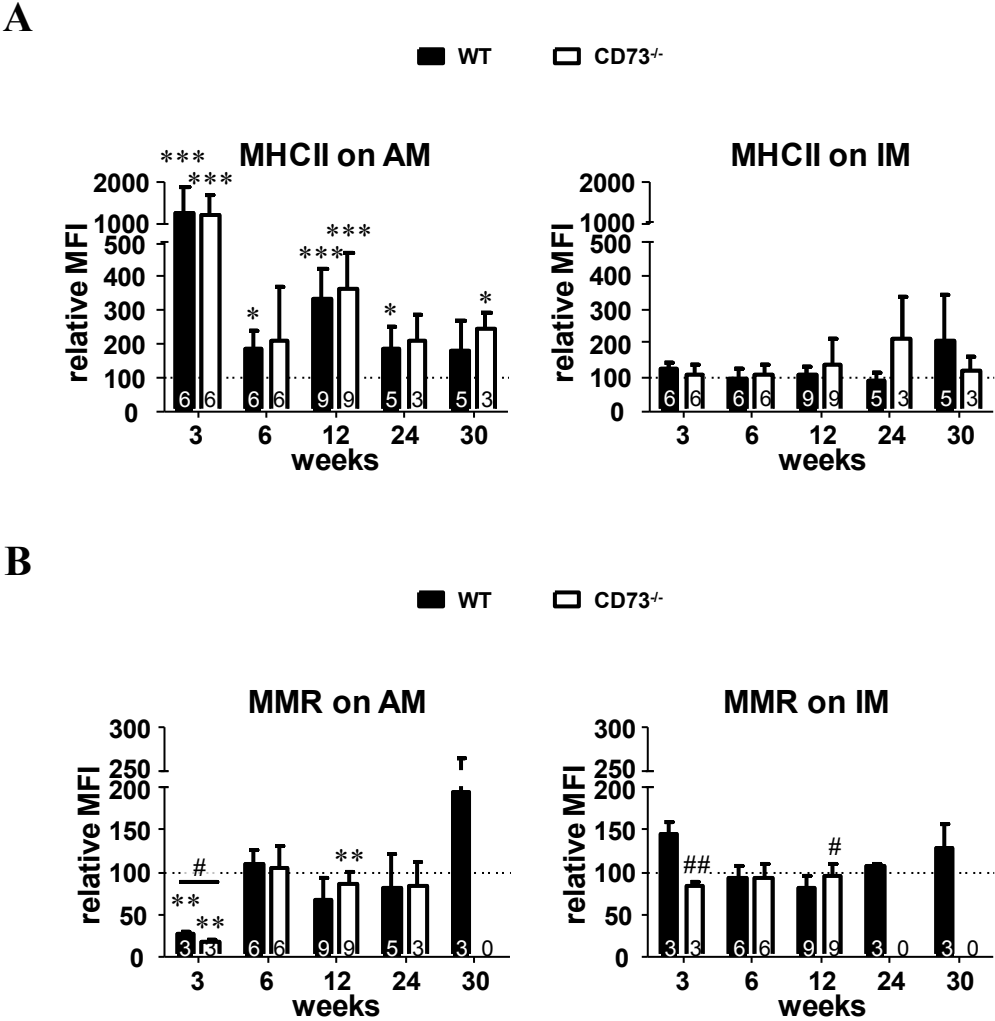


**Fig. 3.17 Analysis of M1 and M2 phenotypes on lung macrophages by flow cytometry.** C57BL/6 wild type (WT) and CD73<sup>-/-</sup> mice received 0 Gy or 15 Gy whole thorax irradiation. Lung tissue isolated at 3, 6, 12, 24 and 30 weeks was used in flow cytometry staining. Alveolar (AM) and infiltrating (IM) macrophages were investigated for the surface expression of MHCII (A) and MMR (B). Timelines show mean values ± SD of the geomean fluorescence intensity (MFI), normalized with respective MFIs of the same populations isolated from control animals. For each time point, the number of mice used is indicated within the bars (\*= 0 Gy vs 15 Gy; #= WT vs CD73) (\*, # p≤0.05; \*\*, ## p≤0.01; \*\*\* p≤0.001; two-tailed unpaired t-test).

Altogether these data indicated that whole thorax irradiation triggers time-dependent changes in the macrophage compartment. Mainly alveolar macrophages of WT and CD73<sup>-/-</sup> mice were differentially affected in their activation state, phenotype and surface expression of CD39 and

CD73, suggesting an active role of these cells in the progression of radiation-induced lung injury.

It might be that the presence of immunosuppressive T cells or of specific T cell subsets is necessary to drive, influence or keep in check the activated cells from the innate and adaptive immune system and to control inflammation-associated tissue damage in the pneumonitic phase. However, an unregulated generation of immunosuppressive cells in the late phase may facilitate fibrosis development.

### 3.2 The contribution of lymphocytes in radiation-induced pneumopathy

To gain insight into the functional relevance of lymphocytes in radiation-induced pneumopathy RAG-2<sup>-/-</sup> mice were enrolled in the study. This mouse strain is lacking mature T and B lymphocytes due to a total inability to initiate V(D)J rearrangement (Shinkai et al., 1992) and therefore represents a useful tool to explore the innate immune response to radiation.

#### 3.2.1 Radiation induced changes in body weight and survival

As previously described, following radiation treatment the body weight of RAG-2<sup>-/-</sup> mice (RAG2) have been monitored weekly for the entire experimental span, and  $\Delta$  weight values were compared with C57BL/6 wild type (WT) mice (**Fig. 3.18 A**).

As expected, control WT and RAG-2<sup>-/-</sup> mice continuously gained in weight until week 24, though to a different extent. Irradiated WT mice, as mentioned in par. 3.2, reached the maximum weight gain at week 22, thereafter slowly decreasing to a  $\Delta$  value of  $1.4 \pm 3.1$  g at week 24 p.i.. On the contrary, in the first week after treatment RAG-2<sup>-/-</sup> mice showed an early weight loss, thereafter recovering until week 8, and with no relevant changes until week 21. In the last 3 weeks of the experiment, irradiated RAG-2<sup>-/-</sup> mice had a rapid decrease in weight reaching approximately the mean starting body weight at week 24. The statistical comparison of  $\Delta$  weight values showed highly significant differences between irradiated and respective

control mice, and interestingly also between irradiated WT and RAG-2<sup>-/-</sup> mice, suggesting that the fibrotic disease may be more pronounced in the absence of T and B cells.

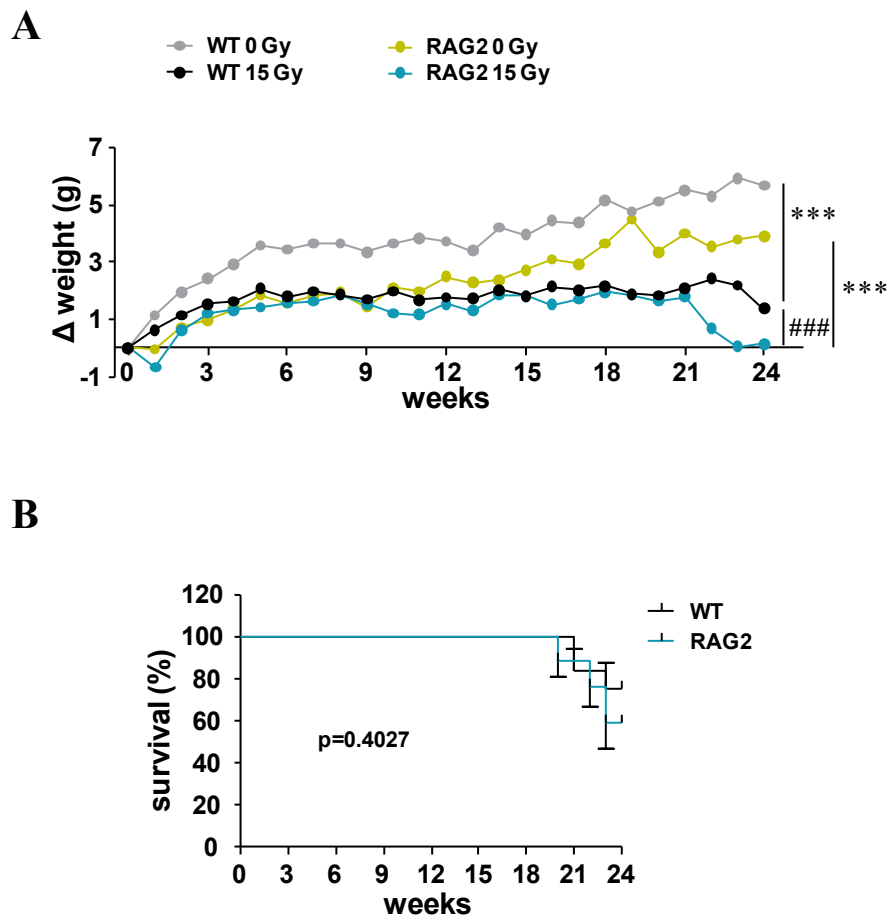


**Fig. 3.18 Changes in body weight and survival in RAG-2<sup>-/-</sup> mice.** Weights and survival of RAG-2<sup>-/-</sup> mice (RAG2) were monitored over time after 15 Gy whole thorax irradiation or sham irradiation, and compared to C57BL/6 wild type mice (WT). **A**) Changes in body weight are represented as mean delta values ( $\Delta$  weight = weight at day X – weight at day 0). Significant difference was calculated using two-way ANOVA test (\*\*\*,###  $p \leq 0.001$ ). **B**) Kaplan-Meier survival curves showing survival percentages of irradiated RAG2 (n=17) and WT mice (n=12). The p value calculated by the log-rank (Mantel-Cox) test is indicated.

Survival percentages of the two mouse strains mice were plotted in the Kaplan–Meier curve. As depicted in **Fig. 3.18 B**, WT and RAG-2<sup>-/-</sup> mice exhibited similar mortality rates after

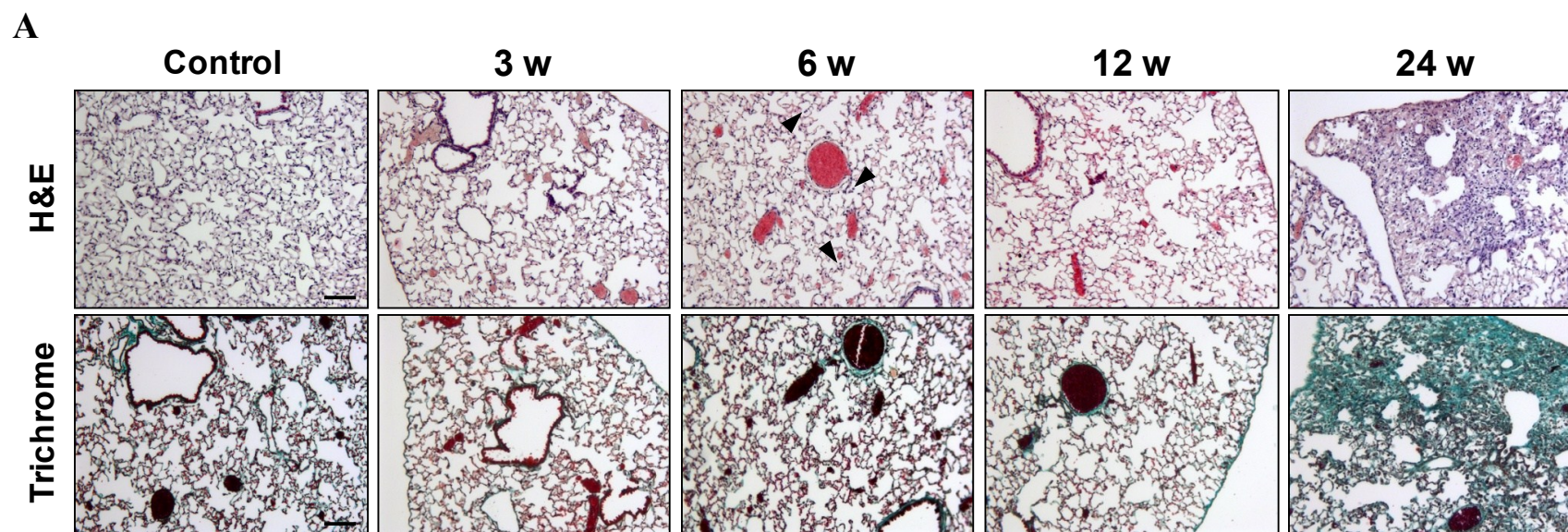
whole thorax irradiation, with percentages corresponding to  $75.0 \pm 12.5$  and  $58.9 \pm 12.0$ , respectively.

### 3.2.2 Histological changes of lung tissues in irradiated RAG-2<sup>-/-</sup> mice

To assess damage after thorax irradiation, lung tissue of irradiated and control RAG-2<sup>-/-</sup> mice was isolated and processed for histological analyses. As shown in **Fig. 3.19 A**, early tissue reactions to irradiation are not obvious by histological analysis of lung sections, even though an increase in inflammatory cell infiltrate is evident at 6 weeks post irradiation (solid arrows). Surprisingly, as a late event, all mice enrolled in the experiment showed enhanced collagen deposition and lung fibrosis already at week 24 after thorax irradiation with 15 Gy, therefore earlier in comparison to C57BL/6 wild type mice.

The increased sensitivity to fibrosis of RAG-2<sup>-/-</sup> mice was further evaluated by immunohistochemical staining of lung sections. Fibrotic areas within the tissue showed high positivity for the presence of the fibrotic markers  $\alpha$ -SMA and TGF- $\beta$  (**Fig. 3.19 B**). In contrast, sham irradiated mice clearly had normal lung structures, with no detectable tissue alterations indicative of fibrosis at this time point.

In order to assess whether the increased sensitivity of RAG-2<sup>-/-</sup> mice to radiation-induced late effects was exclusively a kinetic issue, or was possibly resulting in a higher degree of fibrosis compared to C57BL/6 wild type mice, a quantitative assessment of the extent of lung fibrosis was made. At this purpose, the percentage of fibrotic areas and the number of fibrotic foci per mouse were quantified in both strains. Fibrosis affected almost 20 % of the lung surface in RAG-2<sup>-/-</sup> mice ( $18.0 \pm 13.6$  %), whereas less than 10 % of lung tissue was fibrotic in WT mice ( $6.5 \pm 7.8$  %). Median values represented in the scatter dot plot are equal to 3.1 % for WT mice and 10.4 % for RAG-2<sup>-/-</sup> mice (**Fig. 3.20 A**). The tendency to a higher extent of fibrosis in RAG-2<sup>-/-</sup> mice was associated with a significant increase in the number of fibrotic foci in respect to WT mice, as shown by median values corresponding to 11.7 and 4.7, respectively (**Fig. 3.20 B**).



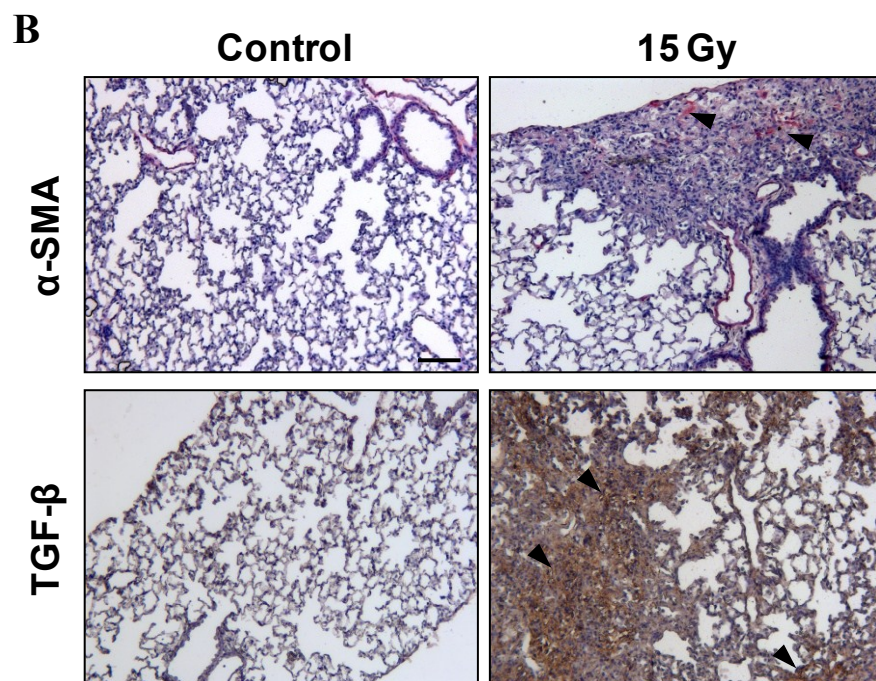


**Fig. 3.19 Lung histological changes in RAG-2<sup>-/-</sup> mice.** Lung tissues were obtained 3, 6, 12 and 24 weeks (w) after whole thorax irradiation with 15 Gy or 0 Gy. **A)** Representative light microscopy pictures of hematoxylin and eosin (H&E) and Masson-Goldner trichrome stained lung sections at all time points analysed. Increased presence of inflammatory cells (solid arrows) was found in lung sections of mice at 6 weeks post irradiation (magnification x100; scale bar: 100 μm). **B)** Representative light microscopy pictures of immunohistochemical stainings for the markers α-SMA and TGF-β on sections of control and irradiated mice at 24 weeks (magnification x100; scale bar: 100 μm). Positive staining within fibrotic areas is indicated by solid arrows.

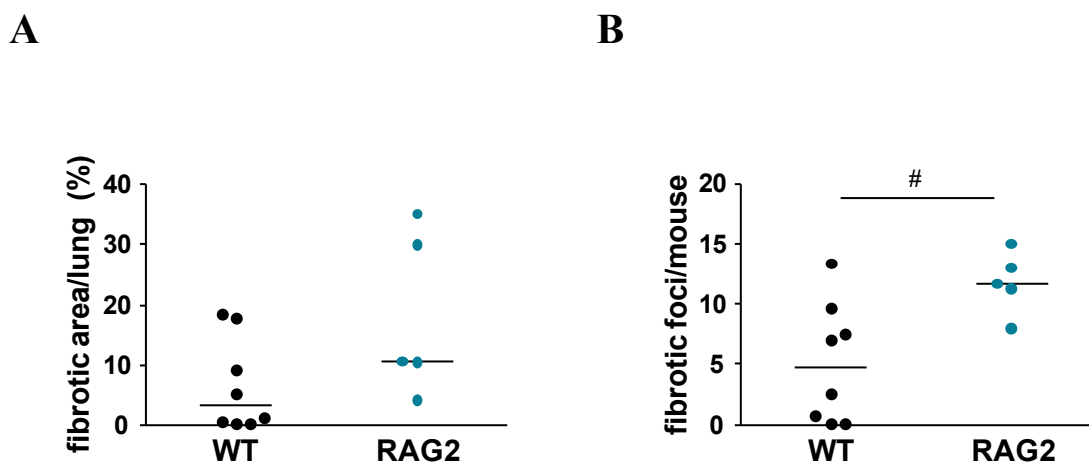


**Fig. 3.20 Quantitative analysis of fibrosis in C57BL/6 wild type and RAG-2<sup>-/-</sup> mice.** Lung sections were obtained from C57BL/6 wild type (WT) and RAG-2<sup>-/-</sup> (RAG2) mice 24 weeks after 15 Gy whole thorax irradiation, stained with H&E and analysed for the amount of fibrosis and the number of fibrotic foci. **A)** Quantification of fibrosis extent in mice 24 weeks after irradiation expressed as percentage of lung area showing fibrosis. **B)** Quantification of fibrotic foci in mice 24 weeks after irradiation. Data represent median values obtained in  $\geq 3$  sections per mouse with a minimum distance of 250  $\mu\text{m}$  in depth (#  $p < 0.05$ ; two-tailed unpaired t-test).

### 3.2.3 Cellular changes of lung tissues in irradiated RAG-2<sup>-/-</sup> mice

To elucidate how the lack of lymphocytes could impact on the infiltration of immune cells in the lung and to independently confirm the increased infiltration observed by histological staining at 6 weeks p.i., tissues from RAG-2<sup>-/-</sup> mice were evaluated by flow cytometry. Due to the absence of cells belonging to the adaptive immune system, exclusively the presence of total leukocytes, macrophages and granulocytes could be compared to the results obtained in C57BL/6 wild type (WT) mice. At 6 weeks (**Fig. 3.21 A**), RAG-2<sup>-/-</sup> mice showed in all cell populations analysed a similar tendency as the one observed in WT mice. In detail, the percentage of leukocytes in RAG-2<sup>-/-</sup> mice increased, whereas granulocyte population was not affected by irradiation. Alveolar macrophages showed a limited increase after treatment whereas a slight but significant infiltration of newly recruited macrophages was noted after 15 Gy irradiation.



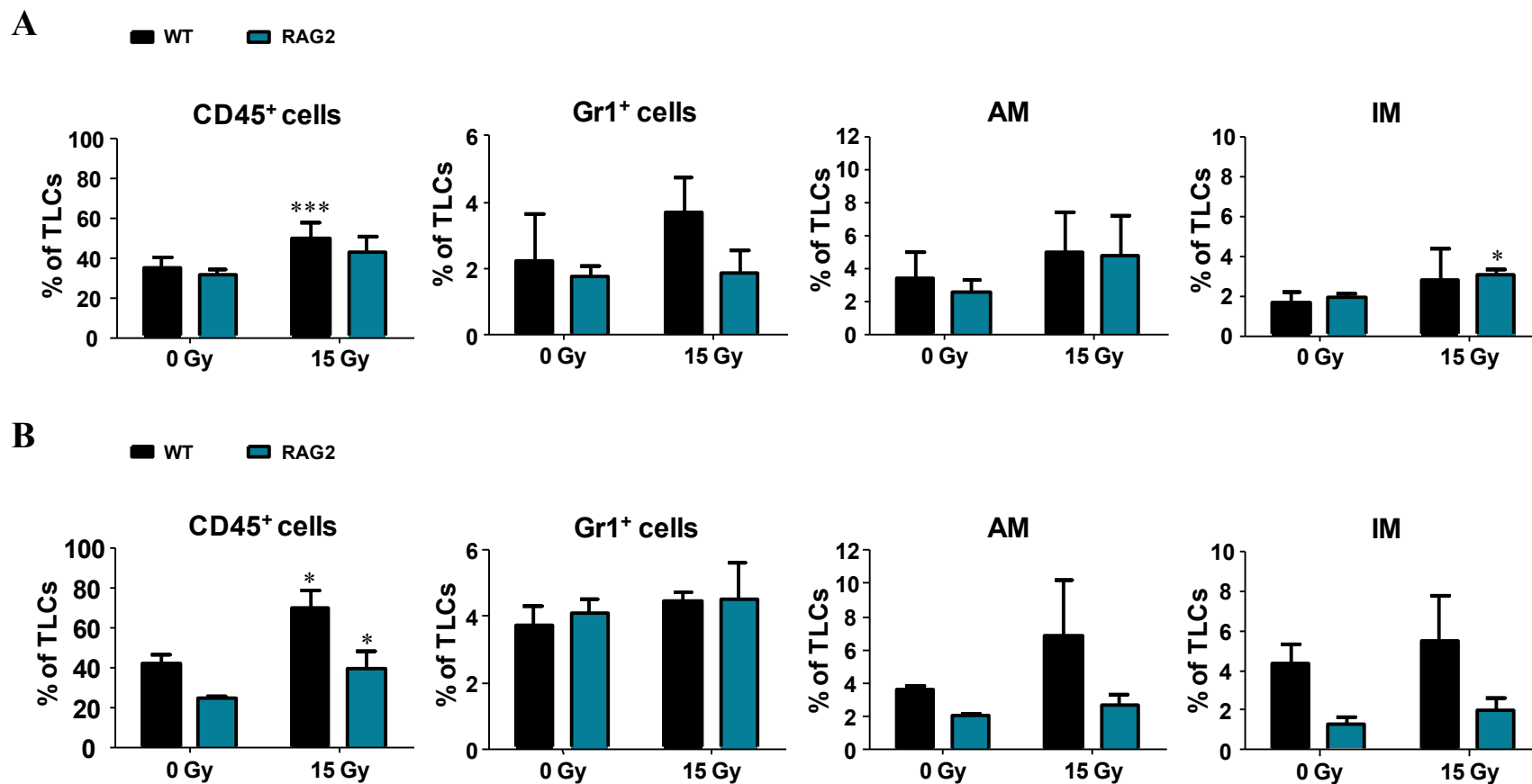


**Fig. 3.21 Determination of leukocyte content in lung tissue.** C57BL/6 wild type (WT) and RAG-2<sup>-/-</sup> mice (RAG2) received 0 Gy or 15 Gy whole thorax irradiation. At 6 (A) and 24 (B) weeks time points lung tissue was digested and used for cell isolation and antibody staining for total leukocytes (CD45<sup>+</sup>), granulocytes (Gr1<sup>+</sup>) and alveolar (AM - F4/80<sup>+</sup>CD11c<sup>+</sup>) or infiltrating (IM - F4/80<sup>+</sup>) macrophages. Shown are mean values  $\pm$  SD of percentages calculated on total lung cells (TLCs). Cells of  $\geq 2$  mice per group were analyzed (\*  $p < 0.05$ ; \*\*\*  $p < 0.001$ ; two-tailed unpaired t-test to respective controls).



When analysing lung immune cells at 24 weeks post irradiation (**Fig. 3.21 B**), once again RAG-2<sup>-/-</sup> mice showed a similar tendency to the one seen in WT mice. The percentage of leukocytes significantly increased of approximately 1.6-folds in both strains after irradiation, and a slight increase was detected in the amount of Gr1 positive cells and macrophages. Remarkably, CD45 positive cells, alveolar macrophages, as well as infiltrating macrophages were significantly lower in RAG-2<sup>-/-</sup> mice as compared to WT mice, respectively with p values of 0.0004, 0.0102 and 0.0014 as measured by two-way ANOVA test. In the specific alveolar macrophages showed 1.9-fold and 1.3-fold increase in WT and RAG-2<sup>-/-</sup> mice respectively, while infiltrating macrophages 1.2-fold and 1.6-fold increase in WT and RAG-2<sup>-/-</sup> mice, respectively.

### 3.2.4 Macrophage characterization

In RAG-2<sup>-/-</sup> mice the lack of B and T lymphocytes leads to an inflammatory response exclusively driven by cells of the innate immunity. Thus, it was important to determine whether macrophages, despite a little change in their percentages, could display altered protein expression, focusing on the same markers analysed in C57BL/6 wild type and CD73<sup>-/-</sup> mice (par. 3.1.6.2, 3.1.6.3 and 3.1.6.4). In **Fig. 3.22**, regulation of CSF-1 receptor (**A**) and CD36 scavenger receptor (**B**) on RAG-2<sup>-/-</sup> alveolar and infiltrating macrophages is shown as relative expression to respective values obtained in sham irradiated mice. In detail, alveolar macrophages of WT mice and RAG-2<sup>-/-</sup> mice displayed a similar expression of CSF-1R at 6 and 24 weeks p.i., but an upregulated expression of the scavenger receptor at 24 weeks p.i..

The scavenger receptor CD36 was indeed 1.4-fold upregulated on alveolar macrophages of RAG-2<sup>-/-</sup> mice, while as previously shown, no changes of this marker were found on lung macrophages of WT mice. Infiltrating macrophages of RAG-2<sup>-/-</sup> mice did not show changes overtime in their expression of CSF-1R and CD36.

To explore the impact of whole thorax irradiation on the adenosinergic pathway in the absence of B and T lymphocytes, lung macrophages were additionally analysed for surface expression of CD39 and CD73. **Fig. 3.23** shows comparison of average values  $\pm$  SD between RAG-2<sup>-/-</sup> and WT mice. Also in RAG-2<sup>-/-</sup> mice alveolar macrophages were more affected by irradiation compared to infiltrating macrophages.

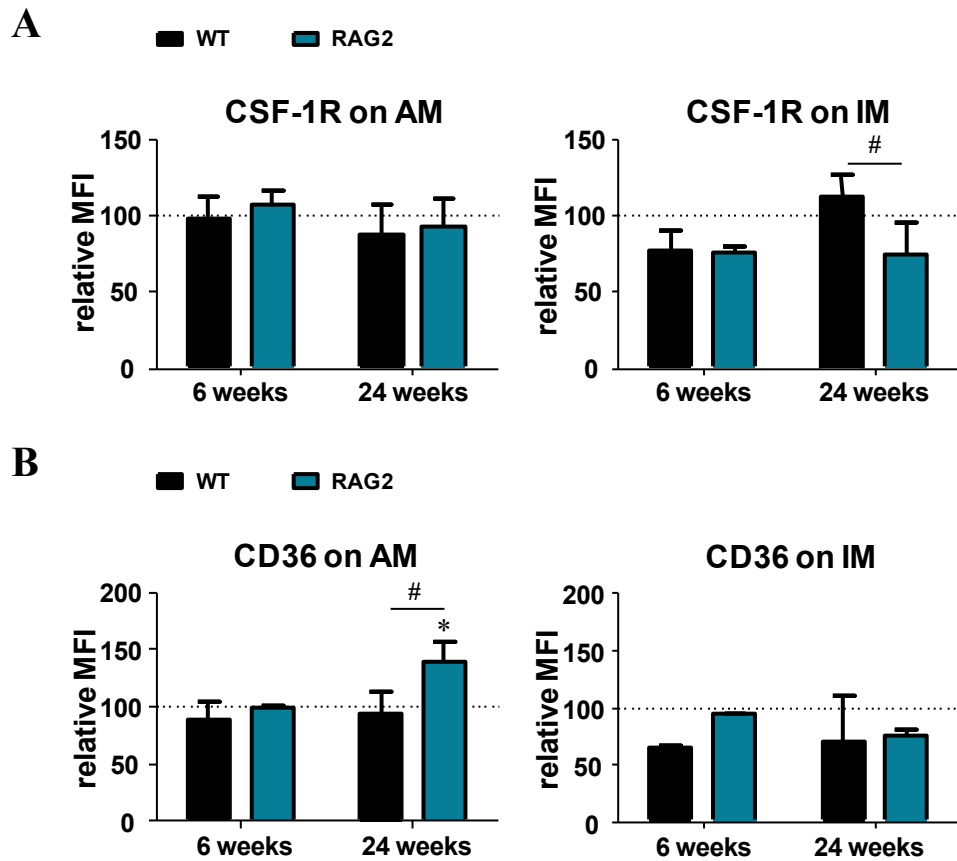


**Fig. 3.22 Determination of macrophage characteristics.** C57BL/6 wild type (WT) and RAG-2<sup>-/-</sup> mice (RAG2) received 0 Gy or 15 Gy whole thorax irradiation. Alveolar macrophages (AM) and infiltrating macrophages (IM) were investigated at 6 and 24 weeks time points for the expression of CSF-1 receptor (A) and CD36 scavenger receptor (B). Shown are mean values  $\pm$  SD of the geometric fluorescence intensity (MFI), normalized with respective MFIs of the same populations isolated from control animals. Cells of  $\geq 2$  mice per group were analyzed (\*= 0 Gy vs 15 Gy; #= WT vs RAG2) (\*,#  $p \leq 0.05$ ; two-tailed unpaired t-test).

Alveolar macrophages of RAG-2<sup>-/-</sup> mice showed even a higher but not significant increase (2.3-folds) in the expression levels of CD39 compared to those isolated from WT mice (1.6-folds) at 24 weeks.

Surprisingly, whole thorax irradiation failed to upregulate CD73 in alveolar macrophages of RAG-2<sup>-/-</sup> mice at the two time points analysed, in contrast to the high upregulation of this enzyme observed in WT mice at 6 weeks. In infiltrating macrophages almost no differences were found in the surface expression of CD73 and CD39 in both mouse strains in response to whole thorax irradiation, with the only exception of a slight CD73 downregulation in RAG-2<sup>-/-</sup> mice at 24 weeks (Fig. 3.22 B).

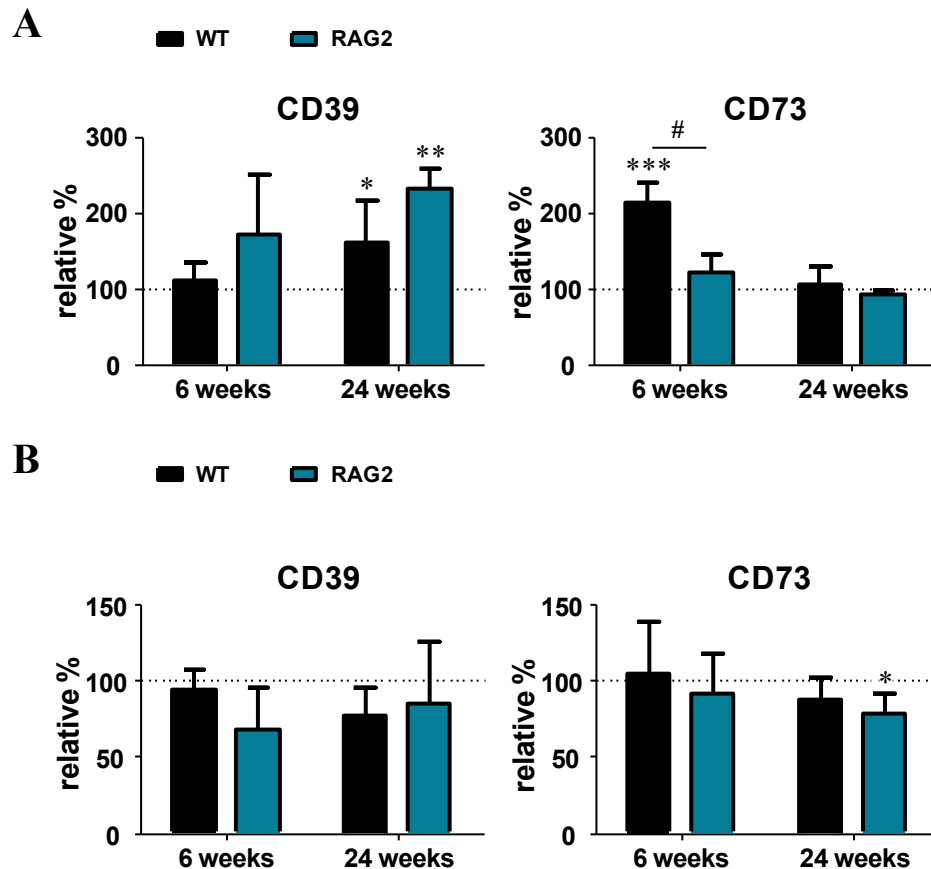


**Fig. 3.23 Determination of CD39 and CD73 expression on lung macrophages.** C57BL/6 wild type (WT) and RAG-2<sup>-/-</sup> mice (RAG2) received 0 Gy or 15 Gy whole thorax irradiation. Alveolar macrophages (A) and infiltrating macrophages (B) were investigated at 6 and 24 weeks time points for the expression of CD39 and CD73. Results are compared with values obtained in C57BL/6 wild type mice (WT). Shown are mean values ± SD of percentages of CD39 or CD73 surface expression on macrophage cells, normalized with respective values obtained from sham irradiated mice. Cells of ≥2 mice per group were analyzed (\*, # p≤0.05; \*\* p≤0.01; \*\*\* p≤0.001; two-tailed unpaired t-test)

To gain insight into potential differences in macrophage activation state in irradiated WT and RAG-2<sup>-/-</sup> mice, it was analysed whether whole thorax irradiation would differentially affect polarization of macrophages into pro-inflammatory (M1) or pro-regenerative (M2) phenotypes. As shown in **Fig. 3.24**, alveolar macrophages of RAG-2<sup>-/-</sup> and WT mice displayed an inflammatory M1 phenotype as an early and late response, almost reaching a 4-fold increase in MHCII surface expression relatively to control MFIs at 24 weeks p.i.. At all time points, the extent of MHCII upregulation was significantly higher in RAG-2<sup>-/-</sup> mice compared to the one detected in WT mice. Effects of radiation on the M2 polarization were comparable in the two mouse strains, though a significant increase (1.2-folds) in alternative activation was present

only in RAG-2<sup>-/-</sup> mice at 6 weeks p.i.. Newly recruited macrophages seemed not to polarize towards an M1 or M2 phenotype in response to tissue irradiation, although a tendency of MHCII upregulation was noted at the time points under investigation (data not shown).

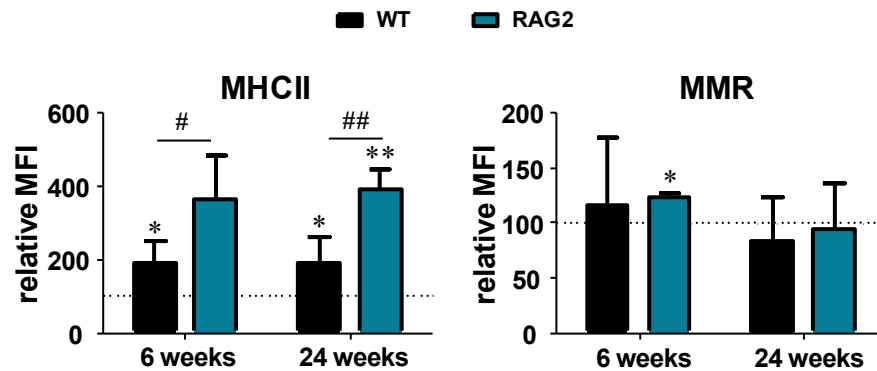


**Fig. 3.24 Determination of alveolar macrophage polarization.** C57BL/6 wild type (WT) and RAG-2<sup>-/-</sup> mice (RAG2) received 0 Gy or 15 Gy whole thorax irradiation. Alveolar macrophages were investigated at 6 and 24 weeks p.i. for the expression of MHCII and MMR. Shown are mean values  $\pm$  SD of the geometric fluorescence intensity (MFI) normalized with respective MFIs of the same populations isolated from sham irradiated mice. Cells of  $\geq 2$  mice per group were analyzed (\*,#  $p \leq 0.05$ ; \*\*,##  $p \leq 0.01$ ; two-tailed unpaired t-test).

## 4 Discussion

Radiation therapy is one of the most important approaches used in the treatment of patients with thoracic and hematologic malignancies. Albeit many progresses have been made in the field of radiotherapy, this therapeutic intervention can generate indirect and adverse effects on normal host tissue. At present, radiation-induced injuries to the lung, known as pneumonitis and fibrosis, still constitute a major complication in the treatment of thorax-associated cancer patients. To date, the molecular mechanisms governing the onset and progression of radiation-induced early and late side effects on the lung tissue are not entirely understood. Moreover, conflicting results have been obtained in the effort to explain a direct link between inflammation and fibrosis development after lung injury.

Therefore, within the present work a mouse model of whole thorax irradiation was used to investigate the role of the CD73/adenosine system of the innate and adaptive immune responses in the pathogenesis of radiation-induced pneumonitis and fibrosis with the ultimate goal to identify novel therapeutic targets for prevention or treatment of early and late radiation-induced lung injuries.

The present work shows for the first time that loss of CD73 protects from radiation-induced fibrosis and that lack of mature T and B cells in RAG-2<sup>-/-</sup> mice causes increased collagen deposition and fibrosis. Notably, loss of CD73 or of mature T and B cells was associated with alterations in the polarization/activation state of specific immune cells suggesting a role of the innate and adaptive immune systems in the pathogenesis of radiation-induced fibrosis.

In more detail, loss of CD73 was associated with a decreased sensitivity to radiation-induced lung fibrosis. Despite a clear trend to decreased collagen deposition in the irradiated lung tissue of CD73<sup>-/-</sup> mice, the semiquantitative evaluation of the extent of lung fibrosis in the two strains failed to detect significant differences between C57BL/6 wild type (WT) and CD73<sup>-/-</sup> mice. This may at least be partially due to some “non-responders” in the WT strain and to the low number of animals analysed. It will be necessary to corroborate the fibrotic changes observed at histological levels with the use of methods such as hydroxyproline or Sircol assays, in order to have a whole lung quantitative analysis of collagen content, and thus of fibrosis development. Nevertheless, deficiency of CD73 was not only associated with decreased collagen deposition but also with a reduced loss of body weight in the irradiated mice when compared to WT mice. This observation corroborates a better general health condition in CD73 deficient mice. In both

strains, few irradiated mice died within the first 10 weeks p.i., and thus probably due to radiation-induced pneumonitis. However, death rates were rather similar during the pneumonitic phase between WT and CD73<sup>-/-</sup> mice. In line with these findings, histological analyses did not show marked differences in the two strains during the pneumonitic phase post irradiation (p.i.) (3-12 weeks). Some mice also died during the time of expected fibrosis development, resulting in a final survival rate that was slightly higher in CD73<sup>-/-</sup> mice. However, 15 Gray (Gy) whole thorax irradiation is usually not sufficient to induce high death rates, although extensive collagen deposition and fibrosis development can be observed.

In addition, the immunostaining results showed that lung sections of WT animals were highly positive for the fibrotic markers  $\alpha$ -SMA and TGF- $\beta$ , whereas CD73 deficient mice showed normal distribution of  $\alpha$ -SMA (around blood vessels and bronchial airways), and no or weak staining for TGF- $\beta$ . These results further corroborate that the two strains differently respond to whole thorax irradiation and, in particular, that CD73<sup>-/-</sup> mice are less sensitive to radiation-induced lung fibrosis. Even more important, it was shown for the first time that in WT mice whole thorax irradiation triggers a time-dependent increase in lung tissue hypoxia, with macrophages being positively stained already at early time points p.i.. Thus, the presence of hypoxia as a consequence of radiation-induced lung injury could result from an increased oxygen consumption by activated macrophages and, in a later phase, from a more general impairment of the normal blood perfusion and gas exchange within the fibrotic lung tissue. Temporal changes in tissue oxygenation have also been found in lung tissue of rats receiving 28 Gy hemithorax irradiation. At week 6 p.i. moderate hypoxia was observed, with gradual increase to severe hypoxia until week 20 p.i.. In these reports, authors proposed hypoxia to be one of the driving forces in initiating and perpetuating radiation induced lung injury (Fleckenstein et al., 2007b; Vujaskovic et al., 2001). Moreover, hypoxia-inducible factor-1 $\alpha$  (HIF-1 $\alpha$ ) deficient mice showed reduced collagen and  $\alpha$ -SMA levels in a model of liver fibrosis (Moon et al., 2009). The transcription factor HIF-1 $\alpha$  is the master regulator of gene expression at low oxygen levels and its activity in normoxic condition is tightly silenced. It is important to mention that mice carrying a mutation in the von Hippel–Lindau (VHL) ubiquitin ligase, which is involved in the oxygen-dependent proteasomal degradation of HIF-1 $\alpha$ , show pulmonary remodeling, macrophage infiltration and fibrosis in the elderly as a consequence of elevated HIF-1 $\alpha$  activity (Hickey et al., 2010). The upregulation of HIF-1 $\alpha$  was also observed in a mouse model of bleomycin (BLM) induced fibrosis during the development of the disease (Tzouveleakis et al., 2007). Therefore, hypoxia could have a major role in the development of radiation-induced fibrosis observed in WT mice in the present study, resulting from

hypoxia-mediated activation of HIF-1 $\alpha$  signalling and HIF-1 $\alpha$  triggered effects. Of note, irradiated CD73<sup>-/-</sup> mice showed a delayed onset and lower levels of tissue hypoxia in association with minimal fibrosis. These observations suggest that hypoxia *per se* is not sufficient to trigger fibrosis. Rather, the presence of a HIF-1 $\alpha$  binding motif in the CD73 gene promoter may imply that the expression of this ecto-enzyme is upregulated as a consequence of tissue hypoxia, thus contributing to increased extracellular adenosine levels in hypoxic tissues (Colgan et al., 2006; Synnestvedt et al., 2002). In conclusion, the early hypoxia after radiation-induced lung injury may, via upregulation of CD73, chronically increase Ado levels and shift the balance towards pro-fibrotic events, which can in turn exacerbate hypoxia. Thus, CD73 may function as a main link between hypoxia, adenosine and fibrosis development, and its absence could be responsible for the protection of CD73<sup>-/-</sup> mice from radiation-induced pulmonary fibrosis. To prove this hypothesis it would be important to measure Ado content in the lung of irradiated WT and CD73<sup>-/-</sup> mice throughout the experimental span.

As mentioned before, many studies have shown a key role of the components of Ado metabolism and signalling in respect to chronic lung pathologies in humans and animal models. In contrast with the obtained results, in a BLM model of acute pulmonary fibrosis CD73 deficient mice challenged with intratracheal BLM displayed enhanced collagen production and deposition when compared to CD73 proficient mice, pointing to a tissue-protective role of the CD73/Ado system (Volmer et al., 2006). Most likely during acute lung injury, increased Ado could be beneficial mainly because of its anti-inflammatory effects, whereas in the radiation model of lung injury chronic elevation of Ado levels could favour the progression to fibrosis. However, the differences in Ado-mediated effects may also largely depend on the diverse activities and distribution of Ado receptors; for example, the high-affinity A<sub>1</sub> and the low-affinity A<sub>2B</sub> receptors have been identified as mediators of anti-inflammatory/tissue protective and pro-fibrotic/tissue destructive effects of adenosine, respectively (Sun et al., 2005; Sun et al., 2006).

In the attempt to find a link between radiation pneumonitis and fibrosis, it was next necessary to show whether the loss of the CD73/Ado system could differently affect the inflammatory response following thorax irradiation, thereby being responsible for the delayed tissue protection found in CD73 deficient mice. A significant infiltration of leukocytes started at week 6 p.i. in irradiated WT and CD73<sup>-/-</sup> mice. Because CD73 expression on endothelial cells has been implicated in tissue barrier function (Koszalka et al., 2004; Lennon et al., 1998), an increased recruitment of immune cells after injury in CD73 deficient mice was expected

(Zernecke et al., 2006). However, CD73<sup>-/-</sup> mice displayed the same ability as WT mice to recruit immune cells to the site of injury. In support of these data, CD73 has been proposed to mediate cell adhesion processes, in that antibodies directed to CD73 could interfere with the binding of human lymphocytes to cultured endothelium (Airas et al., 1995). In addition, CD73 deficient mice maintained higher levels of cellular infiltrates, mainly granulocytes and T cells, until week 30 p.i. suggesting a different ability in the resolution of inflammation after whole thorax irradiation compared to WT mice.

The early drop in T cell and macrophage numbers at week 3 p.i. corroborated a suggested immunosuppressive action of whole thorax irradiation. Surprisingly, the lack of functional CD73 resulted in a less pronounced immunosuppressive effect at this time point. This observation suggests for the first time that the lack of endogenous CD73 leads to a lower sensitivity of lymphocytes to radiation-induced cell death, or to an accelerated recruitment/proliferation of macrophages and T cells after whole thorax irradiation.

Interestingly, radiation effects on CD3<sup>+</sup> cells mainly occurred during the pneumonitic phase and confirmed the radiation-induced increase in T lymphocytes, mainly CD4<sup>+</sup> T cells, typically observed in cancer patients in the so-called alveolar lymphocytosis (Cordier et al., 1984; Gibson et al., 1988; Martin et al., 1999; Nakayama et al., 1996; Roberts et al., 1993). In contrast, in normal conditions C57BL/6 wild type and CD73<sup>-/-</sup> mice have similar cellular composition of lymphoid organs and lymphocytes show comparable proliferative capacity (data not shown)(Thompson et al., 2004).

However the subtle differences observed in the lung immune cell composition were not sufficient to explain the distinct radiation responses of C57BL/6 wild type and CD73<sup>-/-</sup> mice with respect to fibrosis development. Therefore potential differences in radiation-induced changes in T cell functions were investigated focusing on the expression of the adenosinergic pathway at first, and in a second step on T cell polarization. CD39 and CD73 expression on CD3<sup>+</sup> and CD4<sup>+</sup> T cells was differentially regulated in response to whole thorax irradiation, with CD73 being upregulated in the pneumonitic phase and CD39 in the fibrotic phase. In contrast, whole thorax irradiation did not largely affect the surface expression of the 2 ecto-enzymes on CD8<sup>+</sup> T cells. Interestingly, local changes affecting T lymphocytes in regard to sensitivity and adenosinergic pathway regulation were mirrored in T cells isolated from spleen and cervical lymph nodes of irradiated mice. These data show for the first time that whole thorax irradiation not exclusively affects the local T cell population, but also drives adaptive changes in other biological compartments besides the lung. Even more important,



these data demonstrate radiation-induced local changes in the adenosinergic pathway regulation on specific T cell populations.

CD39 and CD73 are part of the immunosuppressive machinery of regulatory T cells ( $T_{reg}$ ) (Deaglio et al., 2007; Kobie et al., 2006). Thus, a differential expression of CD73 and CD39 on (local)  $CD4^+$  T cells of irradiated mice may reflect major changes in the immunoregulatory repertoire of the cells recruited to and/or present in the irradiated lung tissue. Effectively, and mainly in WT mice, lung and peripheral  $T_{reg}$  cells increased at 3 weeks post irradiation. In light of recent reports about the increased radioresistance of these cells both *in vitro* and after whole body irradiation *in vivo* (Cao et al., 2009; Qu et al., 2010), it is not surprising that the decrease in  $CD4^+$  T cells at this time point is accompanied by a higher percentage of  $T_{reg}$  cells. Altogether, these results show for the first time local and systemic alterations in the  $T_{reg}$  cell compartment upon whole thorax irradiation, and suggest that upon radiation-induced lung injury regulatory T cells are recruited *in loco* in the early phase of pneumonitis, therefore being partly responsible for the observed upregulation of the adenosinergic pathway's members on T lymphocytes. The absence of CD73 in this regulatory system could be responsible for the ongoing local inflammation and the sustained  $T_{reg}$  cell levels observed in the periphery, as seen in  $CD73^{-/-}$  mice.

The role of  $T_{reg}$  cells during fibrogenic processes is still controversial. On one hand,  $T_{reg}$  cells may form an important homeostatic mechanism for tissues injured by radiation dampening  $T_H$  responses, regulating detrimental T cell activities, and eventually avoiding excessive immune responses. On the other hand, due to their ability to secrete anti-inflammatory cytokines, such as IL-10 and TGF- $\beta$ , they can contribute to stimulate fibroblast proliferation and activation, as well as collagen deposition. In addition, the ability of regulatory T cells to generate adenosine through the CD39/CD73 pathway should not be underestimated in this complex scenario. During acute lung injury (ALI) after intratracheal administration of LPS,  $T_{reg}$  cells played a central role in the resolution of ALI fibroproliferation by reducing fibrocyte recruitment (Garibaldi et al., 2013). In a more elegant study, the importance of CD73 on  $T_{reg}$  cells was pointed out as essential to mediate endogenous protection from ALI. In this report, lung injury of CD73 deficient mice or RAG deficient mice adoptively transferred with  $CD73^{-/-}$   $T_{reg}$  cells, was more prominent than the one showed by wild type mice or RAG deficient mice adoptively transferred with  $CD73^{+/+}$   $T_{reg}$  cells (Ehrentraut et al., 2013). Nevertheless, ALI is characterized by severe inflammation, therefore it cannot properly represent the specific environmental conditions which drive chronic fibrogenic processes. For example in a model of silica-induced lung fibrosis, it was shown that recruitment and persistence of  $T_{reg}$  cells in the lung contributed

to pulmonary fibrosis, whereas depletion of  $T_{reg}$  cells could attenuate the progress of lung fibrosis (Liu et al., 2010; Lo Re et al., 2011). A very recent study of BLM-induced lung fibrosis demonstrated that  $T_{reg}$  cells depletion with anti-CD25<sup>+</sup> antibody during the early, intermediate, and late phases of the disease could differently influence the outcome of fibrosis. In detail, inflammatory changes and collagen deposition were ameliorated by early depletion of CD4<sup>+</sup>CD25<sup>+</sup>  $T_{reg}$  cells and worsened by late depletion of CD4<sup>+</sup>CD25<sup>+</sup>  $T_{reg}$  cells. The authors suggested that the early suppressive activity of  $T_{reg}$  cells is detrimental, while the late suppressive activity of  $T_{reg}$  cells is beneficial in the chronic stage of the disease (Boveda-Ruiz et al., 2013). In contrast, preliminary experiments in our lab do not support the above hypothesis: DEREK mice depleted in the first 3 weeks p.i. of  $T_{reg}$  cells developed fibrosis at the same extent than irradiated DEREK mice with functional  $T_{reg}$  cells until 30 weeks p.i. (data not shown). At this point, it is relevant to underline that the use of the BLM model rather than the irradiation model of lung fibrosis, might not be the right tool to investigate molecular and cellular mechanisms involved in the pathogenesis of early and late side effects of radiotherapy in lung tissue in detail.

Notably, further own results demonstrate a second increase of  $T_{reg}$  cells during the fibrotic phase in WT mice (Supplementary data, **Fig 7.1**). TGF- $\beta$  is known to contribute to the maintenance of n $T_{reg}$  cells in the periphery and induces Foxp3 in naive T cells in the periphery (iT<sub>reg</sub>) (Chen et al., 2003). Therefore in a TGF- $\beta$ -rich microenvironment like the one observed at 24 and mainly at 30 weeks p.i. in WT mice, could be responsible for the expansion of  $T_{reg}$  cells at this time point. Fibrosis development after whole thorax irradiation was also accompanied by increased hypoxia, which conversely is known to inhibit  $T_{reg}$  cell differentiation through an active process that targets Foxp3 protein for degradation, in addition to directly promote  $T_H17$  differentiation (Dang et al., 2011; Sakaguchi et al., 2008). In the present study, no analysis of  $T_H17$  cells has been done. Whether alterations in the  $T_H17/T_{reg}$  cell balance could influence the chronic development of fibrosis will require additional investigations. However it should also be considered that, within a fibrotic lung, areas with different microenvironments and with different functional immune cell subsets will coexist, therefore spatially confined and distinct compartments in the tissue itself may be defined. It is highly likely that fibrotic areas comprehend molecular and cellular mediators very diverse from non-fibrotic areas.

Whole thorax irradiation could alter many of the features of the T lymphocyte population, therefore it was interesting to analyze radiation-induced changes on the most represented immune cell population in the lung: macrophages.

It is widely demonstrated that lung irradiation leads to resident macrophage depletion followed by rapid expansion of this population through recruitment of new cells or local proliferation, and a further increase in the late fibrotic phase (Chiang et al., 2005; Hong et al., 2003). Therefore, the early drop in macrophage percentages at week 3 p.i. was expected due to the cytotoxic damage of radiation. However, percentages of AM isolated from CD73<sup>-/-</sup> mice were significantly higher as compared to AM of irradiated WT mice, suggesting again a lower sensitivity to radiation or an accelerated recruitment/proliferation of macrophages after whole thorax irradiation in these mice. Possibly, the lower sensitivity may lead to a faster or more efficient resolution of radiation-induced responses in CD73<sup>-/-</sup> mice (24 weeks p.i.). On the contrary, the progressive increase of AM in irradiated WT mice associated to fibrosis development (24 and 30 weeks p.i.) suggests the persistence of the inflammatory/damaging stimulus. Thus, macrophage responses might be prolonged and, at the same time, these cells may actively contribute to the fibrogenic process.

Despite their sensitivity to radiation, alveolar macrophages are the first line of defense and are immediately involved in the removal of apoptotic cells and debris, as well as in the production of cytokines such as IL-1, TNF- $\alpha$  and PDGF- $\beta$  (Coggle et al., 1986; Hong et al., 2003; Morgan and Breit, 1995; Rubin et al., 1992). A common feature of lung macrophages early after thorax irradiation is their foamy appearance. This lipid-filled and enlarged macrophages have been described in the BALF or in the tissue during acute pneumonitis following thoracic irradiation both in human and in animal models (Chiang et al., 2005; Gross and Balis, 1978; Hong et al., 2003). Although it was not completely unexpected to find these characteristic cells, here it is shown for the first time that lipid loaded macrophages appear in the lung tissue up to 6 weeks p.i., and that also other resident cells contain lipid droplets (Cappuccini et al., 2011). This observation suggested that IR disturbs lipid metabolism in the lung tissue. Remarkably, C57BL/6 wild type and CD73<sup>-/-</sup> mice exposed to hemithorax irradiation showed a different amount of foamy macrophage at 3 weeks p.i. with a simultaneous increase at 6 weeks p.i.. The elevated amount of lipid-loaded cells in CD73<sup>-/-</sup> mice suggests that IR affects lipid accumulation/use of macrophages in particular in the absence of CD73. Generally, lipid accumulation in macrophages represents a hallmark of early atherosclerotic lesions (Brown and Goldstein, 1983; Libby, 2002) and has also been described following *Mycobacterium tuberculosis* infections (Hernandez-Pando et al., 1997). Furthermore, presence of foamy cells in

areas of degenerating brain has long been known (Virchow, 1867). The presence of foamy macrophages in the BALF suggested that these cells may represent the alveolar pool rather than interstitial or infiltrating macrophages. In support of that assumption, no correlation was found between foamy cells and Mac-1 cell positivity, a marker with higher expression on infiltrating macrophages compared to mature tissue macrophages (Chiang et al., 2005; Dougherty and McBride, 1984; Duan et al., 2012; Hong et al., 2003). It might be that in CD73<sup>-/-</sup> mice, due to the reduced radiation-sensitivity described for alveolar macrophages compared to WT mice, a higher amount of these cells is available for the uptake of oxidized lipids. Whether the loss of CD73 could directly influence macrophages in their ability to accumulate/degrade cellular lipids has still to be clarified. However, adenosine binding to A<sub>2A</sub> receptor has been shown to stimulate the expression of proteins involved in the reverse cholesterol transport, thereby inhibiting foam cell formation in macrophages (Reiss et al., 2004).

In general, foam cells formation is the consequence of an excessive intracellular deposition of cholesterol due to an alteration in the uptake mainly of oxidized low-density lipoproteins (LDL) by macrophage scavenger receptors. A second main mechanism leading to a dysregulated intracellular cholesterol homeostasis is depending on mediators of cholesterol efflux (Luo et al., 2010). The scavenger receptor CD36 has been indicated as key factor in foam cell formation (Rahaman et al., 2006) and it is upregulated in a time- and dose-dependent manner by IR treatment in cultured blood-derived macrophages; furthermore, irradiation is able to increase the uptake of oxLDL in those cells (Katayama et al., 2008). In own preliminary experiments, bone marrow derived macrophages (BMDM) freshly isolated from CD73<sup>-/-</sup> mice displayed higher CD36 expression in comparison to BMDM of WT mice (data not shown); therefore it was hypothesized that this receptor may be relevant for lipid uptake after whole thorax irradiation. Unfortunately, FACS analysis failed to show a direct correlation between CD36 and the presence of foamy macrophages at 3 and 6 weeks p.i. suggesting that other scavenger receptors, such as scavenger receptors A (SR-A) and class B type I (SR-BI), or a defective cholesterol efflux might play a major role during this phase. In support of the comparable surface regulation of CSF-1R and CD36 in lung macrophages after whole thorax irradiation, is that one effect of macrophage colony stimulating factor (M-CSF) on macrophages is the increase in cholesterol concentration in the cells, suggesting a direct link between the 2 receptors and a similar response to radiation (Dushkin, 2012).

Although in the present study the responsible mediators were not identified, this is the first time that the impact of lung irradiation on lipid metabolism and generation of foamy macrophages has been addressed. Previous publications have tried to identify the activation state of these

foamy macrophages with no clear results. Foamy macrophage formation has been associated with an M1 polarization state in inflammatory processes. Others suggested that these cells actively participate to the resolution of inflammation and that M2 macrophages have a higher expression of CD36, as well as of transporters implicated in cholesterol efflux (Dushkin, 2012; Oh et al., 2012; Pradel et al., 2009). In the effort of shedding light on the role of these peculiar cells in the radiation-induced pneumopathy, and to explain the differences found in the amount of foamy macrophages in C57BL/6 wild type and CD73<sup>-/-</sup> mice, the polarization state of the macrophage compartment was evaluated. Data from immunofluorescence staining on tissue microarrays revealed an early reduction in the M2 phenotype (Arg1) accompanied by a slight increase of the M1 phenotype (iNOS) compared to control animals. The Arg1 positive macrophages expanded particularly at 12 weeks p.i. in WT and CD73<sup>-/-</sup> mice, being underrepresented at later time points when the F4/80<sup>+</sup>IL-10 $\alpha$ <sup>+</sup> cells increased, especially in irradiated WT mice at 30 weeks. Notably, percentages of IL-10 $\alpha$ <sup>+</sup> M2 macrophages were only increased in WT, but not in CD73<sup>-/-</sup> mice. The 13-fold increase in IL-10 receptor positive macrophages observed could indicate an IL-10-rich lung microenvironment during fibrosis development in these mice. In support of this finding, many reports have described a role of IL-10 in fibrotic lung diseases in general (Barbarin et al., 2005; Lee et al., 2002; Sun et al., 2011). Animals overexpressing IL-10 in the lung tissue showed induction of alternatively activated macrophages and irreversible lung fibrosis (Sun et al., 2011) and in other animal models, fibrosis was reduced when development of M2 was inhibited (Laskin et al., 2011). Moreover, TGF- $\beta$  plays a critical role in promoting alternative macrophage activation (Gong et al., 2012), therefore the higher levels of this cytokine in WT mice as compared to CD73 deficient mice at 30 weeks further strengthen histological results.

Phenotypic differences were partially corroborated investigating whole lung macrophages using flow cytometry. Differential regulation of the markers MHCII and MMR was used to characterize M1 and M2 macrophages respectively. Surface expression of MHCII dramatically increased at 3 weeks, whereas a severe decrease in MMR expression in WT and CD73<sup>-/-</sup> mice was observed at that time point. As hypothesized, during the fibrotic phase macrophages of WT mice seemed to switch from M1 to M2 phenotype, while alveolar macrophages from CD73<sup>-/-</sup> mice showed a sustained pro-inflammatory phenotype until this late time point. This observation corroborated the stably high percentages of the F4/80<sup>+</sup>iNOS<sup>+</sup> population seen in CD73 deficient mice in the immunofluorescence analyses. The presence of inflammatory macrophages in CD73<sup>-/-</sup> mice at late time points (24 and 30 weeks p.i.) suggests that these mice may possibly be characterized by continued (mild) inflammation.

The striking differences in the polarization of lung macrophages between WT and CD73<sup>-/-</sup> mice are perfectly in line with the current hypothesis on the role of macrophages in fibrotic diseases. A failure in the regulation of macrophages effector functions can indeed lead to tissue damage and chronic disease. Specifically, in the lung a prolonged M1 response accompanied by uncontrolled release of cytotoxic or pro-inflammatory mediators can lead to acute injury. On the contrary, defects in the M2 functions could induce, through excessive release of fibrogenic mediators, chronic disease and fibrosis.

In addition to a distinct macrophage polarization in C57BL/6 wild type and CD73<sup>-/-</sup> mice, the present work demonstrated for the first time a time-dependent regulation of CD39 and CD73 on macrophage surface in response to whole thorax irradiation. While surface expression of CD73 was reduced on alveolar macrophages at week 3 p.i., a significant increase was found at week 6, followed by normal expression levels at later time points. On the contrary CD39 surface levels were higher at week 3 p.i. when compared to non irradiated controls, reaching normal levels at week 6 and gradually increasing again. It is still not clear what is the functional relevance of these findings and what drives the distinct regulation of these two ecto-enzymes on the surface of macrophages, since they are supposed to act in a concerted manner to produce adenosine. However, the results clearly suggest that after irradiation alveolar macrophages could represent one of the major players in the production of adenosine, or of intermediate components of the adenosinergic pathway, possibly contributing to the development of fibrosis. In this scenario, adenosine is known to influence macrophage effector functions, e.g. their phagocytic ability, production of ROS/NO (decrease), secretion of tumor necrosis factor  $\alpha$  (TNF- $\alpha$ ) and IL-12, as well as induction of IL-10 (Hasko et al., 2007; Hasko et al., 1996; Xaus et al., 1999). In addition, adenosine has been shown to enhance alternative macrophages activation *in vitro* in the presence of IL-4 and IL-13, the two major type 2 cytokines (Barczyk et al., 2010; Bours et al., 2006; Csoka et al., 2012), and to prevent excessive classical macrophage activation (Hasko and Pacher, 2012). It is also known that polarization of peritoneal macrophages is accompanied by differential expression of CD39 and CD73. The M1 macrophages exhibited a downregulation of CD39 and CD73 resulting in a reduced ATP hydrolysis. In contrast, macrophages M2 showed increased ATPase and ADPase activities in relation to M1 macrophages (Zanin et al., 2012). Own preliminary experiments confirmed that BMDM, which do not express CD73, slightly decrease the expression of CD39 following *in vitro* polarization to M1 by stimulation with LPS and IFN- $\gamma$ , while they upregulate CD39 expression when polarized to M2 with IL-4 (data not shown). However, increased expression of CD39 after whole thorax irradiation was not associated to the early appearance of M2

macrophages in the lung tissue of irradiated mice, suggesting that the *in vitro* conditions cannot mimic the *in vivo* situation, where macrophages are exposed to complex microenvironmental changes in the lung tissue regulating their response to injury. Due to the prominent plasticity and the anatomical location of lung macrophages, it is logical to think that they are key players in shaping the initial inflammation following exposure to IR and data showed herein suggest that the CD73/Ado signalling could be one of the mechanisms used by these cells.

Up to now, the role of macrophages in radiation-induced pneumopathy has not yet been defined. Johnston *et al.* depleted lung macrophages using clodronate instillation before 15 Gy lung irradiation. The obtained temporary depletion of macrophages did not alter the number of macrophages and lymphocytes infiltrating the lung 8 weeks p.i. and the increase of macrophages at 16 weeks, when compared to irradiated mice not depleted of macrophages. Unfortunately no information about the effects of macrophages depletion on fibrosis development has been provided in that study (Johnston *et al.*, 2004). Several other studies have tried to define a role of macrophages in fibrotic diseases of distinct origin. Clodronate depletion of alveolar macrophages led to a markedly reduced fibrotic response in a model of silica-induced fibrosis in rats (Elder *et al.*, 2004). In a controlled model of liver fibrosis in rats, characterized by distinct phases of injury, repair and resolution, macrophage depletion during the progressive inflammatory injury had beneficial effect, ameliorating fibrosis. By contrast, the natural resolution of tissue injury after carbon tetrachloride (CCl<sub>4</sub>) treatment failed when depleting macrophages during the recovery phase (Duffield *et al.*, 2005). As it was seen for depletion of T<sub>reg</sub> cells mentioned above, macrophages seem to have a positive role in the resolution phase of the inflammatory process. However, macrophages produce many chemoattractants and growth factors regulating the wound healing response and interfering with those functions can lead to an altered repair process. Consequently, modulation rather than eradication of T<sub>reg</sub> cells and macrophages may be a promising approach for controlling fibrosis.

The dampening of the immune cell response by anti-inflammatory drugs is currently used in the clinic to avoid pneumonitis, but this treatment is not sufficient to prevent late side effects of lung irradiation. The use of the CD73/Ado system in the prevention or treatment of radiation-induced lung injury is of special interest because this immunosuppressive pathway is known to promote tumor growth. Thus, inhibition of CD73/Ado may not only have a beneficial effect on radiation-induced pneumopathy, but at the same time may improve the efficacy of radio(chemo)therapy of lung tumors.

Each fibrotic disease, though sharing common features, could differently progress depending on the initial injury and on the specific resident, immune, and recruited cells involved in the reaction to the provoking stimulus. Therefore it is important to define tissue responses to radiation in an *in vivo* model, and to clarify the role of the immune system in driving pneumonitis and, possibly, fibrosis development. The data presented in this PhD thesis for the first time cope with the effort of elucidating macrophage and T cell responses to whole thorax irradiation through analysis of their phenotype and immunoregulatory functions.

Notably, though the importance of lymphocytes in lung fibrosis development in general has been broadly investigated, after more than 30 years of studies, the influence of lymphocytes on fibrosis development is still not clear. Therefore, to directly address the role of the lymphocyte compartment in radiation-induced fibrosis, RAG-2<sup>-/-</sup> mice lacking mature T and B lymphocytes were analysed in addition. RAG-2<sup>-/-</sup> mice responded to thorax irradiation with reduced gain in weight and a decreased survival rate compared to WT mice, suggesting that the lack of mature lymphocytes causes an increased sensitivity to radiation-induced late adverse effects. Subsequent histological analyses revealed that RAG-2<sup>-/-</sup> mice develop pronounced lung fibrosis already at 24 weeks p.i. A significantly higher amount of fibrotic foci was detected 24 weeks p.i. in these mice when compared to WT mice, though it did not correspond to a significant increase in the fibrotic area. Areas of collagen deposition stained also positive for the two characteristic fibrosis markers  $\alpha$ -SMA and TGF- $\beta$  corroborating the finding that, in the absence of mature T lymphocytes (and B lymphocytes), mice respond to whole thorax irradiation with an earlier onset of fibrosis. In support of this observation, the fibrotic response in SCID mice receiving intratracheal BLM also occurred earlier when compared to WT animals (Helene et al., 1999). Interestingly, the analysis of immune cell infiltrates after whole thorax irradiation (6 and 24 week p.i.), revealed that in RAG-2<sup>-/-</sup> mice the scavenger receptor CD36 was highly upregulated on alveolar macrophages already at 24 weeks p.i., whereas in WT mice CD36 expression on alveolar macrophages increased only at 30 weeks p.i.. This suggests that expression of CD36 may be a common feature of alveolar macrophages in fibrotic tissues and supports the earlier onset of fibrosis in RAG-2<sup>-/-</sup> mice in the absence of appropriate control of the innate immune cells by the adaptive immune system. Whether and how this finding relates to the potential alterations in lipid metabolism and macrophage functions needs further investigations.

Surprisingly, RAG-2<sup>-/-</sup> mice failed to upregulate CD73 on alveolar macrophages at 6 weeks p.i.. In contrast, a slightly more pronounced upregulation of CD39 was observed at this time point



when compared to WT mice. Although the lack of analyses at other time points does not allow a final conclusion, these observations may be indicative for a shift in the response of the adenosinergic pathway on macrophages of RAG-2<sup>-/-</sup> mice to an earlier activation after irradiation. Cells isolated from WT mice indeed significantly upregulated CD39 only 12 weeks p.i..

Of note, the extent of macrophage polarization to a pro-inflammatory M1 phenotype was more pronounced in irradiated RAG-2<sup>-/-</sup> mice when compared to irradiated WT mice at both time points. These data suggest that mature (regulatory) lymphocytes may be required to keep in check activated cells from the innate immune system. Moreover, it could be hypothesized that the more intense inflammation may contribute to the earlier onset of fibrosis observed in RAG-2<sup>-/-</sup> mice. Still, further investigations are required to confirm the hypothesis about a faster degeneration of the lung tissue in irradiated RAG-2<sup>-/-</sup> mice.

In a preliminary experiment RAG-2<sup>-/-</sup> mice received whole thorax irradiation and 1 day after they were adoptively transferred with CD4<sup>+</sup> T cells isolated from WT mice. These cells indeed were the most affected by IR in the previously described experiments. Unfortunately, no changes could be seen in late side effects of whole thorax irradiation, in that RAG-2<sup>-/-</sup> mice and reconstituted RAG-2<sup>-/-</sup> mice showed comparable amount of fibrosis 24 weeks p.i. (Supplementary data, **Fig. 7.2**). These data suggest that the presence of the complete CD4<sup>+</sup> T cell population early after whole thorax irradiation is not sufficient to decrease the pronounced sensitivity of RAG-2<sup>-/-</sup> mice to radiation-induced fibrosis. To identify the beneficial effect of the adaptive immune system it has to be tested whether adoptive transfer of specific T cell subsets, or of B cells, would mimic the delayed response observed in WT mice.

The present work was designed to describe chronological changes in the lung tissue and in the innate and adaptive immune systems in response to thorax irradiation as a model for fibrosis development resulting from chronic lung injury, in an attempt to identify potential innovative therapeutic targets. Overall data obtained in the RAG-2<sup>-/-</sup> model point to an essential role of the adaptive immune system in the control of radiation-induced pneumopathy. However, the CD4<sup>+</sup> T cell subset alone seems not to be sufficient to prevent the earlier onset of radiation-induced late side effects in the lung tissue. Nevertheless, a complete and functional adaptive immune system does not prevent the fibrotic response of the lung tissue after whole thorax irradiation either, as demonstrated by the development of lung fibrosis by week 30 p.i. in WT mice. However, the adaptive immune system seems to participate in the control of the pro-inflammatory phenotype of cells from the innate immune system, thereby decreasing

and/or delaying fibrosis development. Therefore it is highly likely that an uncontrolled response of the innate immune cell compartment, and possibly above all macrophages, extensively contribute to and accelerate the adverse effects of whole thorax irradiation. In this extremely complex scenario, it is necessary to consider that other lung resident cells such as endothelial, epithelial cells, and fibrocytes will additionally influence the lung microenvironment and cooperate with cells of the innate and/or adaptive immune system in driving local tissue damage and destruction of the normal lung architecture in response to lung irradiation. Understanding the contribution of the different macrophage subsets, of soluble mediators secreted by these cells, and of cellular and secreted factors controlling macrophage phenotype will help to find novel ways to redirect the radiation-response of the lung tissue towards a resolution of early inflammation and reestablishment of tissue homeostasis.

Importantly, the CD73 deficient mouse model used in this study helped to demonstrate for the first time a direct role of the CD73/Ado pathway in the progression of late side effects of lung irradiation. Data obtained in CD73<sup>-/-</sup> mice suggest an involvement of the adenosinergic pathway in radiation-induced changes in the lung microenvironment, as well as in the progression of pneumonitis to lung fibrosis. While CD73 expression on immune cells was mostly affected in the early phase, other players, like diffuse tissue hypoxia and increased TGF- $\beta$ , may affect CD73 expression and activity on other resident cells thereby enhancing the amount of regulatory T cells and of alternatively activated macrophages to amplify the fibrotic response. Of course, to determine whether CD73 on resident cells is required to drive fibrosis, CD73 activity and adenosine levels should be measured overtime in the lung tissue and the BALF, respectively. Such investigations are also necessary to identify a possible window of action for a therapeutic strategy targeting the CD73/Ado system.

In conclusion, the present work clearly demonstrated that inflammation constitutes an important process that contributes to the secondary effects of radiation-induced DNA-damage in the lung. Therefore it is highly likely that an appropriate orchestration of inflammatory, repair and regeneration processes could help to avoid early and late side effects in this radiosensitive organ. Of note, complete eradication of specific cell populations from the innate or adaptive immune systems seems to worsen radiation-induced late adverse effects. Thus, a fine tuning of immune cell activation and polarization, rather than complete suppression of specific immune cell populations may be effective in the control of the adverse tissue response to radiation. Therefore, the identification of key regulators/mediators of fibrosis like

CD73/Ado, and/or of the cells responsible for the generation of such regulators/mediators is of utmost importance for developing effective treatment strategies. Because of its dual role in the control of tissue inflammation and fibrosis, the CD73/Ado system may be an attractive therapeutic target for prevention or treatment of radiation-induced pneumopathy. The benefit of inhibitors of CD73 or of adenosine signalling has to be tested in further investigations.

## 5 Summary

Radiation-induced pneumonitis and fibrosis still constitute a major complication in the treatment of patients with thorax-associated neoplasms. To date, the molecular mechanisms governing the onset and progression of these injuries are not entirely understood and no effective therapies are available. Aim of the present study was to gain more insight into the pathogenesis of radiation-induced pneumonitis and fibrosis, with the ultimate goal to provide a molecular basis for the development of novel and effective strategies for prevention or treatment of these pathologies. At this purpose, investigations on immune cells and on the immunomodulatory CD73/adenosine system have been performed *in vivo* in a C57BL/6 mouse model of whole thorax irradiation with 15 Gray (Gy).

In the present work, CD73 was identified as a key mediator of radiation-induced fibrosis, in that CD73 deficient mice showed no or minimal fibrosis at 30 weeks post irradiation (p.i.), while wild type (WT) mice showed extensive collagen deposition, diffuse hypoxia and fibrotic areas positive for  $\alpha$ -SMA and TGF- $\beta$  at this time point. Thus, lack of endogenous CD73 seems to exert a radioprotective effect. Of note, the progression to a more pronounced fibrosis in WT mice was associated with CD73 upregulation on T cells and macrophages during the pneumonitic phase, in addition to an early and late expansion of regulatory T ( $T_{reg}$ ) cells, both locally and systemically. A shift in macrophage phenotype was also noted, with prevalence of pro-inflammatory M1 macrophages during the pneumonitic phase, and a subsequent polarization into an anti-inflammatory M2 phenotype. Surprisingly, lung macrophages and T cells of CD73<sup>-/-</sup> mice were less sensitive to radiation-induced cell depletion in the tissue. Noteworthy, a significantly lower amount of  $T_{reg}$  cells was found in irradiated CD73<sup>-/-</sup> mice as compared to WT mice, within the lung tissue and in peripheral lymphoid organs. The shift of phenotype was not observed in lung macrophages of CD73<sup>-/-</sup> mice, and pro-inflammatory M1 macrophages were still elevated at 30 weeks p.i. In addition, irradiated WT and CD73<sup>-/-</sup> mice displayed a differential regulation of the upstream component of the adenosinergic pathway (CD39) on the immune cells analysed. Thus, endogenous presence or absence of CD73 result in distinct responses within the lung tissue, determining the progression and the final outcome of radiation-induced side effects.

Remarkably, complete absence of mature B and T cells led to an increased sensitivity to radiation-induced fibrosis. Therefore, in WT mice a  $T_{reg}$  cell-mediated control of the innate immune response might help in delaying the damaging effects of IR. However, radiation-induced alterations in the microenvironment, such as chronic upregulation of

adenosine, may subsequently influence the phenotype of macrophages and of other resident cells to promote extensive remodelling and fibrosis.

This model provided evidence for a direct involvement of the immune system in the pathogenesis of lung radiation-induced pneumopathy. Moreover, the herein presented work underlines the importance of the CD73/adenosine system in the regulation of lung responses to IR, therefore it might represent a good target for future combination treatments.

## 6 Bibliography

(2008). *Janeway's immunobiology*, 7. edn (New York u.a.: Garland).

Abid, S.H., Malhotra, V., and Perry, M.C. (2001). Radiation-induced and chemotherapy-induced pulmonary injury. *Current opinion in oncology* 13, 242-248.

Airas, L., Hellman, J., Salmi, M., Bono, P., Puurunen, T., Smith, D.J., and Jalkanen, S. (1995). CD73 is involved in lymphocyte binding to the endothelium: characterization of lymphocyte-vascular adhesion protein 2 identifies it as CD73. *The Journal of experimental medicine* 182, 1603-1608.

Akagawa, K.S., Kamoshita, K., and Tokunaga, T. (1988). Effects of granulocyte-macrophage colony-stimulating factor and colony-stimulating factor-1 on the proliferation and differentiation of murine alveolar macrophages. *J Immunol* 141, 3383-3390.

Barbarin, V., Xing, Z., Delos, M., Lison, D., and Huaux, F. (2005). Pulmonary overexpression of IL-10 augments lung fibrosis and Th2 responses induced by silica particles. *American journal of physiology Lung cellular and molecular physiology* 288, L841-848.

Barczyk, K., Ehrchen, J., Tenbrock, K., Ahlmann, M., Kneidl, J., Viemann, D., and Roth, J. (2010). Glucocorticoids promote survival of anti-inflammatory macrophages via stimulation of adenosine receptor A3. *Blood* 116, 446-455.

Bentzen, S.M. (2006). Preventing or reducing late side effects of radiation therapy: radiobiology meets molecular pathology. *Nature reviews Cancer* 6, 702-713.

Bitterman, P.B., Saltzman, L.E., Adelberg, S., Ferrans, V.J., and Crystal, R.G. (1984). Alveolar macrophage replication. One mechanism for the expansion of the mononuclear phagocyte population in the chronically inflamed lung. *The Journal of clinical investigation* 74, 460-469.

Blackburn, M.R., Datta, S.K., and Kellems, R.E. (1998). Adenosine deaminase-deficient mice generated using a two-stage genetic engineering strategy exhibit a combined immunodeficiency. *The Journal of biological chemistry* 273, 5093-5100.

Blackburn, M.R., Lee, C.G., Young, H.W., Zhu, Z., Chunn, J.L., Kang, M.J., Banerjee, S.K., and Elias, J.A. (2003). Adenosine mediates IL-13-induced inflammation and remodeling in the lung and interacts in an IL-13-adenosine amplification pathway. *The Journal of clinical investigation* 112, 332-344.

Blackburn, M.R., Volmer, J.B., Thrasher, J.L., Zhong, H., Crosby, J.R., Lee, J.J., and Kellems, R.E. (2000). Metabolic consequences of adenosine deaminase deficiency in mice are associated

with defects in alveogenesis, pulmonary inflammation, and airway obstruction. *The Journal of experimental medicine* 192, 159-170.

Bogdan, C., and Nathan, C. (1993). Modulation of macrophage function by transforming growth factor beta, interleukin-4, and interleukin-10. *Annals of the New York Academy of Sciences* 685, 713-739.

Bours, M.J., Swennen, E.L., Di Virgilio, F., Cronstein, B.N., and Dagnelie, P.C. (2006). Adenosine 5'-triphosphate and adenosine as endogenous signaling molecules in immunity and inflammation. *Pharmacology & therapeutics* 112, 358-404.

Boveda-Ruiz, D., D'Alessandro-Gabazza, C.N., Toda, M., Takagi, T., Naito, M., Matsushima, Y., Matsumoto, T., Kobayashi, T., Gil-Bernabe, P., Chelakkot-Govindalayathil, A.L., *et al.* (2013). Differential role of regulatory T cells in early and late stages of pulmonary fibrosis. *Immunobiology* 218, 245-254.

Brown, M.S., and Goldstein, J.L. (1983). Lipoprotein metabolism in the macrophage: implications for cholesterol deposition in atherosclerosis. *Annual review of biochemistry* 52, 223-261.

Burger, A., Loffler, H., Bamberg, M., and Rodemann, H.P. (1998). Molecular and cellular basis of radiation fibrosis. *International journal of radiation biology* 73, 401-408.

Cao, M., Cabrera, R., Xu, Y., Liu, C., and Nelson, D. (2009). Gamma irradiation alters the phenotype and function of CD4+CD25+ regulatory T cells. *Cell biology international* 33, 565-571.

Cappuccini, F., Eldh, T., Bruder, D., Gereke, M., Jastrow, H., Schulze-Osthoff, K., Fischer, U., Kohler, D., Stuschke, M., and Jendrossek, V. (2011). New insights into the molecular pathology of radiation-induced pneumopathy. *Radiotherapy and oncology : journal of the European Society for Therapeutic Radiology and Oncology* 101, 86-92.

Chen, B.D., Mueller, M., and Chou, T.H. (1988). Role of granulocyte/macrophage colony-stimulating factor in the regulation of murine alveolar macrophage proliferation and differentiation. *J Immunol* 141, 139-144.

Chen, W., Jin, W., Hardegen, N., Lei, K.J., Li, L., Marinos, N., McGrady, G., and Wahl, S.M. (2003). Conversion of peripheral CD4+CD25- naive T cells to CD4+CD25+ regulatory T cells by TGF-beta induction of transcription factor Foxp3. *The Journal of experimental medicine* 198, 1875-1886.

Chiang, C.S., Liu, W.C., Jung, S.M., Chen, F.H., Wu, C.R., McBride, W.H., Lee, C.C., and Hong, J.H. (2005). Compartmental responses after thoracic irradiation of mice: strain differences. *International journal of radiation oncology, biology, physics* 62, 862-871.

- Christensen, P.J., Goodman, R.E., Pastoriza, L., Moore, B., and Toews, G.B. (1999). Induction of lung fibrosis in the mouse by intratracheal instillation of fluorescein isothiocyanate is not T-cell-dependent. *The American journal of pathology* *155*, 1773-1779.
- Chunn, J.L., Mohsenin, A., Young, H.W., Lee, C.G., Elias, J.A., Kellems, R.E., and Blackburn, M.R. (2006). Partially adenosine deaminase-deficient mice develop pulmonary fibrosis in association with adenosine elevations. *American journal of physiology Lung cellular and molecular physiology* *290*, L579-587.
- Chunn, J.L., Molina, J.G., Mi, T., Xia, Y., Kellems, R.E., and Blackburn, M.R. (2005). Adenosine-dependent pulmonary fibrosis in adenosine deaminase-deficient mice. *J Immunol* *175*, 1937-1946.
- Chunn, J.L., Young, H.W., Banerjee, S.K., Colasurdo, G.N., and Blackburn, M.R. (2001). Adenosine-dependent airway inflammation and hyperresponsiveness in partially adenosine deaminase-deficient mice. *J Immunol* *167*, 4676-4685.
- Cogle, J.E., Lambert, B.E., and Moores, S.R. (1986). Radiation effects in the lung. *Environmental health perspectives* *70*, 261-291.
- Colgan, S.P., Eltzschig, H.K., Eckle, T., and Thompson, L.F. (2006). Physiological roles for ecto-5'-nucleotidase (CD73). *Purinergic signalling* *2*, 351-360.
- Cordier, J.F., Mornex, J.F., Lasne, Y., Gerard, J.P., Cordier, G., Creyssel, R., and Touraine, R. (1984). Bronchoalveolar lavage in radiation pneumonitis. *Bulletin europeen de physiopathologie respiratoire* *20*, 369-374.
- Cronstein, B.N. (1994). Adenosine, an endogenous anti-inflammatory agent. *J Appl Physiol* *76*, 5-13.
- Csoka, B., Selmeczy, Z., Koscsó, B., Nemeth, Z.H., Pacher, P., Murray, P.J., Kepka-Lenhardt, D., Morris, S.M., Jr., Gause, W.C., Leibovich, S.J., *et al.* (2012). Adenosine promotes alternative macrophage activation via A2A and A2B receptors. *FASEB journal : official publication of the Federation of American Societies for Experimental Biology* *26*, 376-386.
- Dang, E.V., Barbi, J., Yang, H.Y., Jinasena, D., Yu, H., Zheng, Y., Bordman, Z., Fu, J., Kim, Y., Yen, H.R., *et al.* (2011). Control of T(H)17/T(reg) balance by hypoxia-inducible factor 1. *Cell* *146*, 772-784.
- Davis, S.D., Yankelevitz, D.F., and Henschke, C.I. (1992). Radiation effects on the lung: clinical features, pathology, and imaging findings. *AJR American journal of roentgenology* *159*, 1157-1164.
- Deaglio, S., Dwyer, K.M., Gao, W., Friedman, D., Usheva, A., Erat, A., Chen, J.F., Enjyoji, K., Linden, J., Oukka, M., *et al.* (2007). Adenosine generation catalyzed by CD39 and CD73



expressed on regulatory T cells mediates immune suppression. *The Journal of experimental medicine* 204, 1257-1265.

Dianzani, U., Redoglia, V., Bragardo, M., Attisano, C., Bianchi, A., Di Franco, D., Ramenghi, U., Wolff, H., Thompson, L.F., Pileri, A., *et al.* (1993). Co-stimulatory signal delivered by CD73 molecule to human CD45RAhiCD45ROlo (naive) CD8+ T lymphocytes. *J Immunol* 151, 3961-3970.

Dougherty, G.J., and McBride, W.H. (1984). Macrophage heterogeneity. *Journal of clinical & laboratory immunology* 14, 1-11.

Down, J.D., and Steel, G.G. (1983). The expression of early and late damage after thoracic irradiation: a comparison between CBA and C57B1 mice. *Radiation research* 96, 603-610.

Driver, A.G., Kukoly, C.A., Ali, S., and Mustafa, S.J. (1993). Adenosine in bronchoalveolar lavage fluid in asthma. *The American review of respiratory disease* 148, 91-97.

Duan, M., Li, W.C., Vlahos, R., Maxwell, M.J., Anderson, G.P., and Hibbs, M.L. (2012). Distinct macrophage subpopulations characterize acute infection and chronic inflammatory lung disease. *J Immunol* 189, 946-955.

Duffield, J.S., Forbes, S.J., Constandinou, C.M., Clay, S., Partolina, M., Vuthoori, S., Wu, S., Lang, R., and Iredale, J.P. (2005). Selective depletion of macrophages reveals distinct, opposing roles during liver injury and repair. *The Journal of clinical investigation* 115, 56-65.

Dushkin, M.I. (2012). Macrophage/foam cell is an attribute of inflammation: mechanisms of formation and functional role. *Biochemistry Biokhimiia* 77, 327-338.

Ehrentraut, H., Clambey, E.T., McNamee, E.N., Brodsky, K.S., Ehrentraut, S.F., Poth, J.M., Riegel, A.K., Westrich, J.A., Colgan, S.P., and Eltzschig, H.K. (2013). CD73+ regulatory T cells contribute to adenosine-mediated resolution of acute lung injury. *FASEB journal : official publication of the Federation of American Societies for Experimental Biology*.

Elder, A.C., Gelein, R., Oberdorster, G., Finkelstein, J., Notter, R., and Wang, Z. (2004). Efficient depletion of alveolar macrophages using intratracheally inhaled aerosols of liposome-encapsulated clodronate. *Experimental lung research* 30, 105-120.

Fleckenstein, K., Gauter-Fleckenstein, B., Jackson, I.L., Rabbani, Z., Anscher, M., and Vujaskovic, Z. (2007a). Using biological markers to predict risk of radiation injury. *Seminars in radiation oncology* 17, 89-98.

Fleckenstein, K., Zgonjanin, L., Chen, L., Rabbani, Z., Jackson, I.L., Thrasher, B., Kirkpatrick, J., Foster, W.M., and Vujaskovic, Z. (2007b). Temporal onset of hypoxia and oxidative stress after pulmonary irradiation. *International journal of radiation oncology, biology, physics* 68, 196-204.

- Fozard, J.R., and Hannon, J.P. (1999). Adenosine receptor ligands: potential as therapeutic agents in asthma and COPD. *Pulmonary pharmacology & therapeutics* 12, 111-114.
- Franko, A.J., Sharplin, J., Ward, W.F., and Hinz, J.M. (1991). The genetic basis of strain-dependent differences in the early phase of radiation injury in mouse lung. *Radiation research* 126, 349-356.
- Fredholm, B.B. (2007). Adenosine, an endogenous distress signal, modulates tissue damage and repair. *Cell death and differentiation* 14, 1315-1323.
- Garibaldi, B.T., D'Alessio, F.R., Mock, J.R., Files, D.C., Chau, E., Eto, Y., Drummond, M.B., Aggarwal, N.R., Sidhaye, V., and King, L.S. (2013). Regulatory T cells reduce acute lung injury fibroproliferation by decreasing fibrocyte recruitment. *American journal of respiratory cell and molecular biology* 48, 35-43.
- Ghafoori, P., Marks, L.B., Vujaskovic, Z., and Kelsey, C.R. (2008). Radiation-induced lung injury. Assessment, management, and prevention. *Oncology (Williston Park)* 22, 37-47; discussion 52-33.
- Gibson, P.G., Bryant, D.H., Morgan, G.W., Yeates, M., Fernandez, V., Penny, R., and Breit, S.N. (1988). Radiation-induced lung injury: a hypersensitivity pneumonitis? *Annals of internal medicine* 109, 288-291.
- Gong, D., Shi, W., Yi, S.J., Chen, H., Groffen, J., and Heisterkamp, N. (2012). TGFbeta signaling plays a critical role in promoting alternative macrophage activation. *BMC immunology* 13, 31.
- Gordon, S., and Taylor, P.R. (2005). Monocyte and macrophage heterogeneity. *Nature reviews Immunology* 5, 953-964.
- Graves, P.R., Siddiqui, F., Anscher, M.S., and Movsas, B. (2010). Radiation pulmonary toxicity: from mechanisms to management. *Seminars in radiation oncology* 20, 201-207.
- Gross, N.J. (1977). Pulmonary effects of radiation therapy. *Annals of internal medicine* 86, 81-92.
- Gross, N.J., and Balis, J.V. (1978). Functional, biochemical, and morphologic changes in alveolar macrophages following thoracic x-irradiation. *Laboratory investigation; a journal of technical methods and pathology* 39, 381-389.
- Gutensohn, W., Resta, R., Misumi, Y., Ikehara, Y., and Thompson, L.F. (1995). Ecto-5'-nucleotidase activity is not required for T cell activation through CD73. *Cellular immunology* 161, 213-217.

Hasko, G., Linden, J., Cronstein, B., and Pacher, P. (2008). Adenosine receptors: therapeutic aspects for inflammatory and immune diseases. *Nature reviews Drug discovery* 7, 759-770.

Hasko, G., and Pacher, P. (2012). Regulation of macrophage function by adenosine. *Arteriosclerosis, thrombosis, and vascular biology* 32, 865-869.

Hasko, G., Pacher, P., Deitch, E.A., and Vizi, E.S. (2007). Shaping of monocyte and macrophage function by adenosine receptors. *Pharmacology & therapeutics* 113, 264-275.

Hasko, G., Szabo, C., Nemeth, Z.H., Kvetan, V., Pastores, S.M., and Vizi, E.S. (1996). Adenosine receptor agonists differentially regulate IL-10, TNF-alpha, and nitric oxide production in RAW 264.7 macrophages and in endotoxemic mice. *J Immunol* 157, 4634-4640.

Haston, C.K., and Travis, E.L. (1997). Murine susceptibility to radiation-induced pulmonary fibrosis is influenced by a genetic factor implicated in susceptibility to bleomycin-induced pulmonary fibrosis. *Cancer research* 57, 5286-5291.

Heinzelmann, F., Jendrossek, V., Lauber, K., Nowak, K., Eldh, T., Boras, R., Handrick, R., Henkel, M., Martin, C., Uhlig, S., *et al.* (2006). Irradiation-induced pneumonitis mediated by the CD95/CD95-ligand system. *Journal of the National Cancer Institute* 98, 1248-1251.

Helene, M., Lake-Bullock, V., Zhu, J., Hao, H., Cohen, D.A., and Kaplan, A.M. (1999). T cell independence of bleomycin-induced pulmonary fibrosis. *Journal of leukocyte biology* 65, 187-195.

Hernandez-Pando, R., Orozco, H., Arriaga, K., Sampieri, A., Larriva-Sahd, J., and Madrid-Marina, V. (1997). Analysis of the local kinetics and localization of interleukin-1 alpha, tumour necrosis factor-alpha and transforming growth factor-beta, during the course of experimental pulmonary tuberculosis. *Immunology* 90, 607-617.

Hickey, M.M., Richardson, T., Wang, T., Mosqueira, M., Arguiri, E., Yu, H., Yu, Q.C., Solomides, C.C., Morrissey, E.E., Khurana, T.S., *et al.* (2010). The von Hippel-Lindau Chuvash mutation promotes pulmonary hypertension and fibrosis in mice. *The Journal of clinical investigation* 120, 827-839.

Hinz, B., Phan, S.H., Thannickal, V.J., Galli, A., Bochaton-Piallat, M.L., and Gabbiani, G. (2007). The myofibroblast: one function, multiple origins. *The American journal of pathology* 170, 1807-1816.

Hong, J.H., Jung, S.M., Tsao, T.C., Wu, C.J., Lee, C.Y., Chen, F.H., Hsu, C.H., McBride, W.H., and Chiang, C.S. (2003). Bronchoalveolar lavage and interstitial cells have different roles in radiation-induced lung injury. *International journal of radiation biology* 79, 159-167.

Huszar, E., Vass, G., Vizi, E., Csoma, Z., Barat, E., Molnar Vilagos, G., Herjavec, I., and Horvath, I. (2002). Adenosine in exhaled breath condensate in healthy volunteers and in

patients with asthma. *The European respiratory journal : official journal of the European Society for Clinical Respiratory Physiology* 20, 1393-1398.

Jennings, F.L., and Arden, A. (1961). Development of experimental radiation pneumonitis. *Archives of pathology* 71, 437-446.

Johnston, C.J., Williams, J.P., Elder, A., Hernady, E., and Finkelstein, J.N. (2004). Inflammatory cell recruitment following thoracic irradiation. *Experimental lung research* 30, 369-382.

Katayama, I., Hotokezaka, Y., Matsuyama, T., Sumi, T., and Nakamura, T. (2008). Ionizing radiation induces macrophage foam cell formation and aggregation through JNK-dependent activation of CD36 scavenger receptors. *International journal of radiation oncology, biology, physics* 70, 835-846.

Kobie, J.J., Shah, P.R., Yang, L., Rebhahn, J.A., Fowell, D.J., and Mosmann, T.R. (2006). T regulatory and primed uncommitted CD4 T cells express CD73, which suppresses effector CD4 T cells by converting 5'-adenosine monophosphate to adenosine. *J Immunol* 177, 6780-6786.

Koszalka, P., Ozuyaman, B., Huo, Y., Zerneck, A., Flogel, U., Braun, N., Buchheiser, A., Decking, U.K., Smith, M.L., Sevigny, J., *et al.* (2004). Targeted disruption of cd73/ecto-5'-nucleotidase alters thromboregulation and augments vascular inflammatory response. *Circulation research* 95, 814-821.

Lambrecht, B.N. (2006). Alveolar macrophage in the driver's seat. *Immunity* 24, 366-368.

Laskin, D.L., Sunil, V.R., Gardner, C.R., and Laskin, J.D. (2011). Macrophages and tissue injury: agents of defense or destruction? *Annual review of pharmacology and toxicology* 51, 267-288.

Laskin, D.L., Weinberger, B., and Laskin, J.D. (2001). Functional heterogeneity in liver and lung macrophages. *Journal of leukocyte biology* 70, 163-170.

Lee, C.G., Homer, R.J., Cohn, L., Link, H., Jung, S., Craft, J.E., Graham, B.S., Johnson, T.R., and Elias, J.A. (2002). Transgenic overexpression of interleukin (IL)-10 in the lung causes mucus metaplasia, tissue inflammation, and airway remodeling via IL-13-dependent and -independent pathways. *The Journal of biological chemistry* 277, 35466-35474.

Lennon, P.F., Taylor, C.T., Stahl, G.L., and Colgan, S.P. (1998). Neutrophil-derived 5'-adenosine monophosphate promotes endothelial barrier function via CD73-mediated conversion to adenosine and endothelial A2B receptor activation. *The Journal of experimental medicine* 188, 1433-1443.

Libby, P. (2002). Inflammation in atherosclerosis. *Nature* 420, 868-874.

Linden, J. (2006). New insights into the regulation of inflammation by adenosine. *The Journal of clinical investigation* 116, 1835-1837.

Liu, F., Liu, J., Weng, D., Chen, Y., Song, L., He, Q., and Chen, J. (2010). CD4+CD25+Foxp3+ regulatory T cells depletion may attenuate the development of silica-induced lung fibrosis in mice. *PloS one* 5, e15404.

Lo Re, S., Lecocq, M., Uwambayinema, F., Yakoub, Y., Delos, M., Demoulin, J.B., Lucas, S., Sparwasser, T., Renauld, J.C., Lison, D., *et al.* (2011). Platelet-derived growth factor-producing CD4+ Foxp3+ regulatory T lymphocytes promote lung fibrosis. *American journal of respiratory and critical care medicine* 184, 1270-1281.

Lohmann-Matthes, M.L., Steinmuller, C., and Franke-Ullmann, G. (1994). Pulmonary macrophages. *The European respiratory journal : official journal of the European Society for Clinical Respiratory Physiology* 7, 1678-1689.

Luo, D.X., Cao, D.L., Xiong, Y., Peng, X.H., and Liao, D.F. (2010). A novel model of cholesterol efflux from lipid-loaded cells. *Acta pharmacologica Sinica* 31, 1243-1257.

Lupher, M.L., Jr., and Gallatin, W.M. (2006). Regulation of fibrosis by the immune system. *Advances in immunology* 89, 245-288.

Luzina, I.G., Todd, N.W., Iacono, A.T., and Atamas, S.P. (2008). Roles of T lymphocytes in pulmonary fibrosis. *Journal of leukocyte biology* 83, 237-244.

Martin, C., Romero, S., Sanchez-Paya, J., Massuti, B., Arriero, J.M., and Hernandez, L. (1999). Bilateral lymphocytic alveolitis: a common reaction after unilateral thoracic irradiation. *The European respiratory journal : official journal of the European Society for Clinical Respiratory Physiology* 13, 727-732.

Martin, P., and Leibovich, S.J. (2005). Inflammatory cells during wound repair: the good, the bad and the ugly. *Trends in cell biology* 15, 599-607.

Martinez, F.O., Sica, A., Mantovani, A., and Locati, M. (2008). Macrophage activation and polarization. *Frontiers in bioscience : a journal and virtual library* 13, 453-461.

Massaia, M., Perrin, L., Bianchi, A., Ruedi, J., Attisano, C., Altieri, D., Rijkers, G.T., and Thompson, L.F. (1990). Human T cell activation. Synergy between CD73 (ecto-5'-nucleotidase) and signals delivered through CD3 and CD2 molecules. *J Immunol* 145, 1664-1674.

Maus, U.A., Janzen, S., Wall, G., Srivastava, M., Blackwell, T.S., Christman, J.W., Seeger, W., Welte, T., and Lohmeyer, J. (2006). Resident alveolar macrophages are replaced by recruited monocytes in response to endotoxin-induced lung inflammation. *American journal of respiratory cell and molecular biology* 35, 227-235.

Moon, J.O., Welch, T.P., Gonzalez, F.J., and Copple, B.L. (2009). Reduced liver fibrosis in hypoxia-inducible factor-1alpha-deficient mice. *American journal of physiology Gastrointestinal and liver physiology* 296, G582-592.

Moore, B.B., and Hogaboam, C.M. (2008). Murine models of pulmonary fibrosis. *American journal of physiology Lung cellular and molecular physiology* 294, L152-160.

Moore, K.W., de Waal Malefyt, R., Coffman, R.L., and O'Garra, A. (2001). Interleukin-10 and the interleukin-10 receptor. *Annual review of immunology* 19, 683-765.

Morgan, G.W., and Breit, S.N. (1995). Radiation and the lung: a reevaluation of the mechanisms mediating pulmonary injury. *International journal of radiation oncology, biology, physics* 31, 361-369.

Mosser, D.M. (2003). The many faces of macrophage activation. *Journal of leukocyte biology* 73, 209-212.

Mosser, D.M., and Edwards, J.P. (2008). Exploring the full spectrum of macrophage activation. *Nature reviews Immunology* 8, 958-969.

Nakayama, Y., Makino, S., Fukuda, Y., Min, K.Y., Shimizu, A., and Ohsawa, N. (1996). Activation of lavage lymphocytes in lung injuries caused by radiotherapy for lung cancer. *International journal of radiation oncology, biology, physics* 34, 459-467.

Oh, J., Riek, A.E., Weng, S., Petty, M., Kim, D., Colonna, M., Cella, M., and Bernal-Mizrachi, C. (2012). Endoplasmic reticulum stress controls M2 macrophage differentiation and foam cell formation. *The Journal of biological chemistry* 287, 11629-11641.

Ozsahin, M., Crompton, N.E., Gourgou, S., Kramar, A., Li, L., Shi, Y., Sozzi, W.J., Zouhair, A., Mirimanoff, R.O., and Azria, D. (2005). CD4 and CD8 T-lymphocyte apoptosis can predict radiation-induced late toxicity: a prospective study in 399 patients. *Clinical cancer research : an official journal of the American Association for Cancer Research* 11, 7426-7433.

Pauluhn, J., Baumann, M., Hirth-Dietrich, C., and Rosenbruch, M. (2001). Rat model of lung fibrosis: comparison of functional, biochemical, and histopathological changes 4 months after single irradiation of the right hemithorax. *Toxicology* 161, 153-163.

Piguet, P.F., Collart, M.A., Grau, G.E., Kapanci, Y., and Vassalli, P. (1989). Tumor necrosis factor/cachectin plays a key role in bleomycin-induced pneumopathy and fibrosis. *The Journal of experimental medicine* 170, 655-663.

Pixley, F.J., and Stanley, E.R. (2004). CSF-1 regulation of the wandering macrophage: complexity in action. *Trends in cell biology* 14, 628-638.

- Pradel, L.C., Mitchell, A.J., Zarubica, A., Dufort, L., Chasson, L., Naquet, P., Broccardo, C., and Chimini, G. (2009). ATP-binding cassette transporter hallmarks tissue macrophages and modulates cytokine-triggered polarization programs. *European journal of immunology* *39*, 2270-2280.
- Qu, Y., Jin, S., Zhang, A., Zhang, B., Shi, X., Wang, J., and Zhao, Y. (2010). Gamma-ray resistance of regulatory CD4+CD25+Foxp3+ T cells in mice. *Radiation research* *173*, 148-157.
- Rahaman, S.O., Lennon, D.J., Febbraio, M., Podrez, E.A., Hazen, S.L., and Silverstein, R.L. (2006). A CD36-dependent signaling cascade is necessary for macrophage foam cell formation. *Cell metabolism* *4*, 211-221.
- Reiss, A.B., Rahman, M.M., Chan, E.S., Montesinos, M.C., Awadallah, N.W., and Cronstein, B.N. (2004). Adenosine A2A receptor occupancy stimulates expression of proteins involved in reverse cholesterol transport and inhibits foam cell formation in macrophages. *Journal of leukocyte biology* *76*, 727-734.
- Resta, R., Hooker, S.W., Laurent, A.B., Shuck, J.K., Misumi, Y., Ikehara, Y., Koretzky, G.A., and Thompson, L.F. (1994). Glycosyl phosphatidylinositol membrane anchor is not required for T cell activation through CD73. *J Immunol* *153*, 1046-1053.
- Resta, R., and Thompson, L.F. (1997). T cell signalling through CD73. *Cellular signalling* *9*, 131-139.
- Rezvani, M., Heryet, J.C., and Hopewell, J.W. (1989). Effects of single doses of gamma-radiation on pig lung. *Radiotherapy and oncology : journal of the European Society for Therapeutic Radiology and Oncology* *14*, 133-142.
- Roberts, C.M., Foulcher, E., Zaunders, J.J., Bryant, D.H., Freund, J., Cairns, D., Penny, R., Morgan, G.W., and Breit, S.N. (1993). Radiation pneumonitis: a possible lymphocyte-mediated hypersensitivity reaction. *Annals of internal medicine* *118*, 696-700.
- Rubin, P., Finkelstein, J., and Shapiro, D. (1992). Molecular biology mechanisms in the radiation induction of pulmonary injury syndromes: interrelationship between the alveolar macrophage and the septal fibroblast. *International journal of radiation oncology, biology, physics* *24*, 93-101.
- Rubin, P., Johnston, C.J., Williams, J.P., McDonald, S., and Finkelstein, J.N. (1995). A perpetual cascade of cytokines postirradiation leads to pulmonary fibrosis. *International journal of radiation oncology, biology, physics* *33*, 99-109.
- Sakaguchi, S., Yamaguchi, T., Nomura, T., and Ono, M. (2008). Regulatory T cells and immune tolerance. *Cell* *133*, 775-787.

Schrier, D.J., Phan, S.H., and McGarry, B.M. (1983). The effects of the nude (nu/nu) mutation on bleomycin-induced pulmonary fibrosis. A biochemical evaluation. *The American review of respiratory disease* 127, 614-617.

Sharplin, J., and Franko, A.J. (1989). A quantitative histological study of strain-dependent differences in the effects of irradiation on mouse lung during the early phase. *Radiation research* 119, 1-14.

Shinkai, Y., Rathbun, G., Lam, K.P., Oltz, E.M., Stewart, V., Mendelsohn, M., Charron, J., Datta, M., Young, F., Stall, A.M., *et al.* (1992). RAG-2-deficient mice lack mature lymphocytes owing to inability to initiate V(D)J rearrangement. *Cell* 68, 855-867.

Spicuzza, L., Di Maria, G., and Polosa, R. (2006). Adenosine in the airways: implications and applications. *European journal of pharmacology* 533, 77-88.

Stout, R.D., Jiang, C., Matta, B., Tietzel, I., Watkins, S.K., and Suttles, J. (2005). Macrophages sequentially change their functional phenotype in response to changes in microenvironmental influences. *J Immunol* 175, 342-349.

Stout, R.D., and Suttles, J. (2004). Functional plasticity of macrophages: reversible adaptation to changing microenvironments. *Journal of leukocyte biology* 76, 509-513.

Sun, C.X., Young, H.W., Molina, J.G., Volmer, J.B., Schnermann, J., and Blackburn, M.R. (2005). A protective role for the A1 adenosine receptor in adenosine-dependent pulmonary injury. *The Journal of clinical investigation* 115, 35-43.

Sun, C.X., Zhong, H., Mohsenin, A., Morschl, E., Chunn, J.L., Molina, J.G., Belardinelli, L., Zeng, D., and Blackburn, M.R. (2006). Role of A2B adenosine receptor signaling in adenosine-dependent pulmonary inflammation and injury. *The Journal of clinical investigation* 116, 2173-2182.

Sun, L., Louie, M.C., Vannella, K.M., Wilke, C.A., LeVine, A.M., Moore, B.B., and Shanley, T.P. (2011). New concepts of IL-10-induced lung fibrosis: fibrocyte recruitment and M2 activation in a CCL2/CCR2 axis. *American journal of physiology Lung cellular and molecular physiology* 300, L341-353.

Surh, C.D., and Sprent, J. (2008). Homeostasis of naive and memory T cells. *Immunity* 29, 848-862.

Synnestvedt, K., Furuta, G.T., Comerford, K.M., Louis, N., Karhausen, J., Eltzschig, H.K., Hansen, K.R., Thompson, L.F., and Colgan, S.P. (2002). Ecto-5'-nucleotidase (CD73) regulation by hypoxia-inducible factor-1 mediates permeability changes in intestinal epithelia. *The Journal of clinical investigation* 110, 993-1002.



- Szapiel, S.V., Elson, N.A., Fulmer, J.D., Hunninghake, G.W., and Crystal, R.G. (1979). Bleomycin-induced interstitial pulmonary disease in the nude, athymic mouse. *The American review of respiratory disease* *120*, 893-899.
- Tarling, J.D., and Coggle, J.E. (1982). Evidence for the pulmonary origin of alveolar macrophages. *Cell and tissue kinetics* *15*, 577-584.
- Thannickal, V.J., Toews, G.B., White, E.S., Lynch, J.P., 3rd, and Martinez, F.J. (2004). Mechanisms of pulmonary fibrosis. *Annual review of medicine* *55*, 395-417.
- Thompson, L.F., Eltzschig, H.K., Ibla, J.C., Van De Wiele, C.J., Resta, R., Morote-Garcia, J.C., and Colgan, S.P. (2004). Crucial role for ecto-5'-nucleotidase (CD73) in vascular leakage during hypoxia. *The Journal of experimental medicine* *200*, 1395-1405.
- Thompson, L.F., Ruedi, J.M., Glass, A., Low, M.G., and Lucas, A.H. (1989). Antibodies to 5'-nucleotidase (CD73), a glycosyl-phosphatidylinositol-anchored protein, cause human peripheral blood T cells to proliferate. *J Immunol* *143*, 1815-1821.
- Thornton, S.C., Walsh, B.J., Bennett, S., Robbins, J.M., Foulcher, E., Morgan, G.W., Penny, R., and Breit, S.N. (1996). Both in vitro and in vivo irradiation are associated with induction of macrophage-derived fibroblast growth factors. *Clinical and experimental immunology* *103*, 67-73.
- Tiemessen, M.M., Jagger, A.L., Evans, H.G., van Herwijnen, M.J., John, S., and Taams, L.S. (2007). CD4+CD25+Foxp3+ regulatory T cells induce alternative activation of human monocytes/macrophages. *Proceedings of the National Academy of Sciences of the United States of America* *104*, 19446-19451.
- Tsoutsou, P.G., and Koukourakis, M.I. (2006). Radiation pneumonitis and fibrosis: mechanisms underlying its pathogenesis and implications for future research. *International journal of radiation oncology, biology, physics* *66*, 1281-1293.
- Tuder, R.M., Yun, J.H., Bhunia, A., and Fijalkowska, I. (2007). Hypoxia and chronic lung disease. *J Mol Med (Berl)* *85*, 1317-1324.
- Tzouvelekis, A., Harokopos, V., Paparountas, T., Oikonomou, N., Chatziioannou, A., Vilaras, G., Tsiambas, E., Karameris, A., Bouros, D., and Aidinis, V. (2007). Comparative expression profiling in pulmonary fibrosis suggests a role of hypoxia-inducible factor-1alpha in disease pathogenesis. *American journal of respiratory and critical care medicine* *176*, 1108-1119.
- Volmer, J.B., Thompson, L.F., and Blackburn, M.R. (2006). Ecto-5'-nucleotidase (CD73)-mediated adenosine production is tissue protective in a model of bleomycin-induced lung injury. *J Immunol* *176*, 4449-4458.

- Vujaskovic, Z., Anscher, M.S., Feng, Q.F., Rabbani, Z.N., Amin, K., Samulski, T.S., Dewhirst, M.W., and Haroon, Z.A. (2001). Radiation-induced hypoxia may perpetuate late normal tissue injury. *International journal of radiation oncology, biology, physics* *50*, 851-855.
- Westermann, W., Schobl, R., Rieber, E.P., and Frank, K.H. (1999). Th2 cells as effectors in postirradiation pulmonary damage preceding fibrosis in the rat. *International journal of radiation biology* *75*, 629-638.
- Wynn, T.A. (2008). Cellular and molecular mechanisms of fibrosis. *The Journal of pathology* *214*, 199-210.
- Xaus, J., Mirabet, M., Lloberas, J., Soler, C., Lluís, C., Franco, R., and Celada, A. (1999). IFN-gamma up-regulates the A2B adenosine receptor expression in macrophages: a mechanism of macrophage deactivation. *J Immunol* *162*, 3607-3614.
- Yi, E.S., Bedoya, A., Lee, H., Chin, E., Saunders, W., Kim, S.J., Danielpour, D., Remick, D.G., Yin, S., and Ulich, T.R. (1996). Radiation-induced lung injury in vivo: expression of transforming growth factor-beta precedes fibrosis. *Inflammation* *20*, 339-352.
- Zanin, R.F., Braganhol, E., Bergamin, L.S., Campesato, L.F., Filho, A.Z., Moreira, J.C., Morrone, F.B., Sevigny, J., Schetinger, M.R., de Souza Wyse, A.T., *et al.* (2012). Differential macrophage activation alters the expression profile of NTPDase and ecto-5'-nucleotidase. *PloS one* *7*, e31205.
- Zarek, P.E., Huang, C.T., Lutz, E.R., Kowalski, J., Horton, M.R., Linden, J., Drake, C.G., and Powell, J.D. (2008). A2A receptor signaling promotes peripheral tolerance by inducing T-cell anergy and the generation of adaptive regulatory T cells. *Blood* *111*, 251-259.
- Zernecke, A., Bidzhekov, K., Ozuyaman, B., Fraemohs, L., Liehn, E.A., Luscher-Firzlaff, J.M., Luscher, B., Schrader, J., and Weber, C. (2006). CD73/ecto-5'-nucleotidase protects against vascular inflammation and neointima formation. *Circulation* *113*, 2120-2127.
- Zhu, J., Cohen, D.A., Goud, S.N., and Kaplan, A.M. (1996). Contribution of T lymphocytes to the development of bleomycin-induced pulmonary fibrosis. *Annals of the New York Academy of Sciences* *796*, 194-202.
- Zimmermann, H. (2000). Extracellular metabolism of ATP and other nucleotides. *Naunyn-Schmiedeberg's archives of pharmacology* *362*, 299-309.

## 7 Appendix

## 7.1 Supplementary data

## 7.1.1 Radiation response of regulatory T cells in C57BL/6 wild type mice

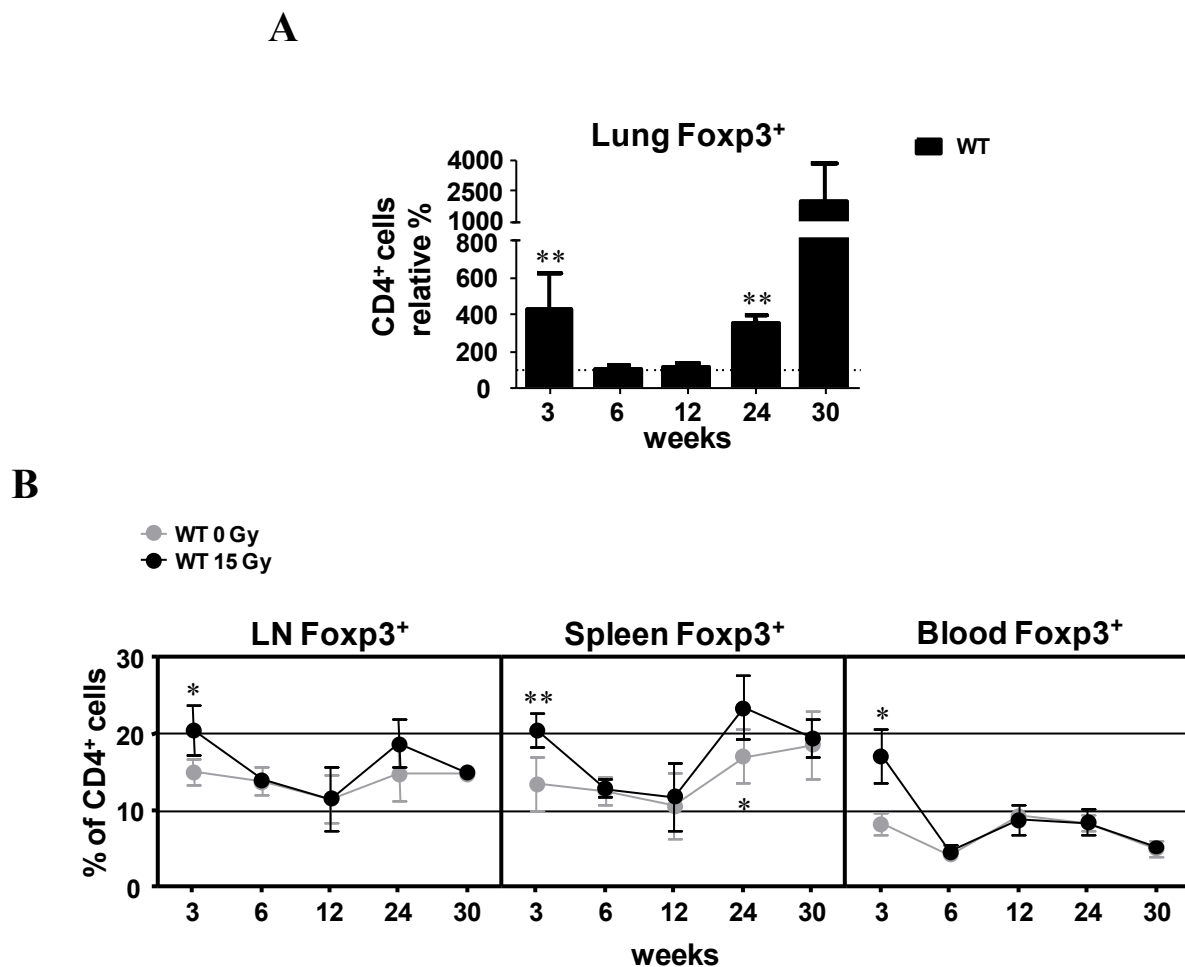


**Fig. 7.1 Determination of local and systemic  $T_{reg}$  cells by flow cytometry.** C57BL/6 wild type (WT) received 0 Gy or 15 Gy whole thorax irradiation. Lymphocytes were isolated from lung (A), blood, spleen and cervical lymph nodes (LN) (B) at 3, 6, 12, 24 and 30 weeks p.i., and used for flow cytometric measurement of  $T_{reg}$  cells. Timelines show relative or absolute percentages  $\pm$  SD of  $CD4^+CD25^+Foxp3^+$  T lymphocyte population in the mentioned tissues of WT mice (\*  $p \leq 0.05$ ; \*\*  $p \leq 0.01$ ; two-tailed unpaired t-test).

### 7.1.2 Effect of CD4<sup>+</sup> T cells on fibrosis development

Most of the significant changes in T lymphocytes of irradiated C57BL/6 wild type mice were observed in CD4<sup>+</sup> T cells, therefore to shed light on the contribution of these cells in radiation-induced fibrosis, in a preliminary experiment RAG-2<sup>-/-</sup> mice were adoptively transferred with CD4<sup>+</sup> T cells 1 day after irradiation or control anaesthesia. Single cell suspensions were obtained from spleens of C57BL/6 wild type mice and used for magnetic separation of CD4<sup>+</sup> T lymphocytes through negative selection. The spontaneous proliferation and generation of memory and effector cells have been already documented after T cell transfer in lymphopenic mice (Surh and Sprent, 2008). Blood samples obtained through eye puncture from reconstituted mice were subjected over time to flow cytometry to confirm T cell persistence also in the radiation model adopted in this study (**Fig 7.2 A**). Similarly to what described before for RAG-2<sup>-/-</sup> mice, lungs of reconstituted mice were isolated 24 weeks after irradiation and processed for histological analysis. As shown in **Fig 7.2 B**, a similar extent of the fibrotic area, as well as a similar amount of fibrotic foci were found in irradiated CD4<sup>+</sup> T cell transferred mice compared to irradiated RAG-2<sup>-/-</sup> mice without adoptive T cell transfer (PBS injected).

These data suggested that the CD4<sup>+</sup> T cells alone seem to be unable to ameliorate fibrosis development in RAG-2<sup>-/-</sup> after whole thorax irradiation.

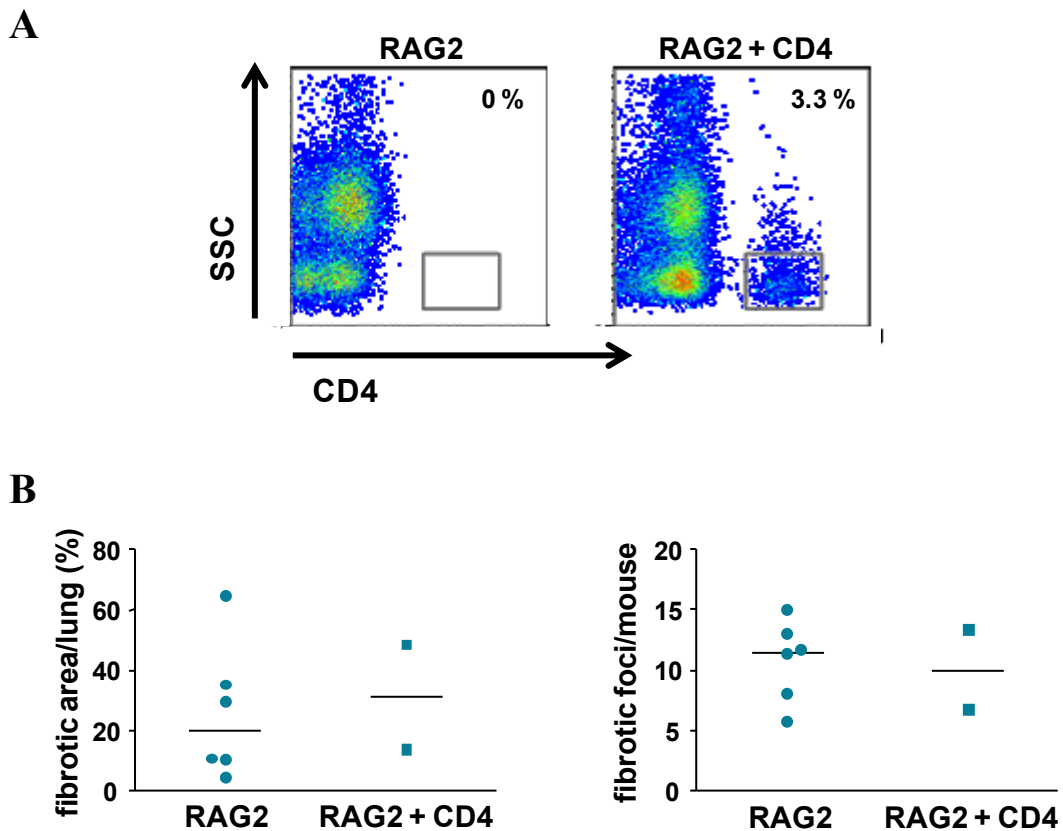


**Fig. 7.2 Fibrosis quantification in RAG-2<sup>-/-</sup> mice adoptively transferred with CD4<sup>+</sup> T cells.** RAG-2<sup>-/-</sup> mice (RAG2) and RAG-2<sup>-/-</sup> mice that were adoptively transferred with CD4<sup>+</sup> T cells (RAG2 + CD4) received 0 Gy or 15 Gy whole thorax irradiation. Blood samples from all groups were regularly assessed for the presence of CD4<sup>+</sup> T cells. At 24 weeks p.i., lung tissue was isolated and used for histological analysis. Paraffin sections obtained from irradiated mice were stained with H&E and evaluated for the amount of fibrosis and the number of fibrotic foci. **A)** Blood samples regularly collected were stained with anti-CD4 antibodies. Representative dot plots for RAG2 mice (left plot) and reconstituted RAG2 mice (right plot) are shown. **B)** Quantification of fibrosis expressed as percentage of fibrotic lung area (left plot), and quantification of the number of fibrotic foci in irradiated mice 24 weeks after irradiation (right plot). Data represent median values obtained in 3 sections per mouse with a minimum distance of 250  $\mu$ m in depth.

## 7.2 Abbreviations

### A

ACK	Ammonium chloride potassium buffer
ADA	Adenosine deaminase
Ado	Adenosine
ADP	Adenosine diphosphate
AECI/II	Alveolar epithelial cell
ALI	Acute lung injury
AM	Alveolar macrophages
AMP	Adenosine monophosphate
ANOVA	Analysis of variance
APAAP	Alkaline phosphatase-anti-alkaline phosphatase
APC	Allophycocyanin or Antigen presenting cell
Arg1	Arginase 1
ATP	Adenosine triphosphate
$\alpha$ -SMA	$\alpha$ -smooth muscle actin

### B

BALF	Bronchoalveolar lavage fluid
BLM	Bleomycin
BSA	Bovine serum albumin

### C

cAMP	Cyclic AMP
CD	Cluster of differentiation
CO <sub>2</sub>	Carbon dioxide
COPD	Chronic obstructive pulmonary disease
CRE	cAMP response element
CREB	CRE binding protein
CSF-1	Colony stimulating factor 1
CSF-1R	Colony stimulating factor 1 receptor
CTL	Cytotoxic T lymphocytes
Cy2/3/5.5/7	Cyanine dyes 2/3/5.5/7

### D

DAB	3,3'-diaminobenzidine
DC	Dendritic cells
ddH <sub>2</sub> O	Double distilled water
DEREG	Depletion of regulatory T cells
DMEM	Dulbecco's modified eagle medium
DNA	Deoxyribonucleic acid

### E

EDTA	Ethylenediaminetetraacetic acid
EtOH	Ethanol

### F

FACS	Fluorescence activated cell sorting
FcR	Fragment crystallizable receptor

**F**

FCS	Fetal calf serum
Fig.	Figure
FITC	Fluorescein isothiocyanate
Foxp3	Forkhead box P3
FSC	Forward-scattered

**G**

GM-CSF	Granulocyte-macrophage colony-stimulating factor
GPI	Glycosyl phosphatidylinositol
Gy	Gray

**H**

H&E	Hematoxylin and eosin
HBSS	Hank's balanced salt solution
HIF-1 $\alpha$	Hypoxia inducible factor 1 $\alpha$
HRE	Hypoxia response element

**I**

i.p.	Intra peritoneal
i.t.	Intra tracheal
IFN	Interferon
IgG	Immunglobulin G
IL	Interleukin
IM	Infiltrating macrophages
iNOS	Inducible nitric oxide synthase
IPF	Idiopathic pulmonary fibrosis
IR	Ionizing radiation

**K**

KHCO <sub>3</sub>	Potassium bicarbonate
-------------------	-----------------------

**L**

LDL	Low-density lipoproteins
LNC	Lymph node cell
LN	Lymph node

**M**

M1	Classically activated macrophages
M2	Alternatively activated macrophages
M-CSF	Macrophage colony-stimulating factor
MHCII	Major histocompatibility complex
MMR	Mannose receptor

**N**

NaCl	Sodium chloride
NGS	Normal goat serum
NH <sub>4</sub> Cl	Ammonium chloride
NK	Natural killer (cells)
NO	Nitric oxide

**P**

p.i	Post irradiation
PBMC	Peripheral blood mononuclear cell
PBS	Phosphate buffered saline
PDGF	Platelet-derived growth factor
PE	Phycoerythrin
PerCP	Peridinin chlorophyll protein complex
PFA	Paraformaldehyde

**R**

RAG	Recombination activating gene
ROS	Reactive oxygen species
rpm	Rounds per minute
RPMI	Roswell park memorial institute medium 1640

**S**

SCID	Severe combined immunodeficiency
SD	Standard deviation
SSC	Side-scattered

**T**

TBS	Tris buffered saline
TGF- $\beta$	Transforming growth factor $\beta$
T <sub>H</sub>	T helper (cell)
TLC	Total lung cells
TMA	Tissue micro array
TNF- $\alpha$	Tumor necrosis factor $\alpha$
T <sub>reg</sub>	Regulatory T (cells)
Tris	Tris(hydroxymethyl) aminomethane
TSC	Total spleen cells

**V**

VHL	von Hippel-Lindau
-----	-------------------

**W**

WT	Wild type
----	-----------

For volume, mass, time or other physical indications, SI (International System of Units) or Legal units were used.



### 7.3 Figure Index

FIG. 1.1 NORMAL WOUND HEALING VS RADIATION INDUCED FIBROSIS.....	9
FIG. 1.2 SCHEMATIC OVERVIEW OF THE EXTRACELLULAR PURINE METABOLISM.....	13
FIG. 2.1 MOUSE MODEL OF WHOLE THORAX IRRADIATION - EXPERIMENTAL SETUP.....	32
FIG. 3.1 CHANGES IN BODY WEIGHT AND SURVIVAL IN C57BL/6 WILD TYPE AND CD73 <sup>-/-</sup> MICE..	43
FIG. 3.2 LUNG HISTOLOGICAL CHANGES IN C57BL/6 WILD TYPE AND CD73 <sup>-/-</sup> MICE..	46
FIG. 3.3 QUANTITATIVE ANALYSIS OF FIBROSIS IN C57BL/6 WILD TYPE AND CD73 <sup>-/-</sup> MICE. ....	47
FIG. 3.4 QUANTITATIVE ANALYSIS OF HYPOXIC AREAS IN C57BL/6 WILD TYPE AND CD73 <sup>-/-</sup> MICE..	49
.....	49
FIG. 3.5 IMMUNOHISTOCHEMICAL STAINING OF TGF-B AND $\alpha$ -SMA IN LUNG SECTIONS. ....	50
FIG. 3.6 DETERMINATION OF LEUKOCYTE CONTENT IN LUNG TISSUE BY FLOW CYTOMETRY. ....	56
FIG. 3.7 DETERMINATION OF CD39 AND CD73 EXPRESSION ON LUNG T CELLS BY FLOW CYTOMETRY.....	57
FIG. 3.8 DETERMINATION OF LUNG CD4 <sup>+</sup> AND CD8 <sup>+</sup> T CELLS AND THEIR CD39 AND CD73 EXPRESSION BY FLOW CYTOMETRY. ....	58
FIG. 3.9 DETERMINATION OF SPLEEN AND LYMPH NODE CD4 <sup>+</sup> TCELLS AND THEIR CD39 AND CD73 EXPRESSIONS BY FLOW CYTOMETRY. ....	61
FIG. 3.10 DETERMINATION OF LUNG T <sub>REG</sub> CELLS BY FLOW CYTOMETRY. ....	62
FIG. 3.11 DETERMINATION OF SYSTEMIC T <sub>REG</sub> CELLS BY FLOW CYTOMETRY. ....	63
FIG. 3.12 FOAMY MACROPHAGES IN C57BL/6 WILD TYPE AND CD73 <sup>-/-</sup> MICE LUNGS .....	65
FIG. 3.13 MACROPHAGES AND iNOS, OR ARG1 OR IL-10RA IMMUNOFUORESCENCE STAINING. ....	67
FIG. 3.14 ANALYSIS OF CSF-1R EXPRESSION ON LUNG MACROPHAGES. ....	69
FIG. 3.15 ANALYSIS OF CD36 EXPRESSION ON LUNG MACROPHAGES.....	69
FIG. 3.16 DETERMINATION OF CD39 AND CD73 EXPRESSION ON MACROPHAGES BY FLOW CYTOMETRY. ....	71
FIG. 3.17 ANALYSIS OF M1 AND M2 PHENOTYPES ON LUNG MACROPHAGES BY FLOW CYTOMETRY. ....	73
FIG. 3.18 CHANGES IN BODY WEIGHT AND SURVIVAL IN RAG-2 <sup>-/-</sup> MICE.....	75
FIG. 3.19 LUNG HISTOLOGICAL CHANGES IN RAG-2 <sup>-/-</sup> MICE.....	78
FIG. 3.20 QUANTITATIVE ANALYSIS OF FIBROSIS IN C57BL/6 WILD TYPE AND RAG-2 <sup>-/-</sup> MICE.....	79
FIG. 3.21 DETERMINATION OF LEUKOCYTE CONTENT IN LUNG TISSUE. ....	80
FIG. 3.22 DETERMINATION OF MACROPHAGE CHARACTERISTICS.....	82
FIG. 3.23 DETERMINATION OF CD39 AND CD73 EXPRESSION ON MACROPHAGES.....	83

FIG. 3.24 DETERMINATION OF ALVEOLAR MACROPHAGE POLARIZATION .....	84
FIG. 7.1 DETERMINATION OF LOCAL AND SYSTEMIC T <sub>REG</sub> CELLS BY FLOW CYTOMETRY .....	115
FIG. 7.2 FIBROSIS QUANTIFICATION IN RAG-2 <sup>-/-</sup> MICE ADOPTIVELY TRANSFERRED WITH CD4 <sup>+</sup> T CELLS .....	117

## 7.4 Table Index

TABLE 2.1 EQUIPMENT _____	25
TABLE 2.2 DISPOSABLES AND MATERIALS _____	26
TABLE 2.3 CHEMICALS, REAGENTS, MEDIA AND KITS _____	27
TABLE 2.4 BUFFERS AND SOLUTIONS _____	28
TABLE 2.5 ANTIBODIES _____	29
TABLE 2.6 FACS STAININGS _____	30
TABLE 2.7 MOUSE STRAINS _____	31

## 7.5 Acknowledgments

**7.6 Curriculum Vitae**

**FEDERICA CAPPUCINI  
CURRICULUM VITAE**

"Not included for reasons of data protection"

"Not included for reasons of data protection"

"Not included for reasons of data protection"

## 7.7 Declarations

### Erklärung:

Hiermit erkläre ich, gem. § 6 Abs. 2, f der Promotionsordnung der Math.-Nat. Fakultäten zur Erlangung der Dr. rer. nat., dass ich das Arbeitsgebiet, dem das Thema „Radiation-induced pneumonitis and fibrosis - Defining the role of immune cells and regulatory molecules“ zuzuordnen ist, in Forschung und Lehre vertrete und den Antrag von Federica Cappuccini befürworte.

Essen, den \_\_\_\_\_

Verena Jendrossek

### Erklärung:

Hiermit erkläre ich, gem. § 7 Abs. 2, c und e der Promotionsordnung der Math.-Nat. Fakultäten zur Erlangung des Dr. rer. nat., dass ich die vorliegende Dissertation selbständig verfasst und mich keiner anderen als der angegebenen Hilfsmittel bedient habe und alle wörtlich oder inhaltlich übernommenen Stellen als solche gekennzeichnet habe.

Essen, den \_\_\_\_\_

Federica Cappuccini

### Erklärung:

Hiermit erkläre ich, gem. § 7 Abs. 2, d und f der Promotionsordnung der Math.-Nat. Fakultäten zur Erlangung des Dr. rer. nat., dass ich keine anderen Promotionen bzw. Promotionsversuche in der Vergangenheit durchgeführt habe, dass diese Arbeit von keiner anderen Fakultät abgelehnt worden ist, und dass ich die Dissertation nur in diesem Verfahren einreiche.

Essen, den \_\_\_\_\_

Federica Cappuccini